NORTH AMERICAN AVIATION, INC.
COLUMBUS DIVISION
COLUMBUS 16, OHIO

23

GENERALIZED HONEYCOMB THERMAL STRESS STUDY

PREPARED BY Lloyd E. Hackman
Lloyd E. Hackman
Specialist
Structural Analysis

C. W. Annis
C. W. Annis
Chief
Structural Mechanics & Computing

APPROVED BY
V. L. Beals, Manager
Structural Mechanics
& Materials Research

J. F. Reagan
Dr. J. F. Reagan
Director of Engineering
Aircraft & Missiles R & D

ABSTRACT

The enclosed development study was performed on the Bureau of Naval Weapons Contract NOw 61-0355-d.

Phase I of this study was initiated to develop a "Generalized Honeycomb Thermal Stress Analysis" which would offer the capability of predicting thermal limits for any aircraft subjected to the effects of a nuclear explosion. The method developed for this contract is based upon a recently developed "Allowable Stress Method" with the capability of predicting the allowable load on any structural cross-section in any flight and thermal exposure environment. The "Allowable Stress Method" is considered one of the most important developments in analysis of aircraft structures in recent years. Such an approach on this contract gives the user not only a nuclear effects analysis method but a "Generalized Allowable Structural Loads Method".

Phase II of this study was initiated to develop design procedures for a weapons system subjected to the effects of a nuclear explosion. The design procedures developed during this study provide a method of deriving the minimum weight configuration to provide the needed delivery or escape capability. The optimization of composite structures with a thermal gradient present is a break-through in automated design methods. The procedure with minor modification can be used for the aerodynamic heating problem as well as the nuclear effects heating problem.

Recognitions

Recognition must be given to R.W. Gehring, Specialist, Structural Development, for his assistance in the preparation of this report and development of the finalized Allowable Stress Method.

Further Recognition must be given to Dr. B.E. Gatewood, Consultant, for the initial derivation and development of the basic Allowable Stress Methods used in this study.

Recognition must also be given to James Richardson, Structures Engineer, Structural Development, for his assistance in the preparation of this report and the development of the skin stringer box beam optimization method.

TABLE OF CONTENTS

TABLE OF CONTENTS (continued)

LIST OF FIGURES AND TABLES

FIGURES

LIST OF FIGURES AND TABLES (Continued)

LIST OF FIGURES AND TABLES (Continued)

LIST OF FIGURES AND TABLES (Continued)

FIGURES

LIST OF FIGURES AND TABLES (Continued)

FIGURES

LIST OF FIGURES AND TABLES (Continued)

TABLES

SYMBOLS

A_{eff}	Effective area, $in.^2$
A_L	Area of lower panel, $in.^2$
A_n	Area of element "n", $in.^2$
A_t	Total area, $in.^2$
A_u	Area of upper panel, $in.^2$
a	Width of loaded edge, in.
b	Maximum value of x_n or length of unloaded edge, in.
b_c	Corrugation length, in.
b_b	Corrugation depth, in.
b_n	Width of plate element "n", in.
b_{n_e}	Effective width of plate element "n", in.
BR	Spar web bend radius, in/in
BRS	Allowable spar web bearing stress, lbs/in^2
b_s	Stringer spacing, in.
b_{st_r}	Lower stringer depth, in.
b_w	box beam depth, in.
C	Core depth, in.
C_n	Effective area coefficient of element "n"
C_1	Proportional limit stress/F_y
C_L	Chord length, in.
c	Maximum value of y_n, in
C_s	Upper cap strain, in/in.

SYMBOLS (continued)

C_{pc}	Specific heat of core, Cal/gm-°F
C_{pf}	Specific heat of face, Cal/gm-°F
E_c	Young's modulus for the core, lbs/in^2
e_L	Lower cap strain, in/in
E_n	Modulus of elasticity at temperature of element "n", lbs/in^2
E_R	Modulus of elasticity at room temperature, lbs/in^2
e_s	Upper cap strain, in/in
E_r	Reduced modulus = $2E\,E_t/E_t + E$
E_s	Secant modulus = $E/1 + .428\,(F_c/F_{cy})^{m-1}$
E_T	Tangent modulus = $E/1 + .428\,m\,(F_c/F_{cy})^{m-1}$
e_{a_p}	Elastic applied load strain, in/in
e_{cr}	Critical column buckling strain, in/in; critical buckling strain of plate element, in/in
e_l	Lower panel strain, in/in
e_{lb}	Bending strain on lower panel, in/in
e_n	Total strain in element "n", in/in
e_{n_o}	Element strain denoting new origin of stress-strain curve, in/in
e_p	Axial strain for inelastic effects, in/in
e_{T_n}	Strain in element "n" at temperature step, in/in
e_w	Spar web strain, in/in
F_{a_p}	Applied elastic stress, lbs/in^2

SYMBOLS (continued)

F_b	Bending stress, lbs/in^2
F_c	Compression stress, lbs/in^2
F_{c_c}	Allowable crippling stress, lbs/in^2
F_{c_o}	Cut-off stress for crippling, lbs/in^2
F_n	Stress in element "n", lbs/in^2
F_{s_u}	Ultimate shear stress, lbs/in^2
F_{t_u}	Ultimate allowable tensile stress, lbs/in^2
F_{y_n}	Tension or compression yield stress of element "n", lbs/in^2
F_{c_y}	Yield stress, lbs/in^2
G_c	Shear modulus of core material; lbs/in^2 heat capacity of honeycomb core, $Cal/cm^2\ ^oF$
G_f	Heat capacity of facing, $Cal/cm^2\ ^oF$
H_s	Heat transfer coefficient, Cal/cm^2 sec ^oF
h	Upper stringer depth, in
I	Moment of inertia, in^4
K_a	Total elastic moment strain, in/in
K_{apx}	Elastic applied moment strain about the x-axis, in/in
K_c	Compression buckling coefficient; thermal conductivity, Cal/cm sec ^oF
$K_{c_{r_n}}$	Compression buckling coefficient for element "n" depending on edge fixity
K_i	Moment strain term for initial deflection, in/in
K_{i_x}	Internal moment strain about x-axis, in/in

SYMBOLS (Continued)

K_n	Element "n" crippling coefficient
K_p	Moment strain to correct for inelastic effects, in./in.
K_s	Shear buckling coefficient
K_T	Thermal moment strain, in./in.
K_w	Moment strain due to deflection, in./in.
K_{w_s}	Spar web shear buckling coefficient
K_{w_c}	Spar web compression buckling coefficient
K_t	Thermal radiation constant, $^{\circ}F$ in.
K_{st_c}	Lower stringer compression buckling coefficient
L	Effective column length, in.
M	Bending moment, in.-lbs.
m	Ramberg-Osgood exponent depending on material
M_u	Primary bending moment compression, in. lbs
M_r	Critical reverse bending upper panel moment, in lbs.
MRD	Maximum rivet diameter, in.
M_{th}	Induced thermal moment, in. lbs
N	Number of waves in buckled panel
P	Axial load, lbs.
P_{ap}	Applied axial load, lbs.
P_m	General buckling coefficient.*
PR	Poisson's ratio
Q	Shear load, lbs.
QT_1	Radiant exposure to the upper panel, Cal/cm^2
QT_2	Radiant exposure to the lower panel, Cal/cm^2

* See Page 6

SYMBOLS (Continued)

s	Cell size, in
T	Temperature, °F
t_c	Core foil thickness, in.
t_F	Facing thickness, in.
t_n	Thickness of element "n", in.
t_v	Lower stringer thickness, in.
t_s	Upper skin thickness, in.
t_w	Web thickness, in.
t_L	Lower skin thickness, in.
t_{str}	Lower stringer thickness, in.
T_b	Base temperature, °F
w	Deflection of structure from its original unloaded position, in., Spar spacing, in.
w_m	Maximum deflection at center of plate element, in.
x_n	Distance from vertical elastic neutral axis to centroid of element "n", in
x_{n_R}	Distance from vertical reference axis to centroid of element "n", in.
y_n	Distance from horizontal elastic neutral axis to centroid of element "n", in.
y_{n_R}	Distance from horizontal reference axis to centroid of element "n", in.
α_n	Thermal coefficient of expansion of element "n", in./in./°F
ρ	Radius of gyration, in.

SYMBOLS (Continued)

μ	Poisson's ratio.
Δ	Incremental change
ϵ'	Honeycomb thermal response parameter
ρ_c	Density of core lbs./in.^{3}
ρ_f	Density of facing lbs./in^3
ΔT_n	Thermal gradient on honeycomb panel °F
ΔT_m	Temperature rise on front face of honeycomb panel °F
η	Time to peak irradiance, sec.
P_M	$= \dfrac{K + \left(\dfrac{Vx}{C4} + Vy\right) F}{1 + L + \dfrac{Vx\, Vy}{C4} F}$
K	$= C_1 + 2C_2 + C_3$
L	$+ (C_1 + \dfrac{1-\mu}{2} C_2) \dfrac{Vx}{C4} + (C_3 + \dfrac{1-\mu}{2} C_2) Vy$
F	$= C_1C_3 - C_2^2 + \dfrac{1-\mu}{2} C_2K$
V_x	$= \dfrac{\pi^2 C\, t_{F_1}\, t_{F_2}\, E_1E_2}{(t_{F_1} E_1 + t_{F_2}E_2)\, a^2\, Gcx\, (1-\mu^2)}$
Vy	$= \dfrac{^2 C\, t_{F_1}\, t_{F_2}\, E_1E_2}{(t_{F_1} E_1 + t_{F_2}E_2)\, a^2\, Gcy\, (1-\mu^2)}$
G'_{cx}	= effective shear modulus of core in x direction, lbs/in^2
G'_{cy}	= effective shear modulus of core in y direction, lbs/in^2

SYMBOLS (Continued)

The constants C_1, C_2, C_3, C_4 are dependent upon the edge fixity conditions of the panel. A listing of these values follows:

Edges simply supported.

$$C_1 = C_4 = \frac{b^2}{n^2a^2} \qquad C_2 = 1 \qquad C_3 = \frac{n^2a^2}{b^2}$$

b = panel length, in. a = panel width, in.

n = number of half waves

Loaded edge simply supported
Unloaded edge clamped

$$C_1 = 5.33\ \frac{b^2}{n^2a^2} \qquad C_2 = 1.33 \qquad C_3 = \frac{n^2a^2}{b^2} \qquad C_4 = 1.33\ \frac{b^2}{n^2a^2}$$

Loaded edge clamped
Unloaded edge simply supported

$$C_2 = 1 \qquad C_3 = \left(\frac{n^4 + 6n^2 + 1}{n^2 + 1}\right) \frac{a^2}{b^2}$$

For n = 1 $\qquad C_1 = .75\ \frac{b^2}{a^2} \qquad C_4 = 3\ \frac{b^2}{a^2}$

For n > 1 $\qquad C_1 = C_4 = \left(\frac{1}{n^2 + 1}\right) \frac{b^2}{a^2}$

All edges clamped

$$C_2 = 1.33 \qquad C_3 = \left(\frac{n^4 + 6n^2 + 1}{n^2 + 1}\right) \frac{a^2}{b^2}$$

For n = 1 $\qquad C_1 = 4C_4 = 4\ \frac{b^2}{a^2}$

For n > 1 $\qquad C_1 = 4C_4 = \frac{5.33}{(n^2 + 1)} \frac{b^2}{a^2}$

SUBSCRIPTS

a	Applied total
ap	Applied
cc	Crippling
c.o.	Cut-off
cr	Critical
cu	Compression ultimate
cy	Compression yield
e	Effective; equivalent
i	Initial; internal
j	Step in temperature-load cycling
m	Middle; extreme fiber
n	Element number
p	Inelastic
ps	Permanent set
r	Iteration step
T	Temperature
x	About x-axis
y	About y-axis; yield
M	Column element number

REFERENCES

1. Thermal Stresses, by B.E. Gatewood, Mc Graw-Hill, 1957.

2. Aircraft Structures, by D.J. Peery, Mc Graw-Hill, 1950.

3. NA59-1957, "Structural Development of Brazed Honeycomb Sandwich Construction for the Model F108 Air Vehicle".

4. NA58H-446, "Criteria and Methods for the Analysis of the Nuclear Weapons Delivery Capability of the A3J-1 Weapons System".

5. MIL-HDBK-5, "Strength of Metal Aircraft Elements".

6. NA56H-525, "Structural Tests - Complete Airplane for the Model A3J-1 Airplane".

7. Forest Products Report Number 1583-B, "Effects of Shear Deformation in the Core of a Flat Rectangular Sandwich Panel".

8. NA60H-288, "Proposal for a Generalized Honeycomb Thermal Stress Analysis".

9. NA60H-633, "Correlation of Calculated and Measured Thermal Stresses in Representative FJ-4B Aircraft Aluminum Structure Exposed to Transient Heating".

1.0 INTRODUCTION

The "Generalized Honeycomb Thermal Stress Study", was initiated in two phases to establish the capability for analysis and design of aircraft subjected to nuclear explosions. Phase I of this study, "Analysis and Tests", is discussed in Sections 2.0, 3.0, 4.0 and 6.0. Phase II, "Optimum Design Procedures", is discussed in Section 5.0.

The analysis procedures developed during the Phase I studies are presented in two sections: a detailed exact method and an approximate hand calculation method. The exact method is based upon a newly developed "Allowable Stress" method. This method provides a tool by which the allowable load for a given structure can be computed for any of three failure criteria; initial instability, yield and ultimate. The initial stability failure is based upon any critically instable element in the structural cross-section. The yield and ultimate failure modes are conversely based upon the yield or ultimate of the total section and not of any one given element as has been the case in the past. The load carrying capability of each element during post-failure as well as pre-failure loading is accounted for to best predict the yield and ultimate of the total structural section. This exact and complex method has been programmed for the IBM 709 Digital Computer and demonstrated on a typical horizontal stabilizer for correlation of the theoretical method against test results.

The hand calculation method was developed from the normal thermal stress analysis approach with the elimination of as much of the detail as possible without completely destroying the accuracy of the method. This method in more detail was used in the past to predict the thermal limits for the FJ4 and A3J airplanes. Limits computed from this abbreviated method can be expected to be as much as + 15% in error depending upon the care taken while making the analysis. From the stress distribution computed with the thermal stress equations, a comparison with element allowables must be made to determine the limits as demonstrated in the example problem presented in Section 3.2. Although this procedure can be accomplished by hand, it is particularly adaptable to desk calculators and small digital computers.

The Phase I study also included high temperature structural tests of a typical horizontal stabilizer and several honeycomb panel configurations. The typical horizontal stabilizer test was made to determine an ultimate failure load under a transient temperature condition. This failure load was then compared with a computed load showing excellent agreement.

The honeycomb panel tests performed during this study established test data for correlation with a general honeycomb panel buckling equation. Previous to this study, honeycomb panel buckling allowables were determined by testing only. With the correlation of the generalized buckling equation,

allowables for all the structural elements can be computed theoretically, thus providing the capability of analysis and design for thermal effects on structures without excessive testing.

The Phase II study has approached the objective of aircraft design for induced thermal gradients as a design optimization problem. In general, the nuclear effects problem has been handled by determining the limit which the aircraft can withstand after the design has been completed. For the case of aircraft vulnerability to defensive weapons, a capability must be designed into the aircraft. In many cases, it would also be a great advantage to predetermine the delivery capabilities as the aircraft is designed. Initially designing for the required capabilities will insure the best design for the weapon system.

The design optimization methods developed during this study include; 1. honeycomb panels with a fixed load, 2. honeycomb panels with a fixed strain, 3. honeycomb box beam with straight or corrugated spar webs, 4. skin-stringer box beam with straight or corrugated webs. In each of these cases, a minimum weight design is computed from a given load and thermal input. The temperature of the hot facing is a variable dependent upon the material thicknesses. The following dependent parameters are also determined in these optimization procedures; honeycomb facing thicknesses, core depth, core cell size and foil thickness, spar spacing, spar web thickness, stringer spacing, stringer thickness and depth.

The methods developed in this study provides a basic tool for nuclear effect capability design. They have also established a basis from which further design methods can be developed.

2.0 GENERAL DISCUSSION OF THE ALLOWABLE STRESS METHOD

When a structure is subjected to a non-uniform temperature distribution, the elements of the cross-section of the structure have varying material properties depending upon the temperature of the element. Thermal stresses may be present due to a non-uniform temperature distribution and/or different materials in the cross-section. The inelastic effects of buckling and stresses beyond the proportional limit produce stress variations and distributions within the cross-section. The strains associated with the stresses vary due to thermal expansion applied axial load and/or bending moment strains and stress variations produced by the temperature distribution.

With the material property stress-strain curve of each element in the cross-section represented analytically by the Ramberg-Osgood equation (Ref. 1) then,

$$\frac{E_n e_n}{F_{y_n}} = \frac{F_n}{F_{y_n}} \left[1 + \frac{3}{7} \left(\frac{F_n}{F_{y_n}} \right)^{m-1} \right] \qquad (2.0.1)$$

where, for element n, F_{y_n} is the yield stress which depends upon temperature, previous temperature and load history of the element; F_n is the stress, E_n is the elastic modulus, and e_n is the element strain associated with the stress.

The following sections show the development of the strain, stress, and equilibrium equations necessary to define the load-deformation curve for any cross-section in any temperature-load environment.

2.1 DEVELOPMENT OF THE ALLOWABLE STRESS METHOD

2.1.1 BASIC STRAIN EQUATIONS

Assuming a plane cross-section to remain plane at all times, then the shape of the strain distribution curve on the cross-section will always be the same shape as the thermal strain distribution curve except for possible rotation through a constant angle. This relationship holds true whether the material is elastic or inelastic and regardless of the presence of buckling. An applied axial load produces a constant strain and an applied moment produces a rotation through a constant angle. A general strain equation may be written for any element n in the cross-section based on the above assumption. The element strain, designated as e_n, consists of the sum of the elastic thermal strain, the elastic applied axial load and bending moment strains, and a correcting linear term to account for all inelastic effects. This strain may be written as

$$e_n = e_{T_n} + \frac{f_{ap_n}}{E_n} + e_{p_n} \qquad (2.1.1)$$

where e_{T_n} is the elastic thermal strain and is defined as follows:

$$e_{T_n} = -(\alpha T)_n + e_T + K_{T_x}\left(\frac{y_n}{c}\right) + K_{T_y}\left(\frac{x_n}{b}\right) \qquad (2.1.2)$$

where

$$e_T = \frac{\sum_n (\alpha T)_n E_n A_n}{\sum_n E_n A_n}$$

$$\left.\begin{aligned} K_{T_x} &= c\left[\frac{M_{T_x}(EI_y) - M_{T_y}(EI_{xy})}{(EI_x)(EI_y) - (EI_{xy})^2}\right] \\ K_{T_y} &= b\left[\frac{M_{T_y}(EI_x) - M_{T_x}(EI_{xy})}{(EI_x)(EI_y) - (EI_{xy})^2}\right] \end{aligned}\right\} \qquad (2.1.3)$$

The temperature moment terms in Eq. (2.1.3) are defined by

$$\left.\begin{aligned} M_{T_x} &= \sum_n (\alpha T)_n \; E_n \; A_n \; y_n \\ M_{T_y} &= \sum_n (\alpha T)_n \; E_n \; A_n \; x_n \end{aligned}\right\} \qquad (2.1.4)$$

and the elastic bending stiffness parameters about orthogonal axes x and y are defined by

$$\left.\begin{aligned} (EI_x) &= \sum_n E_n \; A_n \; y_n^2 \\ (EI_y) &= \sum_n E_n \; A_n \; x_n^2 \\ (EI_{xy}) &= \sum_n E_n \; A_n \; x_n \; y_n \end{aligned}\right\} \qquad (2.1.5)$$

if the bending stiffness of each element about its own elastic neutral axis is neglected.

From the arbitrary reference axes x_R and y_R the values x_n and y_n are defined by

$$\left.\begin{aligned} x_n &= x_{n_R} - \frac{\sum_n E_n \; A_n \; x_{n_R}}{\sum_n E_n \; A_n} \\ y_n &= y_{n_R} - \frac{\sum_n E_n \; A_n \; y_{n_R}}{\sum_n E_n \; A_n} \end{aligned}\right\} \qquad (2.1.6)$$

The elastic applied axial load and bending moment strain term in Eq. (2.1.1) is

$$\frac{F_{ap_n}}{E_n} = e_{ap} + K_{ap_x} \left(\frac{y_n}{c}\right) + K_{ap_y} \left(\frac{x_n}{b}\right) \qquad (2.1.7)$$

where the elastic applied axial load strain is

$$e_{op} = \frac{P}{\sum_n E_n A_n} \tag{2.1.8}$$

and the elastic applied bending moment strains on the extreme fiber elements are

$$K_{opx} = c\left[\frac{M_x (EI_y) - M_y (EI_{xy})}{(EI_x)(EI_y) - (EI_{xy})^2}\right]$$
$$K_{ap_y} = b\left[\frac{M_y (EI_x - M_x (EI_{xy})}{(EI_x)(EI_y) - (EI_{xy})^2}\right] \tag{2.1.9}$$

In Eq's. (2.1.8) and (2.1.9) P, M_x, and M_y are the applied axial load, bending moment about the horizontal elastic neutral axis, and bending moment about the vertical elastic neutral axis, respectively, for any given cross-section.

The inelastic correcting strain is determined by

$$e_{pn} = e_p + K_{p_x}\left(\frac{y_n}{c}\right) + K_{p_y}\left(\frac{x_n}{b}\right) \tag{2.1.10}$$

where the values of the inelastic correcting strains e_p, K_{px}, and K_{py} are defined by the iteration procedures of Section 2.1.7 such that the stresses F_n corresponding to the strains e_n satisfy the equilibrium equations

$$P = \sum_n F_n A_n C_n$$
$$M_x = \sum_n F_n A_n C_n y_n$$
$$M_y = \sum_n F_n A_n C_n x_n \tag{2.1.11}$$

where C_n is the effective area factor for local buckling of element n as defined in Section 2.1.6.

2.1.2 TEMPERATURE AND LOAD STRAIN EQUATIONS

Since the applied load may already be present when the temperature is applied to the structure, a non-uniform temperature distribution may be present when the load is applied, the temperature may cycle with a steady load acting, or both load and temperature may vary with time, it is necessary to write the strain equations to account for sequence application and removal of load and temperature. These equations must then allow for the strain, stress, and temperature histories of the structural elements. Various factors involved are the true permanent set strains at the end of any given sequence of temperature and load cycling, strain accumulation produced by temperature cycling, variation of material properties as the temperature varies with time, and the recovery of material properties after a given exposure time at temperature. Under sequence application and/or removal of load and temperature, unloading of some elements from an inelastic position on the stress-strain curve may occur. For unloading, the element strain is assumed to follow a straight line of slope E_n (elastic) to zero stress and then follow a stress-strain curve with a new origin when loading in the opposite direction. The shift in origin for any element is defined as:

$$e_{n_o} = e_n - \frac{F_n}{E_n} \qquad (2.1.12)$$

(See Figure 2.1.)

If reloading takes place from any point on the straight line or from an elastic position on the new stress-strain curve, then the straight line is followed up to the original stress-strain curve (for strain hardening materials) and the original stress-strain curve followed for larger strains. If reloading occurs from an inelastic point on the new stress-strain curve, then the element may follow a new stress-strain curve from a new origin as shown by (6) in Figure 2.1. The effect that actually occurs depends upon the amount of yielding that has occurred in the reverse direction. Until more test data is available to establish definitive criteria for reloading, it may be reasonably assumed that a new stress-strain curve can arise whenever unloading occurs from any point on the stress-strain curve where:

$$\frac{F_n}{F_{y_n}} \geq 0.80 \qquad (2.1.13)$$

FIGURE 2.1

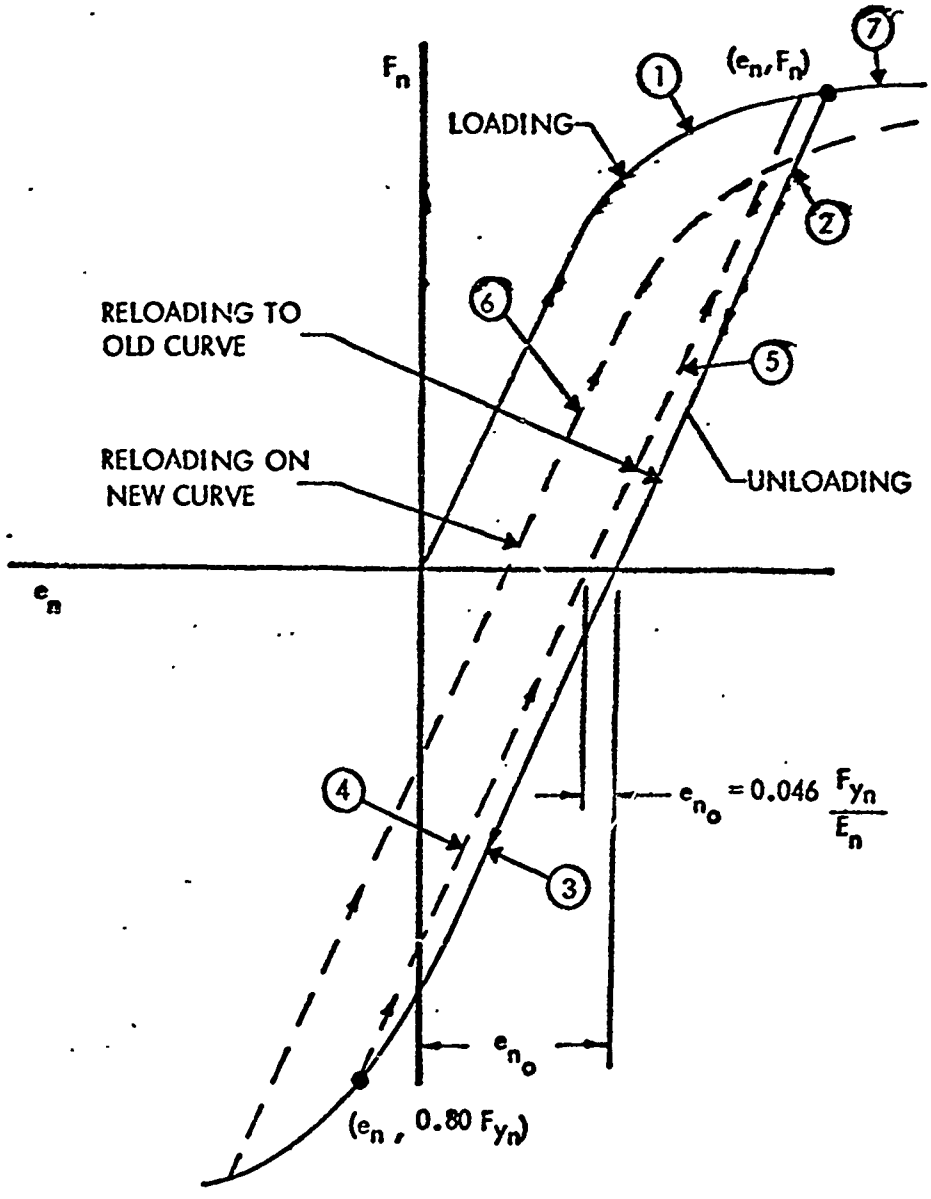

SHIFT IN ORIGIN OF STRESS-STRAIN CURVES

This corresponds to a shift in origin of the stress-strain curve defined by

$$e_{a_0} \geq 0.046 \left(\frac{F_{y_m}}{E_n} \right) \qquad (2.1.14)$$

if the stress-strain curve is represented by the Ramberg-Osgood equation with m = 10. (See Figure 2.1) where reloading to the old stress-strain curve at the maximum permissible origin shift defined by Eq. (2.1.14) is illustrated by (5). It is apparent, then, that with various elements in the cross-section loading, unloading, or reloading at any step in the temperature-load sequence, that the strains and stresses must depend upon the previous steps in the sequence to define the proper stress-strain curve and origin. If at each step in the temperature-load sequence the strain e_n is assumed to start from a new origin as defined by Eq. (2.1.12), then the element strain Eq. (2.1.1) at any step j can be written in terms of the previous step j-1 and the load or temperature application or removal at step j as:

$$e_{nj} = \frac{F_{nj-1}}{E_{n,j-1}} - (\alpha T)_{n_j} + (e_T + e_{ap} + e_p)_j + (K_{T_x} + K_{ap_x} + K_{px})_j \frac{y_n}{c} + (K_{T_y} + K_{ap_y} + K_{py})_j \frac{x_n}{b}$$

$$= \frac{F_{n,j-1}}{E_{n,j-1}} + \Delta e_{n_j} \qquad (2.1.15)$$

where $E_{n,j-1}$ is the elastic modulus at step j-1. Eq. (2.1.15) is general since it includes both the thermal elastic strain of Eq. (2.1.2), the elastic applied load and/or moment strains of Eq. (2.1.7), all inelastic effects which are represented by e_p, K_{px}, and K_{py}, and the stress effects of the previous steps.

Since the calculations are performed for temperature-load sequences where the effects of temperature and load are not applied simultaneously, the general strain equation (2.1.15) is written as follows. For any temperature application or removal step; the element strain is:

$$\epsilon_{n_j} = \frac{F_{n,j-1}}{E_{n,j-1}} + \Delta e_{n_j}$$

$$= \frac{F_{n,j-1}}{E_{n,j-1}} - (\alpha T)_{n_j} + (e_T + e_p)_j + (K_{T_x} + K_{p_x})_j \frac{x_n}{c} + (K_{T_y} + K_{p_y}) \frac{x_n}{b} \qquad (2.1.16)$$

In Eq. (2.1.16) the temperature T_{n_j} is the incremental change in temperature of element n from the last temperature application or removal step. The temperature terms e_{T_j} and K_{T_j} are essentially as shown in Eq. (2.1.3) and specifically for any temperature application or removal step are calculated as follows:

$$e_{T_j} = \frac{\left(\sum_n (\alpha T)_n E_n A_n\right)_j}{\left(\sum_n E_n A_n\right)_j}$$

$$K_{T_{x_j}} = c_j \left[\frac{\left(\sum_n (\alpha T)_n E_n A_n y_n\right)_j \left(\sum_n E_n A_n x_n^2\right)_j - \left(\sum_n (\alpha T)_n E_n A_n x_n\right)_j \left(\sum_n E_n A_n x_n y_n\right)_j}{\left(\sum_n E_n A_n y_n^2\right)_j \left(\sum_n E_n A_n x_n^2\right)_j - \left(\sum_n E_n A_n x_n y_n\right)_j^2}\right]$$

$$K_{T_{y_j}} = b_j \left[\frac{\left(\sum_n (\alpha T)_n E_n A_n x_n\right)_j \left(\sum_n E_n A_n y_n^2\right)_j - \left(\sum_n (\alpha T)_n E_n A_n y_n\right)_j \left(\sum_n E_n A_n x_n y_n\right)_j}{\left(\sum_n E_n A_n y_n^2\right)_j \left(\sum_n E_n A_n x_n^2\right)_j - \left(\sum_n E_n A_n x_n y_n\right)_j^2}\right] \qquad (2.1.17)$$

For any load application or removal step j the element strain is

$$e_{n_i} = \frac{F_{n_{i-1}}}{E_{n_{i-1}}} + \Delta e_{n_i}$$

$$= \frac{F_{n_{i-1}}}{E_{n_{i-1}}} + (e_{ap} + e_p)_i + (K_{ap_x} + K_{p_x})_i \frac{y_n}{c} + (K_{ap_y} + K_{p_y})_i \frac{x_n}{b} \qquad (2.1.18)$$

where,

$$e_{ap_i} = \frac{P_i}{(\sum_n E_n A_n)_i}$$

$$K_{ap_{x_i}} = c_i \left[\frac{M_{x_i} (\sum_n E_n A_n x_n^2)_i - M_{y_i} (\sum_n E_n A_n x_n y_n)_i}{(\sum_n E_n A_n y_n^2)_i (\sum_n E_n A_n x_n^2)_i - (\sum_n E_n A_n x_n y_n)_i^2} \right]$$

$$K_{ap_{y_i}} = b_i \left[\frac{M_{y_i} (\sum_n E_n A_n y_n^2)_i - M_{x_i} (\sum_n E_n A_n x_n y_n)_i}{(\sum_n E_n A_n y_n^2)_i (\sum_n E_n A_n x_n^2)_i - (\sum_n E_n A_n x_n y_n)_i^2} \right] \qquad (2.1.19)$$

where P_i, M_{x_i}, and M_{y_i} are the incremental loads and bending moments applied or removed at any step i.

In Equations (2.1.15) and (2.1.18) e_{n_i} is the strain directly associated with the stress F_{n_i} either as an elastic value or as a value on the stress-strain curve upon reloading. In this case the strain associated with the stress is taken as:

$$e_{n_i} + q_{n_i}; \text{ where } q_{n_i} = \sum_{i=k}^{i-m} e_{no_i} \qquad (2.1.20)$$

where e_{no_i} is determined by Equation (2.1.12) but is not included in the sum unless it also satisfied the condition of Equation (2.1.14). k is the step at

which the last sign reversal of e_{no_i} occurred, and j-m is the last step at which e_{no_i} satisfied Equation (2.1.14).

The stress equations of Section 2.1.5 and the logic table in Table 2.1 are required for the solution of the strains and stresses at any step j in the temperature-load sequence.

2.1.3 SHIFT IN ORIGIN OF STRESS-STRAIN CURVES

Figure 2.1 illustrates the various stress-strain relationships which can arise during the sequence application or removal of temperature and load. Each element in the cross-section is considered to behave according to one of these conditions at any step in the temperature-load sequence. Analytically these conditions are described by the Ramberg-Osgood Eq: (2.1.22) and the logic table of Table 2.1 which allow for the stress and strain histories of the elements.

Curve (1) represents loading on the original stress-strain curve from the 0,0 origin. Assuming no change in material properties due to temperature change, (2) represents unloading of the element from an inelastic point on (1) on an elastic line which has the same slope (E_n) as the elastic portion of the original curve (1). Unloading of the element may continue until the element begins to load in the opposite direction. In this case, a new stress-strain curve (3) is followed which has a new origin defined by the offset strain e_{n_o} where e_{n_o} is found by Eq. (2.1.12). The elastic unloading lines (4) show unloading from two different points on the stress-strain curve(3). One elastic line is similar to elastic unloading line (2) and takes place from an inelastic point on the offset stress-strain curve (3). Continued unloading of the element may produce reloading of the element in the same direction as the original loading. This reloading is assumed to take place along a new stress-strain curve (6) which has a different origin than either (1) or (3). The other unloading line (4) begins at a point on (3) defined by $F_n = 0.80\ F_{y_n}$ which is the assumed limitation for reloading back to the original stress-strain curve (1). This defines a maximum permissible offset shown by Eq. (2.1.14) for the Ramberg-Osgood curve with m = 10. Continued application of strain on the element produces reloading on an extension of the original stress-strain curve (1) which is designated by (7).

2.1.4 SIGN CONVENTION

The use of the equations of Sec. 2.1.1 and 2.1.2 requires that definite sign conventions be established for compatibility throughout the temperature-load sequencing. The following table shows the terms requiring algebraic sign definition and the proper signs.

EQUATION TERM	ALGEBRAIC SIGN
T	(+) if temperature increases from datum (-) if temperature decreases from datum
x_n, y_n	(+) dimension toward the extreme fiber element having the highest positive value of (αT). In the case of symmetrical temperature distribution and geometry any convenient sign convention may be selected if the applied moment values have consistent signs.
F_n, F_m	(+) tension (-) compression
c, b	(+)
e_{ap}	(+) tension (-) compression
K_{ap_x}	(+) if the applied bending moment M_x puts compression on elements having $-y_n$ values. (-) if M_x puts compression on elements having $+y_n$ values.
K_{ap_y}	(+) if the applied bending moment M_y puts compression on elements having $-x_n$ values. (-) if M_y puts compression on elements having $+x_n$ values.

2.1.4 SIGN CONVENTION (continued)

EQUATION TERM	ALGEBRAIC SIGN
P	(+) Tension (-) compression
M_x	(+) if moment produces compression on elements having $-y_n$ values. (-) if moment produces compression on elements having $+y_n$ values.
M_y	(+) if moment produces compression on elements having $-x_n$ values. (-) if moment produces compression on elements having $+x_n$ values.
e_n, e_m	(+) tension (-) compression
e_{cr}, e_{cr_n}	(-)

2.1.5 STRESS EQUATIONS

Since all calculations for the cross-section are performed using the strain equation (2.1.1) it is necessary to obtain the stress F_n associated with the strain e_n from a stress-strain curve for each element corresponding to the temperature of the element. The stress-strain curve for each element in the cross-section is represented analytically by the non-dimensional Ramberg-Osgood equation as shown in Reference (1).

$$\frac{E_n e_n}{F_{y_n}} = \frac{F_n}{F_{y_n}} \left[1 + \frac{3}{7} \left(\frac{F_n}{F_{y_n}} \right)^{m-1} \right] \qquad (2.1.21)$$

where the slope of the elastic portion of the curve, the yield stress, and a shape factor define the stress-strain curve.

For the stresses at any step j in the temperature-load sequence corresponding to the strains of Equation (2.1.16) or (2.1.18) the Ramberg-Osgood Equation (2.1.21) is modified to

$$\frac{E_{n_j}}{F_{y_{n_j}}} \left(e_{n_j} + q_{n_j} \right) = \frac{F_{n_j}}{F_{y_{n_j}}} \left[1 + \frac{3}{7} r_{n_j} \left(\frac{F_{n_j}}{F_{y_{n_j}}} \right)^{m-1} \right] \qquad (2.1.22)$$

where

$$q_{n_j} = 0 \text{ or } \sum_{i=k}^{j-m} e_{n_{o_i}} \quad , \quad r_{n_j} = 0 \text{ or } 1$$

according to the stress and strain histories of the elements with the values of q_{n_j} and r_{n_j} defined by the logic table of Table 2.1. In the modified Ramberg-Osgood Equation (2.1.22) E_{n_j} is the elastic modulus of element n at step j, $F_{y_{n_j}}$ is the yield stress of element n at step j, and r_n is the shape factor which depends primarily upon the material.

LOGIC TABLE FOR SELECTION OF ELEMENT STRESS-STRAIN CURVE

TABLE 2.1

FOR ANY STEP IN THE TEMPERATURE-LOAD SEQUENCE

$r_{n_{j-1}}$	$\frac{F_{n_{j-1}}}{E_{n_{j-1}}}$	Δe_{n_j}	e_{n_j}	$s_{n_j} = e_{n_j} + \sum_{i=k}^{j-m} e_{no_i}$				$(e_{n_o})_{j-m} \geq .046 \left(\frac{F_{yn}}{E_n}\right)_{j-m}$	r_{n_j}	q_{n_j}
				$> s_{n_{j-m}}$	$= s_{n_{j-m}}$	$< s_{n_{j-m}}$	$\gtrless s_{n_{j-m}}$			
1	+	+	+				X	+,0	1	$\sum_{i=k}^{j-m} e_{no_i}$
0	+	+	+		X	X		+	0	0
0	+	+	+	X				+	0	$\sum_{i=k}^{j-m} e_{no_i}$
0	+	+	+				X	-,0	1	0
1	-	-	-				X	-,0	1	$\sum_{i=k}^{j-m} e_{no_i}$
0	-	-	-	X	X			-	0	0
0	-	-	-			X		-	0	$\sum_{i=k}^{j-m} e_{no_i}$
0	-	-	-				X	+,0	1	0
1,0	+	-	+				X	+,0	0	0
1,0	-	+	-				X	+,0	0	0
1,0	+	-	-				X	+,0	0	0
1,0	+	-	-	X	X			-	0	0
1,0	+	-	-			X		-	0	$\sum_{i=k}^{j-m} e_{no_i}$
1,0	-	+	+				X	-,0	1	0
1,0	-	+	+		X	X		+	0	0
1,0	-	+	+	X				+	0	$\sum_{i=k}^{j-m} e_{no_i}$
1	+	+	+				X	-	1	0
1	-	-	-				X	+	1	0

2.1.6 BUCKLING AND CRIPPLING LOADS

For stresses below the local buckling stresses of the elements of the structure, the effective area coefficients as defined by C_n in the iteration equations of Sec. 2.1.7, are taken as unity. However, after some elements buckle, the stress and strain distribution on the elements change due to the change in length of the buckled element from the deflection. Since some part of the buckled element (one or more edges) does not deflect, the strain in this undeflected portion of the element may be taken as the reference strain for the element and for the strain to be associated with the strains of the other elements.

Now the buckling strain of the element n can be approximated by:

$$e_{crn} = K_{crn} \left(\frac{t_n}{b_n}\right)^2 \qquad (2.1.23)$$

where the buckling curve is taken to be the same as the stress-strain curve (see Figure 6 - 5 in reference 1). The temperature of the element is assumed to be uniform. In most cases, this will be approximately true. If not, an average temperature of the element can be used. Define the reference strain for the element after buckling by:

$$e_n = K_n \left(\frac{t_n}{b_{ne}}\right)^2 \qquad (2.1.24)$$

where b_{ne} is an effective width, K_n depends on the restraints after buckling of the element, and e_n is given by Eq. 2.1.24 with local bending of the element neglected but with e_p including the area change effect.

From Eqs. (2.1.23) and (2.1.24)

$$\frac{b_{ne}}{b_n} = \left(\frac{e_{crn}}{e_n} \quad \frac{K_n}{K_{crn}}\right)^{1/2} = C_n \qquad (2.1.25)$$

and

$$e_{ap} = \frac{\sum_n F_n A_n C_n}{\sum_n E_n A_n}$$

$$C_n = 1, \; e_n \leq e_{crn} \qquad (2.1.26)$$

$$C_n = \left(\frac{e_{cm}}{e_n} \cdot \frac{K_n}{K_{cm}}\right)^{1/2} \quad , e_n \geq e_{crn} \qquad (2.1.26)$$

Note that e_{ap} is based on the original areas.

Consider Eq. (2.1.26) for a single element so that:

$$e_{ap} = \frac{F}{E}\sqrt{\frac{e_{cr}}{e}} \sqrt{\frac{K}{K_{cr}}} \quad ; e \geq e_{cr} \qquad (2.1.27)$$

or

$$\frac{E\ e_{ap}}{F_{cy}} = \frac{F}{F_{cy}} \sqrt{\frac{E\ e_{cr}/F_{cy}}{E\ e/F_{cy}}} \cdot \sqrt{\frac{K}{K_{cr}}} \qquad (2.1.28)$$

From Eq. (2.0.1) with $m = 10$,

$$\left(\frac{E\ e_{ap}}{F_{cy}}\right)^2 = \left(\frac{E\ e_{cr}}{F_{cy}}\right) \left(\frac{K}{K_{cr}}\right) \frac{F/F_{cy}}{1+\frac{3}{7}\left(\frac{F}{F_{cy}}\right)^9} \qquad (2.1.29)$$

The maximum value of e_{ap} is:

$$\frac{F_{cc}}{F_{cy}} = \left(\frac{E\ e_{ap}}{F_{cy}}\right)_{max.} = 0.88 \sqrt{\frac{E\ e_{cr}}{F_{cy}}} \sqrt{\frac{K}{K_{cr}}} \quad \text{at} \quad \frac{F}{F_{cy}} = 0.87$$

$$\frac{E\,e}{F_{cy}} = 0.98 \geq \frac{Ee_{cr}}{F_{cy}} = \frac{F}{F_{cy}} \quad \text{at} \quad \frac{E\,e}{F_{cy}} = \frac{E\,e_{cr}}{F_{cy}} \geq 0.98 \qquad (2.1.30)$$

Equation (2.1.30) indicates that if the buckling strain is less than the elastic yield strain F_{cy}/E then the maximum crippling stress occurs at the elastic yield strain while if the buckling strain is greater than the elastic yield strain the maximum stress occurs at the buckling strain.

For large e_{cr}, with the cut-off stresses in Figure 6-5 in Ref. (1) being applicable, Eq. (2.1.27) becomes:

$$e_{op} = \frac{F_{c.o.}}{E} \sqrt{\frac{e_{cr}}{e}} \quad e \geq e_{cr} \tag{2.1.31}$$

Thus, the crippling load can be determined provided Eq. (2.1.26) is used instead of Eq. (2.1.8) with C_n in Eq. (2.1.26) evaluated as described above. In machine calculations approximate results can be obtained by making $K_{cr}/K_{cm} = 1$ and cutting off the stress-strain curve at $F/F_{cy} = 1.0$.

Therefore, a good approximation of the effective area coefficient is:

$$C_n = 1 \qquad e_n \leq e_{cm}$$

$$C_n = \left(\frac{e_{cm}}{e_n}\right)^{1/2} \qquad e_n \geq e_{cm} \tag{2.1.32}$$

2.1.7 ITERATION EQUATIONS

The final strains and stresses at any step j in the temperature-load sequence are obtained by the iteration of the strain equations (2.1.16) where the inelastic effects represented by e_{p_j}, $K_{p_{x_j}}$ and $K_{p_{y_j}}$ are determined by axial load and bending moment equilibrium on the cross section. At any temperature or load step j the strains are calculated by Eq. (2.1.16) or Eq. (2.1.18) with e_{p_j}, $K_{p_{x_j}}$, and $K_{p_{y_j}}$ taken as zero for a first approximation. These strains are used to obtain the element stresses from Eq. (2.1.22) and the logic table of Table 2.1. If inelastic effects are present, these stresses will give values of P_r, M_{x_r}, and M_{y_r} in Eq. (2.1.11) different from the values of $\sum_i P_i$, $\sum_i M_{x_i}$, and $\sum_i M_{y_i}$ used in Eq. (2.1.34).

The inelastic effects for successive approximations are defined by the following equilibrium iteration equations at any step j in the temperature-load sequence. The axial load and bending moment equilibrium iteration equations are shown below for any step r in the iteration.

$$\begin{aligned}
\left(e_{p_j}\right)_r &= \left(e_{p_j}\right)_{r-1} - \left(e_{ap_j}\right)_{r-1} + \sum_i e_{ap_i} \\
\left(K_{px_j}\right)_r &= \left(K_{px_j}\right)_{r-1} - \left(K_{ap_{x_j}}\right)_{r-1} + \sum_i K_{ap_{x_i}} \\
\left(K_{py_j}\right)_r &= \left(K_{py_j}\right)_{r-1} - \left(K_{ap_{y_j}}\right)_{r-1} + \sum_i K_{ap_{y_i}}
\end{aligned} \tag{2.1.33}$$

where the extemal applied loads are represented by:

$$\sum_i e_{ap_i} = \frac{\sum_i P_i}{\left(\sum_n E_n A_n\right)_i}$$

$$\sum_i' K_{ap_{x_i}} = c_j \left[\frac{\sum_i M_{x_i} \left(\sum_n E_n A_n x_n^2\right)_i - \sum_i M_{y_i} \left(\sum_n E_n A_n x_n y_n\right)_i}{\left(\sum_n E_n A_n y_n^2\right)_i \left(\sum_n E_n A_n x_n^2\right)_i - \left(\sum_n E_n A_n x_n y_n\right)_i^2} \right] \tag{2.1.34}$$

$$\sum_i K_{op_{y_i}} = b_i \left[\frac{\sum M_{y_i} \left(\sum_n E_n A_n y_n^2 \right)_i - \sum M_{x_i} \left(\sum_n E_n A_n x_n y_n \right)_i}{\left(\sum_n E_n A_n y_n^2 \right)_i \left(\sum_n E_n A_n x_n^2 \right)_i - \left(\sum_n E_n A_n x_n y_n \right)_i^2} \right] \qquad (2.1.34)$$

The internal axial loads and bending moments for equilibrium of the cross-section are calculated at each iteration step r by the following equations:

$$\left(e_{op_i} \right)_{r-1} = \frac{\left(\sum_n F_{n_{r-1}} A_n C_n \right)_i}{\left(\sum_n E_n A_n \right)_i}$$

$$\left(K_{op_{x_i}} \right)_{r-1} = c_i \left[\frac{\left(\sum_n F_{nr-1} A_n C_n y_n \right)_i \left(\sum_n E_n A_n x_n^2 \right)_i}{\left(\sum_n E_n A_n y_n^2 \right)_i \left(\sum_n E_n A_n x_n^2 \right)_i - \left(\sum_n E_n A_n x_n y \right)_i^2} \right.$$

$$\left. \frac{- \left(\sum_n F_{n_{r-1}} A_n C_n x_n \right)_i \left(\sum_n E_n A_n x_n y_n \right)_i}{\left(\sum_n E_n A_n y_n^2 \right)_i \left(\sum_n E_n A_n x_n^2 \right)_i - \left(\sum_n E_n A_n x_n y_n \right)_i^2} \right] \qquad (2.1.35)$$

$$\left(K_{op_{y_i}} \right)_{r-1} = b_i \left[\frac{\left(\sum_n F_{n_{r-1}} A_n C_n x_n \right)_i \left(\sum_n E_n A_n y_n^2 \right)_i}{\left(\sum_n E_n A_n y_n^2 \right)_i \left(\sum_n E_n A_n x_n^2 \right)_i \left(\sum_n E_n A_n x_n y_n \right)_i^2} \right.$$

$$\left. \frac{- \left(\sum_n F_{n_{r-1}} A_n C_n y_n \right)_i \left(\sum_n E_n A_n x_n y_n \right)_i}{\left(\sum_n E_n A_n y_n^2 \right)_i \left(\sum_n E_n A_n x_n^2 \right)_i \left(\sum_n E_n A_n x_n y_n \right)_i^2} \right]$$

The iteration continues until the successive approximations of Eq. (2.1.33) produce:

$$e_{p_i} = \left(e_{p_i}\right)_r = \left(e_{p_i}\right)_{r-1}, \quad K_{px_i} = \left(K_{px_i}\right)_{r-1}, \text{ and}$$
$$K_{py_i} = \left(K_{py_i}\right)_r = \left(K_{py_i}\right)_{r-1} \text{ within a specified tolerance.}$$

A practical range of tolerances has been established as:

$$\left(e_{p_i}\right)_r - \left(e_{p_i}\right)_{r-1} = \pm 0.00003 \text{ to } \pm 0.00006$$
$$\left(K_{px_i}\right)_r - \left(K_{px_i}\right)_{r-1} = \pm 0.00003 \text{ to } \pm 0.00006$$
$$\left(K_{py_i}\right)_r - \left(K_{px_i}\right)_{r-1} = \pm 0.00003 \text{ to } \pm 0.00006$$

2.1.8 COLUMN PROCEDURES

For a structural cross-section which contains column elements, it is first necessary to define the load-deformation curve of the column element if a satisfactory representation is to be made as described in Sec. 2.1.9. The Ramberg-Osgood stress-strain curve (2.1.21) adequately describes many elements in the cross-section except those subject to either column or local instability. The load-deformation characteristics of members with local instability are defined by the methods of Sec. 2.1.6 where the Ramberg-Osgood stress-strain curve and an effective area which depends upon the critical buckling strain of the element define the load-deformation characteristics. The column, however, may have an unsymmetrical temperature distribution through the cross-section or a secondary bending moment may be acting on the column element thus producing deflections normal to the neutral plane of the column. An axial load acting on the column element will affect these deflections by producing a bending moment due to the deflections. If symmetrical bending only is considered, the net bending moment strain consists of two parts, one due to applied secondary bending moments and one due to deflection.

$$K_{a_x} = K_{a_{px}} + K_{w_x} \tag{2.1.36}$$

The deflection moment strain may be described in terms of e_{ap} and the deflection W as follows:

$$K_{wx} = \frac{W}{c} e_{a_p} \frac{\sum_M E_M A_M}{\sum_M E_M A_M \left(\frac{y_M}{c}\right)^2} = \frac{W}{c} e_{a_p} \left(\frac{c}{\rho}\right)^2 \tag{2.1.37}$$

In many problems the applied secondary bending moment may be related to the applied axial load as

$$M_{ap_x} = p\, P_{ap} \tag{2.1.38}$$

In this case Eq. (2.1.37) may also be written

$$\frac{K_{ax}}{e_{ap}} = \frac{W + P}{c} \left(\frac{c}{\rho}\right)^2 \tag{2.1.39}$$

If z is the variable along the length of the structure, then W depends on z and the end conditions, while p may depend on z if the applied moment is variable. For simple beams, Reference (2) gives:

$$\frac{d^2W}{dz^2} = \frac{M}{EI} = \frac{K}{c} \qquad (2.1.40)$$

The net rotational strain of any cross-section through the column may be written

$$K_x = K_{i_x} + K_{w_x} + K_{ap_x} + (K_{T_x})_{i-1} + K_{p_x} + \sum_{j=1}^{i-1} K_{px_i} \qquad (2.1.41)$$

for the temperature-load sequence + T, + P where K_i represents the initial deflection or eccentricity of the load. In Eq. (2.1.41) K_{p_x} is a function of z depending upon the amount of inelastic action at the various cross-sections throughout the span or length of the column. Eq. (2.1.40) can be written

$$\frac{d^2K_{w_x}}{dz^2} = \left(\frac{e_{a_p}}{\rho^2}\right) K_x \qquad (2.1.42)$$

where, with K as a table of values for selected values of z, then K_{w_x} can be obtained from Eq. (2.1.42) by an area-moment numerical integration or by a double summation.

If K_{ap_x}, K_{T_x} and K_{i_x} are constant along the beam, then K_{p_x} will be constant except for the effect of W. Assume K_{p_x} is constant along the span so that Eq. (2.1.42) can be integrated to give

$$K_{w_x} = (K_{i_x} + K_{a_{p_x}} + (K_{T_x})_{j-1} + \sum K_{p_{x_i}} + K_{p_x}) f(z)$$

$$f(z) = \frac{\cos q\,(1 - \frac{2z}{L}) - \cos q}{\cos q} \quad \text{(compression)} \qquad (2.1.43)$$

$$= \frac{\cosh q\,(1 - \frac{2z}{L}) - \cosh q}{\cosh q} \quad \text{(tension)}$$

where

$$q^2 = -\frac{e_{a_p} L^2}{4\rho^2} \tag{2.1.44}$$

for a simply supported beam-column

$$\text{let} \quad e_{cr} = -\frac{\pi^2 \rho^2}{L^2}, \quad q^2 = \frac{\pi^2}{4} \cdot \left(\frac{e_{a_p}}{e_{cr}}\right) \tag{2.1.45}$$

so that the maximum deflection in Eq.(2.1.43) at $z = \frac{L}{2}$ is

$$(K_{w_x})_{max.} = \left(K_{i_x} + K_{a_{p_x}} + (K_{T_x})_{i-1} + \sum_{i=1}^{i-1} K_{p_{x_i}} + K_{p_x}\right) f_{max.}\left(\frac{e_{ap}}{e_{cr}}\right) \tag{2.1.46}$$

Eq.(2.1.41) may be written

$$K_x = \left[1 + f_{max.}\left(\frac{e_{ap}}{e_{cr}}\right)\right](K_{ix} + K_{ap_x} + (K_{T_x})_{i-1} + \sum_{i=1}^{i-1} K_{p_x} + K_{p_x}) \tag{2.1.47}$$

The temperature-load sequence of primary importance for defining the column load-deformation curve is apply temperature (+T), then apply load (+P). For any given temperature distribution through the column cross-section a range of loads is applied to establish the shape and the peak of the column load-deformation curve. This curve provides the data for the column representation methods of Section 2.1.9.

The strain equation for the temperature application step for the column is essentially that shown by Eq. (2.1.16). For the applied load step in the temperature-load sequence the element strains are found by the following equation

$$e_{M_i} = \frac{F_{M_{i-1}}}{E_{M_{i-1}}} + (e_{a_p} + e_p)_i + (K_{a_{p_x}} + K_{w_x} + K_{p_x})_i \frac{y_M}{c} \tag{2.1.48}$$

where

$$K_{wx_i} = \left(K_{in_i} + K_{T_{x_{i-1}}} + K_{ap_{x_i}} + K_{p_{x_i}} + \sum_{i=1}^{i-1} K_{p_{x_i}}\right) C_{l_x}$$

and

$$C_{l_x} = \frac{1 - \cos \pi/2 \left(\frac{e_{ap}}{e_{cr}}\right)}{\cos \pi/2 \left(e_{ap}/e_{cr}\right)}$$

when a compression load is acting.

e_{pj} and K_{px_i} must be determined by an iterative procedure to satisfy the following equilibrium conditions.

$$e_{ap_i} = \frac{\sum_M F_{M_i} A_M}{\sum_M E_M A_M} \qquad (2.1.49)$$

$$(K_{apx_i} + K_{w_{x_i}}) = \frac{\sum_M F_{M_i} A_M \left(\frac{y_M}{c}\right)}{\sum_M E_M A_M \left(\frac{y_M}{c}\right)^2}$$

In Eq. (2.1.47) the stresses F_{M_i} are determined by the procedures of Section 2.1.5. The iteration equations for the equilibrium condition are:

$$(e_{pj})_r = (e_{pj})_{r-1} + e_{apj} - \frac{\sum_M (F_{Mj})_{r-1} A_M}{\sum_M E_M A_M}$$

$$(K_{pxj})_r = (K_{pxj})_{r-1} \pm \left[K_{ap_{xj}} + (K_{wxj})_{r-1} - \frac{\sum_M (F_{Mj})_{r-1} A_M \left(\frac{y_M}{c}\right)}{\sum_M E_M A_M \left(\frac{y_M}{c}\right)^2}\right] \qquad (2.1.50)$$

Two sets of answers are provided at convergence of the iteration equations (2.1.50) with the second set defining a post-buckling point on the column load-deformation curve.

The column procedures presented in this section are based on constant moments and a maximum value of K_{wxj}. Further column studies have shown this approximation to be quite accurate for practical design use. Comparisons of column load-deformation curves using the approximate procedures of this section and by integrating the inelastic effects along the length of the column show good correlation between the two methods with the approximate procedures being slightly conservative.

2.1.9 COLUMN REPRESENTATION

Since many structures contain column members in the form of stringers, truss members, etc. it is most convenient to consider the column as a single element in the cross-section when defining the allowable load-deformation curve using the general allowable stress procedures described in Sections 2.1.1 through 2.1.7. The load-deformation characteristics of the column may not, however, be defined directly by a simple stress-strain relationship such as the Ramberg-Osgood representation of material property stress-strain curves. The post-buckling portion of the column curve as shown in Section 2.1.8 is defined by bending moment equilibrium where the applied axial load must be less than the critical peak buckling load. The column, however, is analagous to the plate buckling problem since the critical buckling strains of both are based on the Euler equation. Therefore, a good approximation of the column load-deformation curve can be obtained by the use of the effective area coefficient for any column element n as follows:

$$C_n = \left(e_{cr_n}/e_n\right)^{1/2} \qquad (2.1.51)$$

as described in Sec. 2.1.6 of this report and Sec. 7-5 of Ref. (1). This allows an equivalent Ramberg-Osgood stress-strain curve defined by Eq. (2.0.1) to be used in the calculations for the particular cross section.

The equivalent Ramberg-Osgood stress-strain curve for the column element must be obtained for the particular temperature distribution, geometry, and material variations in the column cross-section for the unrestrained condition. From this stress-strain curve the slope representing the equivalent modulus of elasticity, the equivalent yield stress defined by $E_{sec} = 0.7E$, and the Ramberg-Osgood stress-strain shape parameter m are obtained. These values are used in the structural cross-section to define the equivalent Ramberg-Osgood stress-strain curve represented by Eq. (2.0.1).

For the column element in the cross-section analysis a value of e_{cr_n} must be determined to define the effective area coefficient given by Eq. (2.1.32). First, the column load-deformation curve is computed by the procedures of Sec. 2.1.8 including the effects of local buckling. From the column load-deformation curves the two significant values required to define the equivalent critical buckling strain are the peak stress defined by (F_{ap}) max, and the foreshortening strain at which the peak stress occurs defined by e_{max}.

The equivalent ecr_n for the column element is defined by the following relationships. For load equilibrium on the column cross-section at the strain associated with the peak stress:

$$(F_c)_e C_n \Sigma A_M = (e_{ap})_{max.} \Sigma E_M A_M \qquad (2.1.52)$$

where the subscript M denotes element number in the column cross-section, and n is column element n in the composite structure. In terms of the effective stress on the total cross-section area of the column

$$(F_c)_e C_n = (e_{ap})_{max.} \frac{\Sigma E_M A_M}{\Sigma A_M} \qquad (2.1.53)$$

Substituting Eq. (2.1.49) into Eq. (2.1.51)

$$(F_c)_e \frac{(e_{cr_n})^{1/2}}{(e_{max.})^{1/2}} = (e_{ap})_{max.} \frac{\Sigma E_M A_M}{\Sigma A_M} \qquad (2.1.54)$$

Solving for e_{cr_n}

$$(e_{cr_n})^{1/2} = (e_{ap})_{max.} (e_{max.})^{1/2} (E_c)_e \frac{\Sigma E_M A_M}{\Sigma A_M} \qquad (2.1.55)$$

$$e_{cr_n} = (e_{max.}) \left[\frac{(e_{ap})_{max} \Sigma E_M A_M}{(F_c)_e \Sigma A_M}\right]^2 = (e_{max.}) \left[\frac{(F_{ap})_{max.}}{(F_c)_e}\right]$$

where e_{max} is the foreshortening strain associated with the peak stress of the column load-deformation curve and $(F_c)_e$ is the stress associated with $e_{max.}$ as determined from the equivalent Ramberg-Osgood compression stress-strain curve.

Since each element in the column cross-section may have a different area, modulus of elasticity, yield stress, temperature, and coefficient of thermal expansion, an equivalent value for the temperature expansion strain is required for the solution of more complex structures which treat the column as a single structural element. This temperature expansion strain may be expressed as:

$$(\alpha T)_{equiv.} = e_t = \frac{\Sigma E_M A_M (\alpha T)_M}{\Sigma E_M A_M} \qquad (2.1.56)$$

where the subscript M denotes element number in the column cross-section. Input data for the Allowable Stress IBM Program (E2119) requires separate input values for α and T for each element. Therefore, when using this program for cross-sections which contain columns as a single element it may be necessary to compute an equivalent temperature change from datum. For the column as a single element in a cross-section select a reference value of α_R and compute the equivalent temperature change by

$$(T)_{equiv.} = \frac{E_M A_M (\alpha T)_M}{\alpha_R \Sigma E_M A_M} \qquad (2.F.57)$$

$(T)_{equiv.}$ and α_R are the input values for the column element.

The curves on page 40 demonstrate the use of the effective area approximation and provide justification for the use of this approximation.

FIGURE 2.2

COLUMN EFFECTIVE AREA APPROXIMATION

•	C_n	F_c	$F_{equiv.}$
.0025	.902	20,000	18,040
.003	.823	23,500	19,370
.004	.712	29,250	20,800
.005	.637	32,500	20,700
.006	.582	34,100	19,850
.008	.504	36,900	18,600
.010	.451	38,600	17,400
.014	.381	40,750	15,530

$$(e_{cr})_e = \left[e_{max}\frac{(F_{op})_{max}}{(F_c)_e}\right]^2$$

$$= .004\left(\frac{20500}{28750}\right)^2$$

$$= -.002033$$

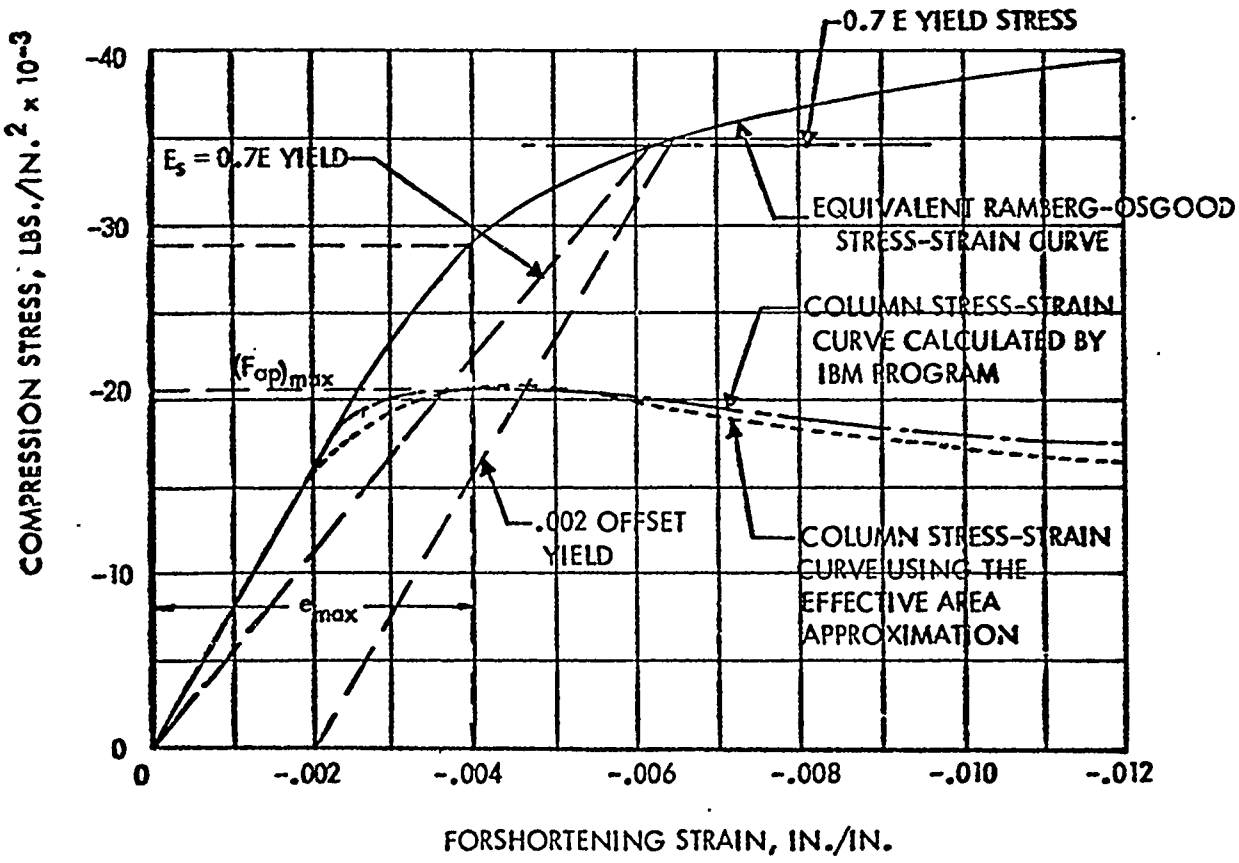

2.1.10 FAILURE CRITERIA

In order to specify thermal limits it is necessary to derive suitable allowable stresses for individual elements in the complex structure. Standard allowables, such as for crippling, buckling, and compression yield, are relatively simple to describe for variations in temperature. Other allowables, such as honeycomb general buckling are more difficult to acquire.

In determining the critical honeycomb panels to be analyzed, six possible modes of failure must be considered. The first and simplest mode is a tension failure of the tension face due to bending in the panel. Another failure which can be produced by bending is core shear for which the allowable may be expressed as:

$$q^{x}_{core} = (t_c/S)^2 \left(F_{su} K_s E_c\right)^{1/2} .2h \qquad (2.1.58)$$

The loads inducing failure in this mode are not appreciably changed by the thermal loading and therefore is not considered as an important failure mode for this study. A third failure mode in bending which can be considered is core crushing, the allowable for which is expressed as:

$$F_c' = (C_1 F_{cy})^{2/3} (K_c E_c)^{1/3} 2(t_c/S)^{5/3} = \frac{(2t_{F1}) F_c F_b}{hE_s} \qquad (2.1.59)$$

This mode of failure has been found not to occur in practical design cases and is therefore also not considered in the present study. A fourth mode of failure which can occur in either bending or compression panels is wrinkling of the facing for which the allowable is:

$$F_{cw} = 0.5 \left[0.055 (t_c/S)^2 G_c E_c (E_s + 3E_T)\right]^{1/3} \qquad (2.1.60)$$

The fifth failure mode which may occur in bending as well as compression is called intercell-buckling which has an allowable expressed as:

$$F_{ci} = 0.9 E_R (t_{F1}/S)^{3/2} \qquad (2.1.61)$$

The honeycomb allowable Equations 2.1.60 and 2.1.61 can be computed independent of the final structural arrangement in a general form of e_{ci} or F_{ci} Vs t_F/S and e_{ca} or F_{cw} VS t_c/S. Such a plot is then needed only for each material used. Therefore, to reduce the computing time of the "Allowable Stress Program" this data is entered as a table rather than being

computed each time through the program. Furthermore, it was found that by plotting e_{ci} and e_{cw} against the respective parameters there was no significant change with temperature within the realistic range of the allowable strains. Thus, if the calculation of data is done for a medium range temperature the data will be satisfactory for the full temperature range (see Fig. 2.3 and 2.4). The normal allowable strain range for the 2024-T4 material plotted in Fig. 2.3 and 2.4 is from .003 to .0065. Further discussion of the I&M 709 computer program for producing this data can be found in appendix D of this report.

The final failure mode can occur only in compression of the panel and is referred to as general-buckling for which the allowable is expressed as:

$$F_{ccR} = \frac{P_M \pi^2 t_{F_1} t_{F_2} E_{s_1} E_{s_2} \left(C + \frac{t_{F_1} + t_{F_2}}{2} \right)^2}{a^2 (1 - \upsilon^2) (t_{F_1} E_{s_1} + t_{F_2} E_{s_2}) (t_{F_1} + t_{F_2})} \qquad (2.1.62)$$

$$P_M = \frac{K + \left(\frac{Vx}{C4} + Vy \right) F}{1 + L + \frac{Vx\, Vy}{C4} F}$$

$$K = C_1 + 2C_2 + C_3$$

$$L = \left(C_1 + \frac{1 - \mu}{2} C_2 \right) \frac{Vx}{C4} + \left(C_3 + \frac{1 - \mu}{2} C_2 \right) Vy$$

$$F = C_1 C_3 - C_2^2 + \frac{1 - \mu}{2} C_2 K$$

$$Vx = \frac{\pi^2 C t_{F_1} t_{F_2} E_1 E_2}{(t_{F_1} E_1 + t_{F_2} E_2) a^2 G'_{cx} (1 - \mu^2)}$$

$$Vy = \frac{\pi^2 C t_{F_1} t_{F_2} E_1 E_2}{(t_{F_1} E_1 + t_{F_2} E_2) a^2 G'_{cy} (1 - \mu^2)}$$

G'_{cx} = effective shear modulus of core in x direction

G'_{cy} = effective shear modulus of core in y direction

The constants C_1, C_2, C_3, C_4 are dependent upon the edge fixity conditions of the panel. A listing of these values follows:

Edges simply supported

$$C_1 = C_4 = \frac{b^2}{n^2a^2} \qquad C_2 = 1 \qquad C_3 = \frac{n^2a^2}{b^2}$$

b = panel length

n = number of half waves

Loaded edge simply supported
Unloaded edge clamped

$$C_1 = 5.33\ \frac{b^2}{n^2a^2} \qquad C_2 = 1.33 \qquad C_3 = \frac{n^2a^2}{b^2} \qquad C_4 = 1.33\ \frac{b^2}{n^2a^2}$$

Loaded edge clamped
Unloaded edge simply supported

$$C_2 = 1 \qquad C_3 = \left(\frac{n^4 + 6n^2 + 1}{n^2 + 1}\right)\ \frac{a^2}{b^2}$$

For n = 1 $\quad C_1 = .75\ \frac{b^2}{a^2} \qquad C_4 = 3\ \frac{b^2}{a^2}$

For n > 1 $\quad C_1 = C_4 = \frac{1}{n^2 + 1}\ \frac{b^2}{a^2}$

All edges clamped

$$C_2 = 1.33 \qquad C_3 = \frac{(n^4 + bn^2 + 1)}{n^2 + 1}\ \frac{a^2}{b^2}$$

For n = 1 $\quad C_1 = 4C_4 = 4\ \frac{b^2}{a^2}$

For n > 1 $\quad C_1 = 4C_4 = \frac{5.33}{(n^2 + 1)}\ \frac{b^2}{a^2}$

These last three failure modes are the most important in the design of honeycomb panels and constitute the primary failure modes found in conventional honeycomb structures subjected to thermal stresses. These modes along with the tension mode make up the failure modes used in this study.

Unlike the allowables F_{ci} and F_{cw}, F_{ccR} must be computed within the allowable stress program. This computation takes place within subroutine HKM which is diagrammed in Appendix D.1 of this report. The Equation 2.1.62 has been substantiated by a test program presented in Appendix A and discussed in Section 4.0 of this report.

Equations (2.1.58) through (2.1.62) were substantiated by tests performed by the NAA Los Angeles Division (See Reference 3). A production full depth honeycomb component was tested and failed in the mode of face wrinkling, showed very good agreement between test data and the applicable allowable stress Equation (2.1.60) (Ref. 4, Figure D.5).

For tension elements in the structure the failure criteria is defined as a maximum strain or elongation of the material. Compression elements which buckle locally will reach a peak load causing further increases of load and/or moment to be taken by remaining members of the structure when some member will eventually reach the strain cut-off or the crippling cut-off defined by the following equation.

Crippling of compression elements is considered to occur if:

$$F_n C_n \geq F_{y_n} \qquad (2.1.63)$$

A tension ultimate stress cut-off is used on all Ramberg-Osgood stress-strain curves with a compression yield stress cut-off used on all Ramberg-Osgood stress-strain curves used to represent a column element.

FIGURE 2.3

ALLOWABLE INTER-CELLULAR BUCKLING STRAIN DIAGRAM
2024-T4 ALUMINUM ALLOY

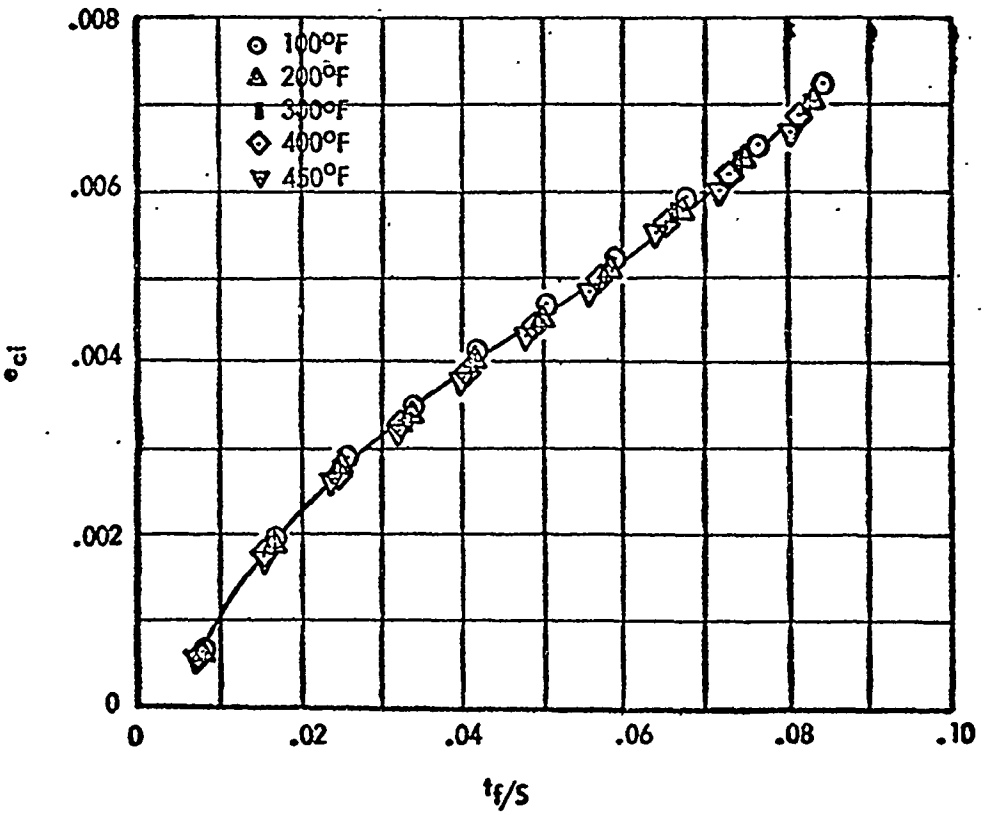

FIGURE 2.4

ALLOWABLE FACE WRINKLING STRAIN DIAGRAM
2024-T4 ALUMINUM ALLOY

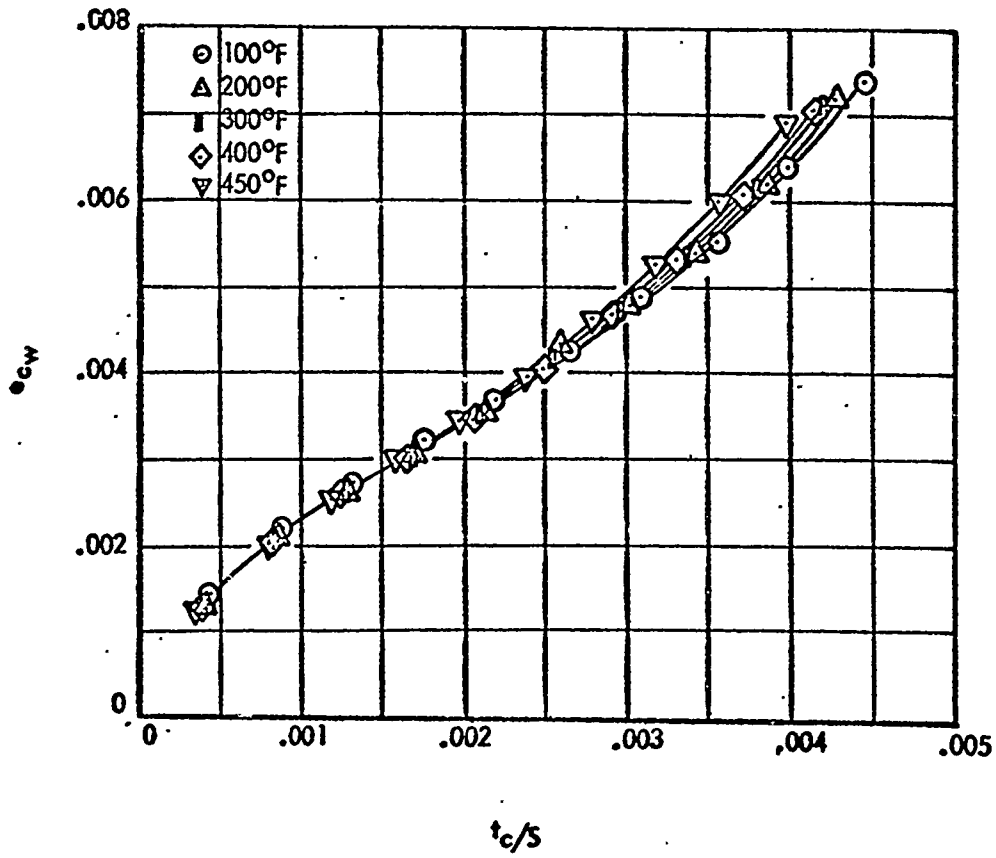

2.1.11 LOAD-DEFORMATION CURVES

The previous sections describe the procedures for obtaining the element strains and stresses at any particular step in the temperature-load sequence. Convergence of the iteration procedures of Section 2.1.7 produces the final values of e_{p_i}, K_{px_i}, and K_{py_i} at each step in the temperature-load sequence. At any step j, the total inelastic effects for all steps on any element n in the cross-section may be expressed by

$$ep_{s_n} = \Sigma_j \, e_{p_j} + (\Sigma_j \, K_{px_j}) \frac{y_n}{c} + (\Sigma_j \, K_{py_j}) \frac{x_n}{b} \qquad (2.1.64)$$

where ep_{s_n} represents the permanent set on each element of the cross-section if step j ends with the removal of all load and temperature and assuming that the residual stresses do not change due to creep at room temperature.

If the procedures of the previous sections are followed for given geometry, materials, temperature distribution, and temperature-load sequence for a range of values of applied axial loads and bending moments then an allowable load or moment vs. strain curve can be constructed. In this case, the primary bending moment (M_x) may be plotted against $F_{ap_m}/E_m + e_{ps_m}$. It is essential, however, that fixed ratios exist between P_j, M_{x_j}, and M_{y_j} if a single moment-strain curve is to be used to define the first instability failure, yield and ultimate load for the cross-section.

For a range of values of load and/or bending moment, the elastic strain term (F_{ap_m}/E_m) may be defined as follows:

$$F_{ap_m}/E_m = \Sigma_j \, e_{ap_j} + (\Sigma_j \, K_{ap_x}) \frac{y_m}{c} + (\Sigma_j \, K_{ap_{y_j}}) \frac{x_m}{b} \qquad (2.1.65)$$

where m designates the element with the maximum permanent set as defined by Eq. (2.1.64).

2.2 SAMPLE PROBLEM

To provide substantiation for the newly developed methods presented in this report a sample problem on the computer was made for comparison with tests performed during this study. Two comparisons are made in this section. The first comparison and computer run was made to predict the allowable load for the skin stringer columns found in the test horizontal stabilizer. The computer run was made with the column allowable program E2140 described in Appendix C.1. This column allowable was computed without the lateral bending effect discussed in Section 2.2.1. The lateral bending was not used in this case because of the test conditions would not produce the tension loads caused by buckling because of the lack of edge restraint (see Figure B.30). Also because of the end restraint conditions the column end fixity was a different value in this comparison problem than in the test horizontal stabilizer problem. The results of this computed column allowable and the test allowable can be found in Section 2.2.3.

The second comparison and computer run was made to predict the ultimate failure load for the typical horizontal stabilizer with an induced temperature gradient. Before making the actual computer run it was necessary to compute several groups of input data. The first group of data required was the honeycomb allowable strains against the parameters t_F/S and t_c/S as a function of temperature. This data was compiled through the use of the computer program E2128 described in Appendix C.2 of this report. This data is then used as a table input as described in Appendix D.1.3 for the final computer run.

The second group of data required is compiled through the use of computer program E2140 described in Appendix C.1. In addition to the straight axial load a laterally induced bending moment was also used as discussed in Section 2.2.1. This data was then used as element buckling coefficients for the input data such as described in Appendix D.1.3.

Another important part of the input data is the material properties E, F_{ty}, F_{t_n}, and the Ramberg-Osgood coefficient (m). The derivation of this data for the specific test horizontal stabilizer problem is discussed in detail in Section 2.2.2. Although tensile coupon tests were made in this case to insure greatest accuracy it was found that the use of Reference 5 would give very satisfactory results.

2.2.1 SKIN-STRINGER COMPRESSION ALLOWABLES INCLUDING THE EFFECTS OF INDUCED LATERAL BENDING

The allowable compression stresses (F_{cr}) or the critical buckling strains (e_{cr}) of skin-stringer column elements may not be accurately determined by the application of direct compression loads either analytically or experimentally since the compression load alone does not always represent the only load acting on the stringer. More representative allowables could be determined experimentally, however, by box beams with applied bending moments where the chordwise restraint to the skin panels and the effects of radius of curvature are present. Essentially, the major effect of the bending radius of curvature of the box beam is to force inward buckling of the skin panels between the stringers. This inward buckling on both sides of a stringer coupled with chordwise restraint of the skin panels produces chordwise tension stresses. Components of these stresses normal to the plane of the stringer produce bending moments on the stringer which are acting simultaneously with the applied compression loads. In many structures, these effects may be quite small but the induced bending moments in shallow depth stringers may produce substantial losses in allowable compression strength.

The skin-stringer panels in the typical test horizontal stabilizer represent the type of structure where the induced lateral bending due to skin panel buckling should be investigated. The following analysis is a conservative approximation to allow for the induced bending effects.

One typical skin-stringer panel is considered where $b_s = 3.73$ inches (between stringer $\mathcal{L}$ and $t_s = .042$ in. Temperature is uniform at 375°F. For the panel simply supported on all four edges, the critical buckling strain is

$$e_{cr} = K\left(\frac{t}{b}\right)^2 = 3.62\left(\frac{.042}{3.73}\right)^2 = .000459 \text{ in./in.}$$

Considering the center strip of the buckled plate to act as a column, the deflection may be approximated by

$$W_m = \frac{2\rho}{\sqrt{e_{cr}}}\sqrt{\frac{\Delta L}{L}}$$

where ρ is the radius of gyration of the strip element, e_{cr} is the buckling strain of the panel, and $(\Delta L/L)$ is the foreshortening of the panel after buckling. This foreshortening is taken as the difference between the strain at which the skin-stringer column peak occurs and the critical buckling strain. From Figure 2.5, the column peak occurs at .00365 in./in.

thus

$$\frac{\Delta L}{L} = .00365 - .000459 = .003191 \text{ in./in.}$$

The radius of gyration of the plate element is

$$\rho = \frac{t}{\sqrt{12}} = \frac{.042}{\sqrt{12}} = .01212 \text{ in.}$$

The maximum deflection at the center of the buckled plate is

$$W_m = \frac{2(.01212)}{\sqrt{.000459}} \sqrt{.003191} = .064 \text{ in.}$$

To determine the lateral load on the stringer, the skin panel is assumed to act as a membrane and an equivalent normal load is calculated which will produce the same maximum panel deflection as the buckling.

From Section 8-5 of Reference (1) the deflection of an element strip may be approximated as

$$W = \frac{px}{2N}(b - x)$$

or the maximum deflection at $x = \frac{b}{2}$ is

$$W_m = \frac{pb^2}{8N}$$

where $N = \left[\frac{p^2 b^2 h_s E}{24(1-\mu^2)}\right]^{1/3}$

Substituting and solving for the normal surface pressure, p

$$p^{1/3} = \frac{8W_m\left[\frac{b^2 h_s E}{24(1-\mu^2)}\right]^{1/3}}{b^2} = \frac{8(.064)\left[\frac{(3.48)^2(.042)(9.5\times 10^6)}{24(1-.09)}\right]^{1/3}}{(3.48)^2}$$

$$p^{1/3} = 2.58 \quad , \quad p = 17.15 \text{ psi}$$

A conservative normal load distribution along the length of the stringer is
w = 17.15 (3.48) = 59.7 lbs./in.

The maximum bending moment at the center of the column span is

$$M = \frac{w L^2}{8} = \frac{59.7 (8.17)^2}{8} = 497.5 \text{ in.} - \text{lbs.}$$

An applied bending moment rotational strain on the column cross-section is calculated by

$$K_{ap_x} = \frac{M_c}{(EI)_x} = \frac{497.5 (.334)}{73700} = .00226 \text{ in/in. at extreme fiber.}$$

The values of e_{cr_n} for the column elements are determined by the procedures of Section 2.1.9 with some typical results shown in Figure 2.5 for the critical column element. From the column load-deformation curves e_{cr_n} is calculated in the table below for each stringer in the compression cover.

FIGURE 2.5

TYPICAL SKIN-STRINGER COLUMN ALLOWABLE CURVES

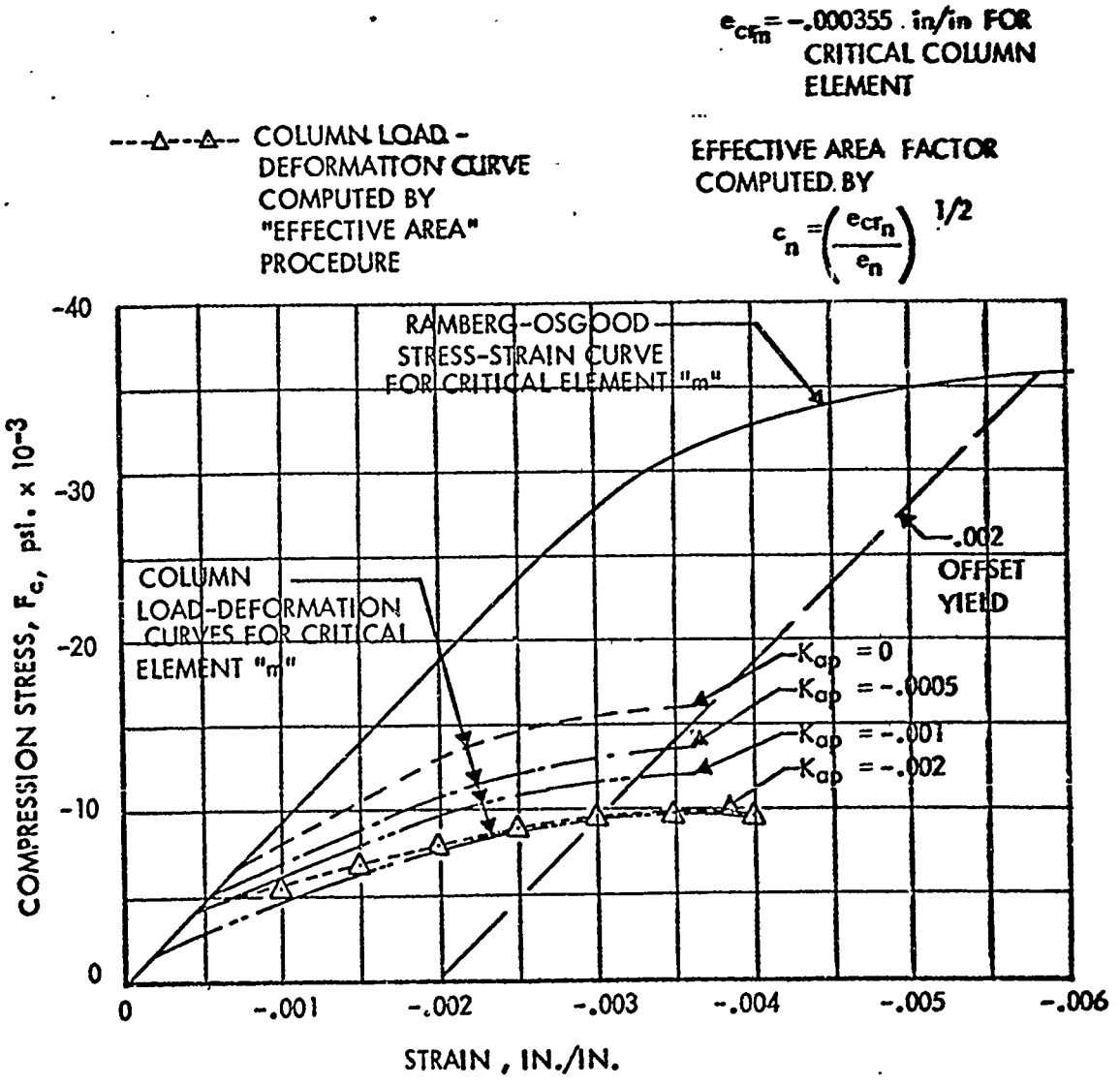

TABLE 2.2

Effective Column e_{cr} Values Including the Effects of Induced Lateral Bending

Column	T, °F.	(F_{ap}) max.	Lateral Bending Factor	(F_{ap}) max. corrected	$e_{max.}$	E/F_y	$\frac{e_{max.}E}{F_y}$	F/F_y	$(F_c)_e$
1.	340	16350	.625	10220	.0037	245.5	.908	.862	35150
2.	360	16160		10100		253.5	.938	.878	33600
3.	375	15930		9970		260.5	.964	.89	32700
4.	390	15720		9840		268	.992	.902	31750
5.	375	15930		9970		260.5	.964	.89	32700
6.	360	16160		10100		253.5	.938	.878	33600
7.	345	16270	.625	10180	.0037	246.5	.912	.864	34200

$$e_{cr} = .0037 \left(\frac{10220}{35150}\right)^2 = .000313$$

$$e_{cr} = .0037 \left(\frac{10100}{33600}\right)^2 = .000334 = e_{cr_7}$$

$$e_{cr} = .0037 \left(\frac{9970}{32700}\right)^2 = .000344 = e_{cr_6}$$

$$e_{cr} = .0037 \left(\frac{9840}{31750}\right)^2 = .000355$$

$$e_{cr} = .0037 \left(\frac{10180}{34200}\right)^2 = .000328$$

2.2.2 MATERIAL PROPERTIES

The tension stress-strain curves used in the analysis and represented by the Ramberg-Osgood equation

$$\frac{eE}{F_y} = \frac{F}{F_y}\left[1 + \frac{3}{7}\left(\frac{F}{F_y}\right)^{14}\right]$$

are shown in Figure 2.6. The curve of Figure 2.7 shows the data from two tensile coupons which was used to determine the Ramberg-Osgood shape parameter, m. The stress-strain curves shown in Figure 2.7 were obtained from standard NAA tensile coupons taken from the test stabilizer between H.S. Sta. 167 and H.S. Sta. 177.

The material properties obtained from these coupons showed a distinct permanent loss due to the elevated temperature curing of the high temperature strain gages in the test area (H.S. Sta. 187 to H.S. Sta. 197). The entire horizontal stabilizer was placed in an oven and heated to 350°F for two hours and then to 450°F for one-half hour for the curing process. The tensile coupons were taken from the stabilizer skins after the failing load test was completed. Therefore, the coupons and the test area had the same temperature history prior to the beginning of the tests. The primary cause of the permanent loss of material properties was the temperature of 450°F for one-half hour. Data obtained from short time elevated temperature tensile coupon tests is plotted in Figure 2.8 and used as material property input data for the analytical portion of the program. The room temperature values of Ft_y and Ft_u on Figure 2.9 are specifically noted for comparison with the expected recovery values after exposure to the elevated temperature environment required for strain gage curing. Using data from Reference (5) and Figure 3.2.7.1.1 the expected room temperature recovery points are also plotted. From Figure 2.9 the room temperature recovery factors are found to be

$$Ft_u/Ft_{uR.T.} = 0.785 \quad \text{and} \quad Ft_y/Ft_{yR.T.} = 0.722$$

The room temperature material allowables are taken as $Ft_u = 78000$ psi. and $Ft_y = 68000$ psi. from Table 3.2.7.0 (b) of Reference (5). For the temperature time history of the stabilizer the room temperature material allowables may be expected to recover to $Ft_u = 0.785\ (78000) = 61200$ psi. and $Ft_y = 0.722\ (68000) = 49100$ psi. Although good correlation is obtained from room temperature recovery properties it is impossible to predict what the expected recovery values should be at temperatures between room temperature and the maximum soaking temperature due to a lack of test data. Since it appears that the recovery problem can be quite serious it would also indicate that a worthwhile program could be established to determine recovery properties at temperatures above room temperature for

the aluminum alloys used most frequently. Studies conducted by the Columbus Division of NAA indicate the material recovery problem to be most serious in aluminum alloys.

FIGURE 2.6

TENSION STRESS-STRAIN CURVES
RECOVERY CURVES AFTER EXPOSURE TO 350° F FOR 2 HR.
AND 450° F FOR 1/2 HR.

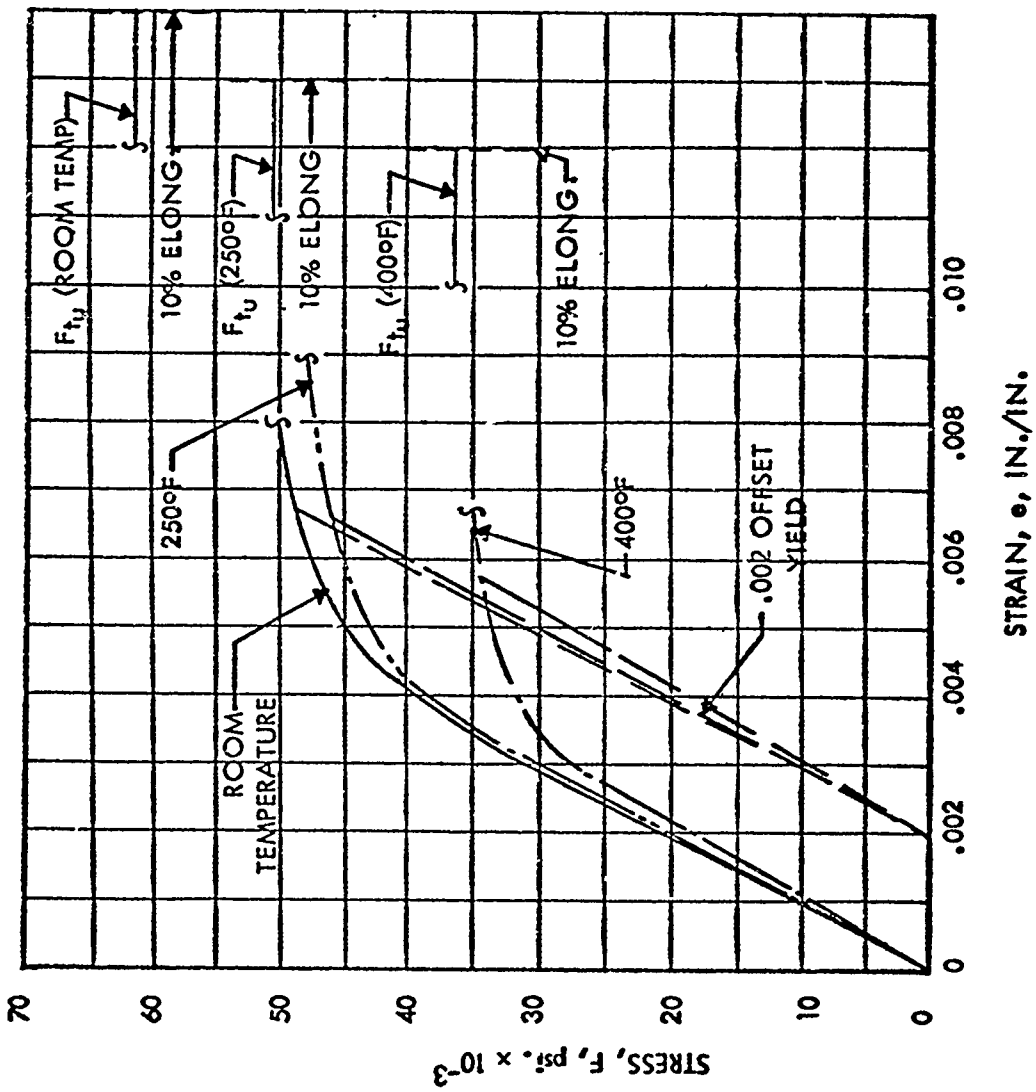

FIGURE 2.7

ROOM TEMPERATURE TENSILE COUPON STRESS-STRAIN CURVES AND EQUIVALENT RAMBERG-OSGOOD EQUATION

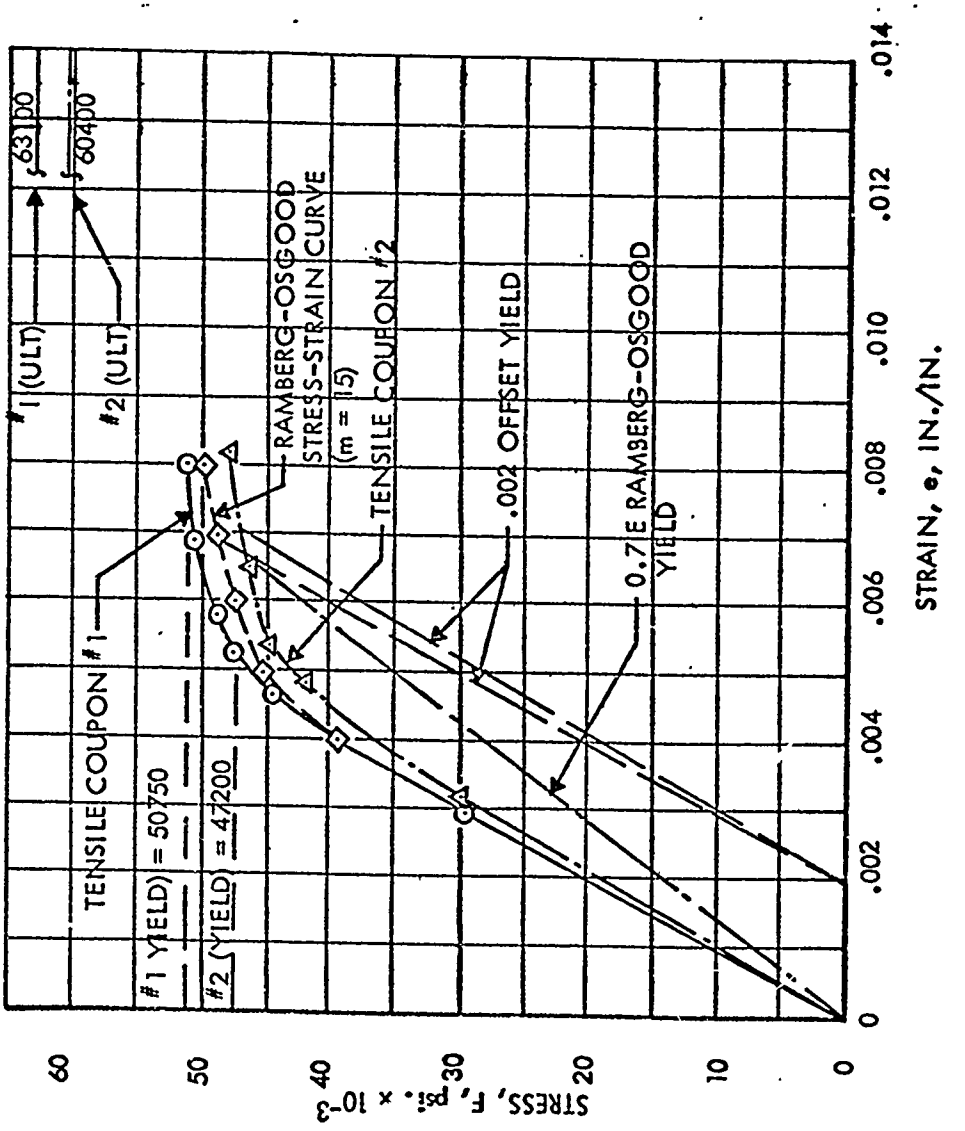

FIGURE 2.8

EFFECT OF TEMPERATURE ON THE MECHANICAL PROPERTIES OF 7075-T6 BARE ALUMINUM ALLOY FOR A TEMPERATURE HISTORY OF 350°F FOR TWO HOURS AND 450°F FOR 1/2 HOUR

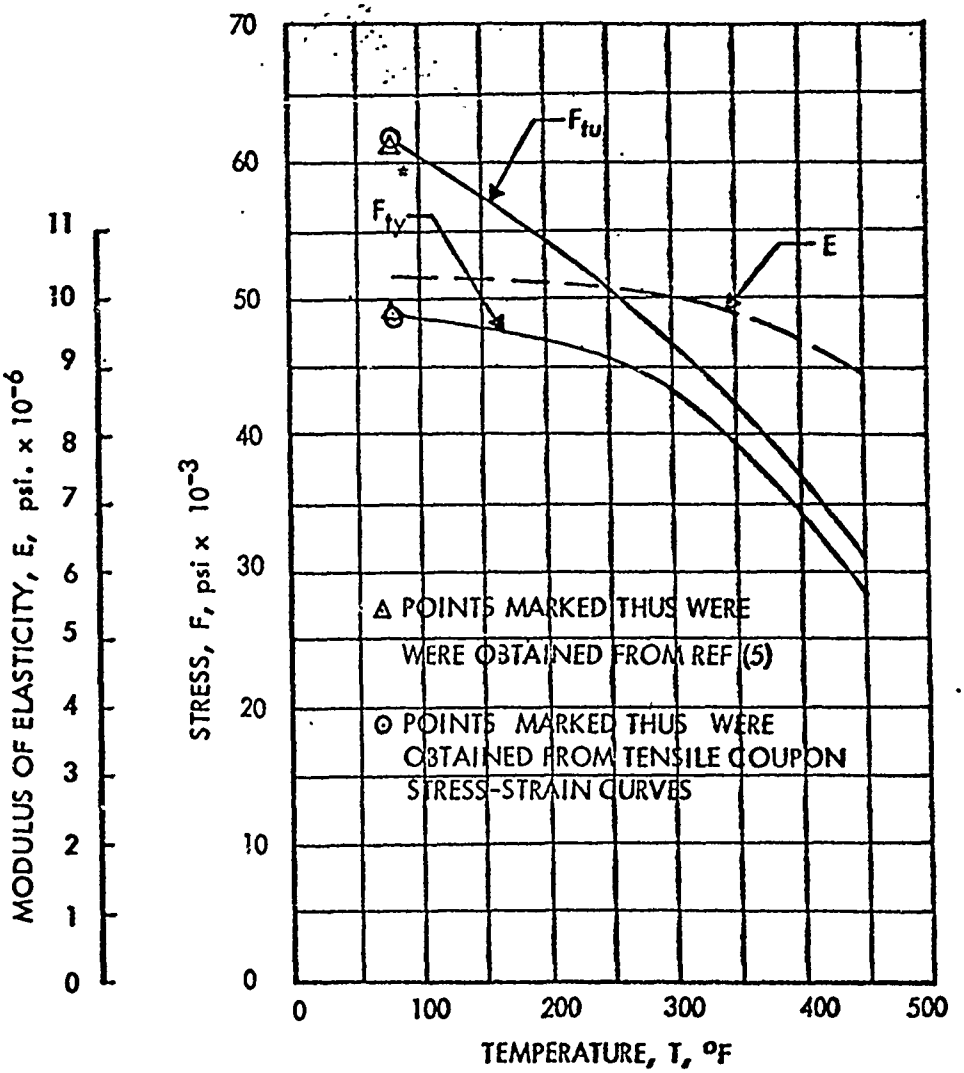

* F_{ty} IS THE 0.002 IN./IN. OFFSET YIELD STRESS

FIGURE 2.9

MATERIAL RECOVERY PROPERTIES

$F_{tu_{R.T.}}$ = 78000 psi

$F_{ty_{R.T.}}$ = 68000 psi

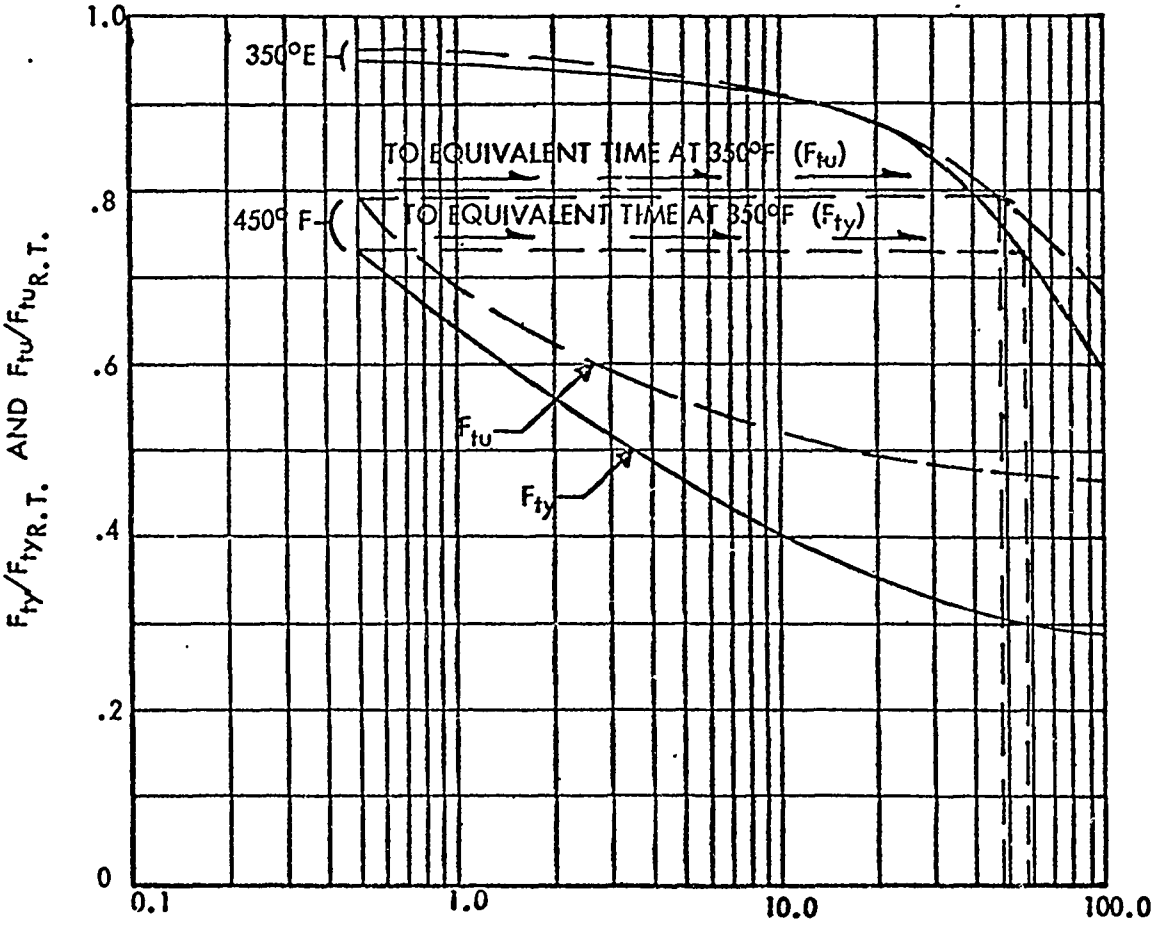

PREVIOUS TEMPERATURE HISTORY
2 HOURS AT 350°F
4 HOURS AT 450°F

2.2.3 COMPUTED AND TEST DATA COMPARISON

A test was performed on two skin stringer panels taken from the test horizontal stabilizer. This test was made to substantiate the prediction of column allowables to be used in the allowable stress computer program. The test set up and results are presented in Appendix B. The test specimen was failed under a varying temperature which produced the desired temperature gradients. Since the computer program cannot exactly simulate the varying temperature, the allowable load was computed for the temperature distribution in the panel at the time of failure. The comparison of test and computed results are shown in Figure 2.10. This comparison shows excellent agreement between the maximum test load and the load computed with the temperature distribution at the time of failure. From these tests, it was concluded that the column allowable program Appendix C was satisfactory for estimating column input data for the main program.

The test set up and results of the test horizontal stabilizer are presented in Appendix B. Again the temperature distribution at the time of failure was used to compute the allowable moment for the test section. The test section was broken into 37 structural elements as shown in Figure 2.11. The honeycomb element allowables (F_{cw}, F_{ci}) were computed using the IBM program E2128 presented in Appendix C.2. The skin stringer element buckling coefficients required were computed from the column allowable program E2140 in Appendix C.1. Allowables for other elements were computed as described in Section 2.1.

The first computer run results plotted in Figure 2.12 showed an allowable bending moment M_X of 186,000 in#. This moment is 112% of the actual test failure load. At this point, further investigation into laterally induced bending loads on the skin stringer elements was done as presented in Section 2.1.8. Following this investigation, the second computer run plotted in Figure 2.12 was made showing an ultimate allowable bending moment of the section as 171,000 in#. This computed allowable moment is 103% of actual failing load.

Figure 2.13 shows a comparison of measured and calculated strains vs. chord at H.S. Sta. 192. The measured strains are shown for an applied load of 4,390 lbs. and the calculated strains are shown for the nearest calculated applied load of 4,410 lbs. The calculated strains are shown for the temperature-load sequence +T, +P and reflect the effects of the non-uniform temperature distribution as well as the applied load.

From this data, it has been concluded that the proposed allowable stress method developed in this study will meet the requirements for predicting nuclear effects temperature limits within the accuracies required.

FIGURE 2.10

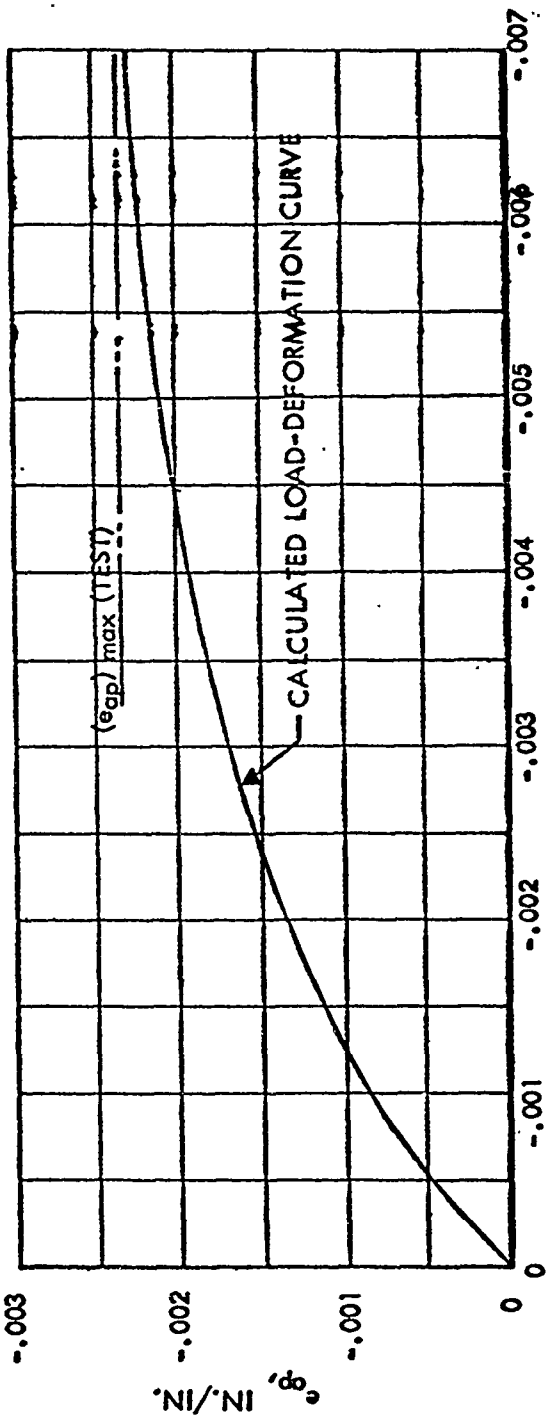

SKIN-STRINGER BUCKLING PANEL LOAD-DEFORMATION CURVE

FIGURE 2.11

SCHEMATIC OF TYPICAL CROSS SECTION

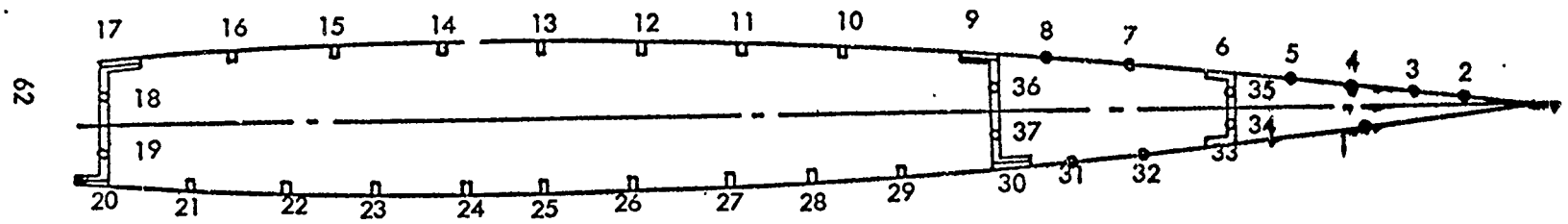

NUMBERS INDICATE ELEMENT NUMBER

1 NO COMPRESSION YIELD CUT-OFF OR INDUCED LATERAL BENDING CONSIDERED FOR SKIN-STRINGER COLUMNS

2 COMPRESSION YIELD CUT-OFF AND INDUCED LATERAL BENDING FOR SKIN-STRINGER COLUMNS

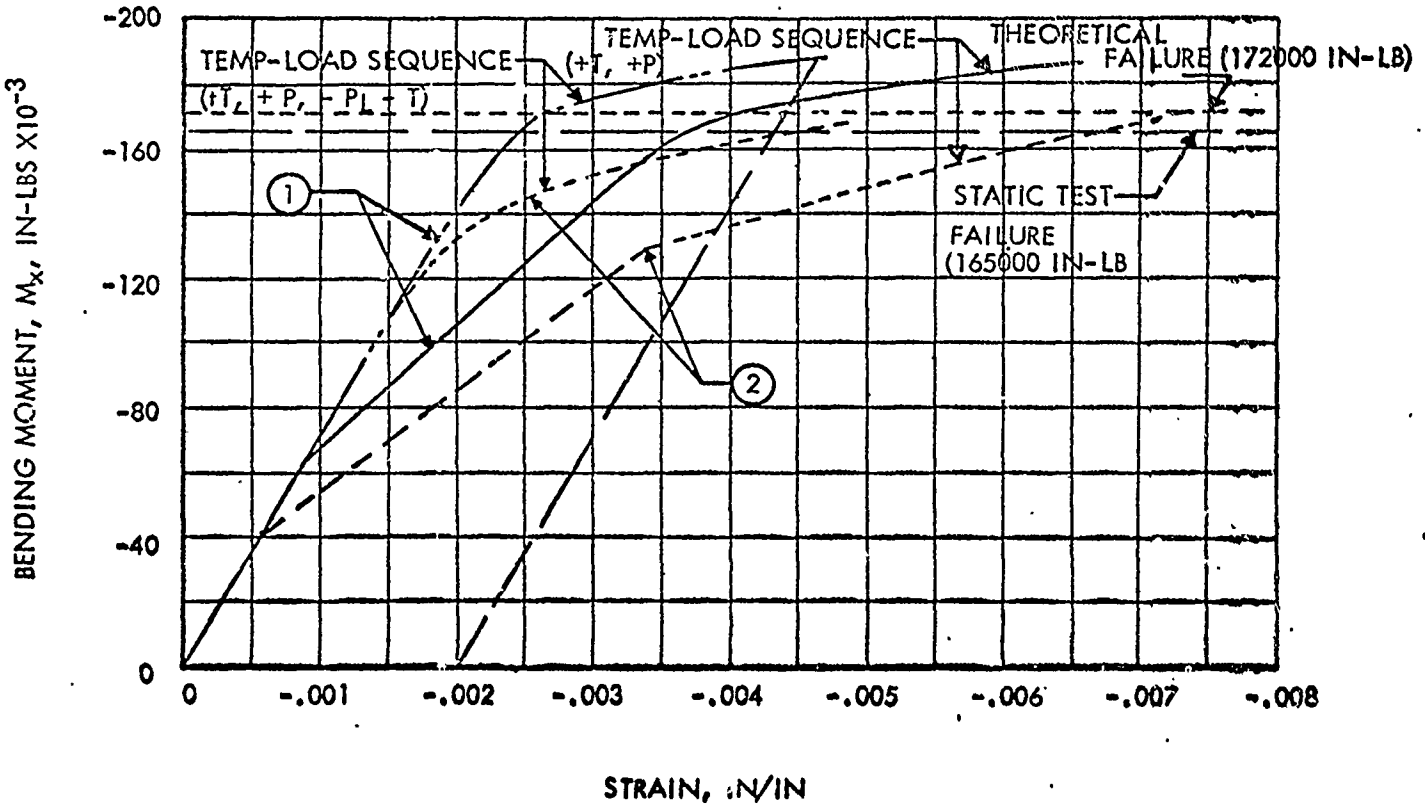

FIGURE 2.12
MOMENT DEFORMATION CURVE

NORTH AMERICAN AVIATION, INC.
COLUMBUS DIVISION
COLUMBUS 16, OHIO

NORTH AMERICAN AVIATION, INC.
COLUMBUS DIVISION
COLUMBUS 16, OHIO

FIGURE 2.13

CHORDWISE STRAIN DISTRIBUTION AT 350°F

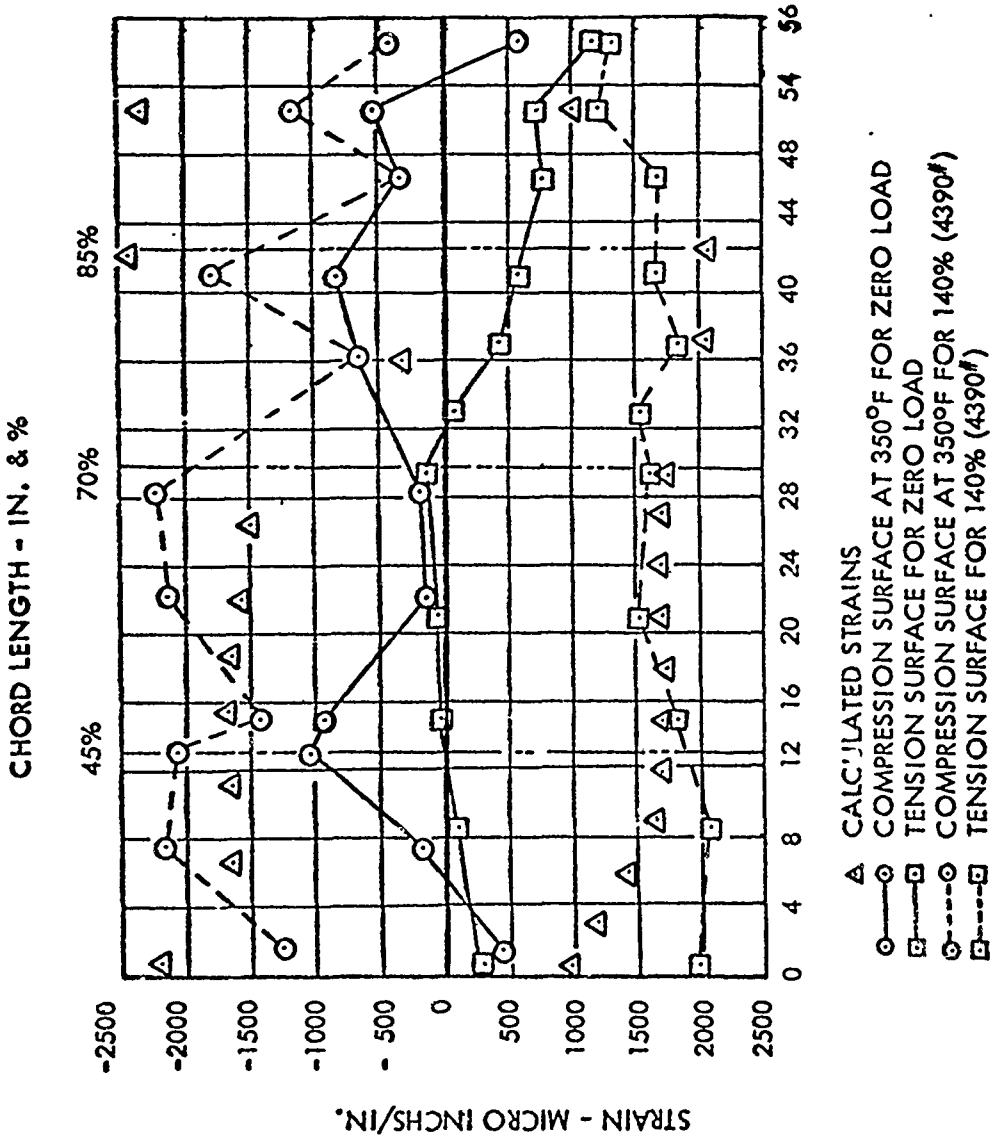

3.0 A SIMPLIFIED HAND CALCULATION METHOD

The hand calculation method presented in this report was selected to provide reasonable accuracy without excessive detail. This detail which accounts for the last increments of accuracy can be eliminated from the thermal stress analysis to greatly simplify the computations required.

The first step in the elimination of detail was made by eliminating chordwise bending effects from the analysis. This chordwise effect accounts for a maximum of 10% of the total stress in most cases. The location of the critical area forward and aft on the surface actually determines the magnitude of the induced error. If the critical area being analyzed is close to the forward and aft center of area, essentially no errors exist. If the critical areas are on the leading or trailing edge of the surface, an error of + 10% may exist. The existence of this error is dependent upon the temperature distribution on the structure. An evaluation of the thermally induced drag moment will indicate the sign of the error.

A direct elimination of detail can be made in the selection of structural elements to be included in the analysis. The object of element selection is to group similar detailed elements according to failure mode, temperature, and distance from the x axis. Using this procedure, all similar column elements with approximately the same temperature and moment arm can be considered as one element at an average temperature, moment arm and buckling allowable. The induced error from such a procedure should remain within + 2%. The magnitude of this error is dependent upon the accuracies with which the average values are computed for the combined elements. Selection of typical elements is demonstrated in the sample problem of this section.

3.1 SIMPLIFIED METHOD DEVELOPMENT

3.1.1 THERMAL STRESS EQUATION

Thermal stress distributions can be calculated for appropriate flight loads and temperature distributions with a general equation (3.1.7) which was derived by an expansion of information obtained from Reference (1) as follows.

Assume a one-dimensional temperature distribution T(y).

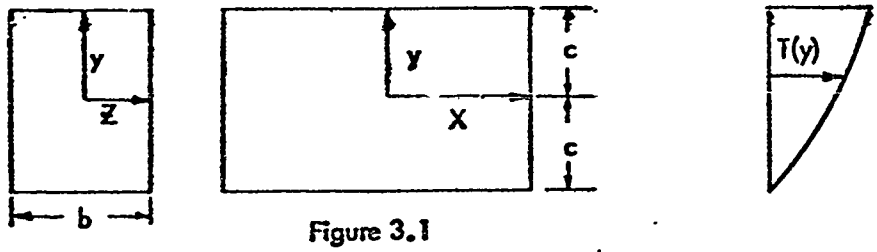

Figure 3.1

With the assumed temperature distribution T(y) and the plate fully restrained with no buckling, the stress distribution becomes:

$f_x = \alpha E T(y)$

α = coefficient of thermal expansion (3.1.1)

E = modulus of elasticity

If we free the plate of end but not bending restraints a relief stress is realized. This relief stress is superposed on the full restraint stresses. The total tensile load P_x may be written as:

$$P_x = \int_{-c}^{c} \alpha E T(y)\, b\, dy$$

The resultant relief stress becomes

$$(f_x)_t = \frac{P_x}{A_t} = \frac{-1}{A_t} \int_{-c}^{c} \alpha E T(y)\, dA_t \qquad (3.1.2)$$

A_t = total area of section

$dA_t = b\, dy$

Since the temperature distribution is unsymmetrical the tensile forces have a resultant moment. Thus when the plate is unrestrained in bending an unbalanced relief moment results:

$$M_z = \int_{-c}^{c} \alpha ET(y)\, b\, dy\, dy$$

The resulting relief stress becomes:

$$(f_x)_{b(z)} = -\frac{MzY}{I_z} = -\frac{Y}{I_z} \int_{-c}^{c} \alpha ET(y) y dA_t \qquad (3.1.3)$$

Y = distance to element C.G.

The one dimensional thermal stress equation is formed by compiling Equations 3.1.1, 3.1.2, and 3.1.3 as follows:

$$f_x = \alpha ET(y) - \frac{1}{A_t}\int_{-c}^{c} \alpha ET(y)\, dA_t - \frac{y}{I_z}\int_{-c}^{c} \alpha ET(y) y dA_t \qquad (3.1.4)$$

The stress from the external bending moment M_z can be expressed as:

$$f_x = \frac{MY}{I_z} \qquad (3.1.5)$$

Thus by combining equations 3.1.4 and 3.1.5, the final stress equation becomes:

$$f_x = -\alpha ET(y,z) + \frac{1}{A_t}\int_{-c}^{c} \alpha ET(y) dA_t + \frac{y}{I_z}\int_{-c}^{c} \alpha ET(y) dA_t + \frac{M_z y}{I_z} \qquad (3.1.6)$$

For the use of numerical integration Equation 3.1.6 becomes:

$$f_x = \alpha ET(y,z) - \frac{1}{A_t}\sum \alpha EAT(y) - \frac{y}{I_z}\sum \alpha EAyT(y) + \frac{M_z y}{I_z} \qquad (3.1.7)$$

where:

A = area of small elements in section

Equation 3.1.7 is modified for stresses above the proportional limit by the use of the Ramberg-Osgood Equation as follows:

$$E \text{ becomes } E_s = \frac{E}{1 + 3/7(F/F_y)^{m-1}} \qquad (3.1.8)$$

F = actual stress

F_y = yield stress

m = coefficient dependent on material stress strain curve

The equation is also modified for buckling by changing the effective area of a buckling element. The following equation is used to modify A:

$$A_{EFF} = A\sqrt{F_{cR}/F} \qquad (3.1.9)$$

F_{cR} = buckling stress of element

NORTH AMERICAN AVIATION , INC.
COLUMBUS DIVISION
COLUMBUS 16, OHIO

FIGURE 3.2
SKIN TEMPERATURE VERSUS SKIN THICKNESS

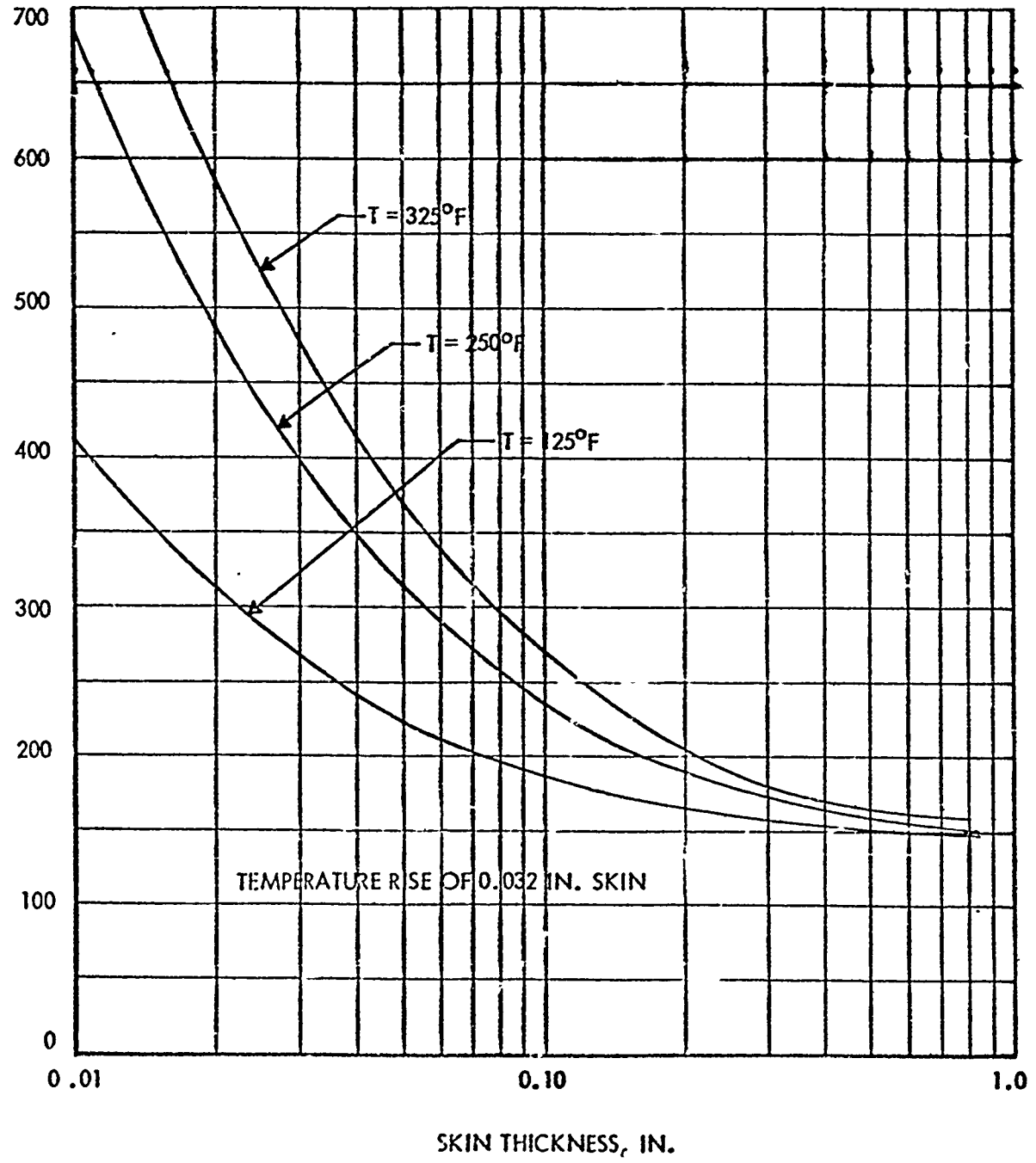

3.1.2 ANALYSIS DEVELOPMENT

The development of the thermal stress equation into a usable thermal limits analysis requires several complementary steps. Each of these steps are presented here in a form to simplify the computations as much as possible. The developed analysis method is also readily adaptable to small digital or desk type calculators.

The first step in deriving a thermal limit for a complex aircraft structure is to determine the temperature distribution on the structure. Knowing the Mach numbers and altitude at which the limit is desired a curve of skin thickness vs average element temperature for the given boundary layer temperature and reference ΔT rise can be constructed such as Figure 3.2. From such a curve an approximate temperature distribution can be determined for any given structure. It is recommended that a reference ΔT rise be selected in the range of from 300 to 400°F in .032 aluminum to insure some proximity to the final limit rise. The respective honeycomb element temperatures must be computed for the specific configuration to complete the structural temperature distribution.

At this time the structure should be broken down into structural elements as described in paragraph 3.0 of this report. With the number of elements and temperatures determined a table of computations can be started to determine the stress distribution. The following is a listing by column of the necessary tabular data and computations to arrive at an approximate Stress distribution.

Column 1. Element number or identification

2. The actual area of each element of Column 1.

3. The temperature rise of the element above room temperature.

4. Young's Modulus E_o at the element temperature.

5. Corrected Area computed by the following equation:

$$A_{corr} = \text{Area} \times E_o/10^7 \qquad (3.1.10)$$

6. The moment arm Y of each element from a reference X axis.

7. The products of the Corrected Area and moment arm Y for each element are summed and divided by the summation of column 5 to compute $\bar{Y}$.

8. The corrected moment arm Ycorr listed for each element, computed by the following equation:

$$Y_{corr} = Y - \bar{Y} \qquad (3.1.11)$$

9. The moment of inertia of each element about the X axis summed to give the total moment of inertia of the section. Computed by the following equation:

$$I_{xx} = A_{corr} \times Y^2_{corr} \qquad (3.1.12)$$

10. The full fixity thermal stress computed by equation 3.1.1.

11. The summation of the thermal tension relief load ($\Sigma 5 \times 10$), and the thermal relief stress as computed by equation 3.1.2 where $A_t = A_{corr}$.

12. The summation of the thermal bending relief moment ($\delta \times 11$) as computed by equation 3.1.3.

13. The applied bending stress as computed by equation 3.1.5 (the bending moment used should be for the normal load factor N_z of greatest interest). $I_z = I_{xx}$ and $Y = Y_{corr}$.

14. Thermal bending relief stress computed by using the equation

$$f_{bth} = \frac{M_{th} \cdot Y_{corr}}{I_{xx}} \qquad (3.1.13)$$

Where $M_{th} = \sum$ Column 12.

Column 15. Total thermal stress on each element as computed by Equation 3.1.4.

16. The actual corrected applied bending stress on each element as computed by the following equation:

$$f_{bact} = F_b \quad \frac{A_{corr}}{A} \qquad (3.1.14)$$

17. The actual corrected total thermal stress on each element as computed by the following equation:

$$f_{th\ act} = f_{th} = \frac{A_{corr}}{A} \qquad (3.1.15)$$

18. Final total element stress (16 + 17)

Upon the completion of the computation of the Final Total element stress each element stress must be checked against the respective element buckling allowable or yield stress, whichever is applicable, with the buckling, if critical, taking precedence. If an element is found to be stressed above the allowable buckling a correction must be made to the effective area, A_{corr}, using equation 3.1.9 where A is the last Acorr and A_{EFF} is the new A_{corr}. If an element stress is found which exceeds .6 Fcy a correction of the Acorr must be made for this element also using the following equation:

$$\left(\frac{(OLD)\ A_{corr}}{2x\ Area} + \frac{E_s}{2x10^7}\right) \qquad Area = (NEW)A_{corr} \qquad (3.1.16)$$

Where E_s is computed using equation 3.1.8 with $E = E_o$ and F is the final total element stress. Upon correcting the areas for these elements the computation must be again performed and repeated until the final total element stresses converge within required error limits.

When final element stress convergence has been accomplished the element nearest to becoming critical or most critical can be selected. The approximate limiting temperature rise or moment can then be estimated by one of the following methods:

3.2 SAMPLE PROBLEM

The sample problem computed in tables 3.1 through 3.5 were computed for a typical horizontal stabilizer at a flight condition of Mach 1.2 at 20,000 ft. altitude and a reference temperature rise of 450°F. on .032 aluminum skin. Figure 3.3 shows a layout of the horizontal stabilizer section and areas included in each structural element used in this analysis.

The most critical element in this analysis is element 9 which is the full depth honeycomb trailing edge. The final element stress was computed to be 31,800 psi. The allowable stress for this element at 483°F. is computed using Equation (3.1.2), the reference rise on .032 skin becomes:

$$450^{\circ} = \text{reference rise used in table}$$

$$450^{\circ}\left(\frac{33500 - 4100}{27700}\right) = 476^{\circ}\text{F allowable rise on .032 at } N_Z = 2$$

If the change in temperature rise was great enough in this problem a correction of the allowable for the increased or decreased temperature should be accounted for by recalculating the allowable. The allowable rise computed here agrees reasonably well with the allowable calculated for the same condition using past methods. The single mission limit for this condition using the more exact method was computed as 445°F rise on .032 during that study. This shows a 6.3% error in the proposed hand calculation method for this problem.

CASE I

If the element thermal stress (column 16) is greater than the element allowable stress the following equation should be used:

$$(T_{ELE} - T_{BOUNDARY})\frac{(F_{allow} - f_{b\ act})}{f_{th\ act}} = (T_{ELE} - T_{BOUNDARY})_{allow} \qquad (3.1.17)$$

$f_{b\ act}$ = column 17

$f_{th\ act}$ = column 16

F_{allow} = element allowable stress

T_{ELE} = element total temperature

$T_{BOUNDARY}$ = Boundary Layer temperature

The new allowable element temperature rise calculated is for the moment used in the stress distribution table. From this moment a value of N_Z can be obtained to plot versus the limit temperature rise. By changing the applied moment and f_b in the table proportionately another approximate limit temperature rise can be obtained without recomputing the entire table.

CASE II

If the thermal stress is less than the allowable and the total stress is greater than the allowable the applied bending moment can be reduced by the following equation:

$$M\frac{(F_{allow} - f_{th\ act})}{f_{b\ act}} = M_{allow} \qquad (3.1.18)$$

This allowable moment is for the temperature rise used in the computation of the actual stress distribution. If the allowable moment should become less than that at an $N_Z = 1$ the limit temperature rise should be adjusted as in Case I.

CASE III

If the allowable stress is greater than the total stress either the moment or the temperature rise limit can be computed using the respective equations 3.1.17 and 3.1.18 of the preceding paragraphs. In any of the discussed equations if the element temperature is changed the allowable element stress should be adjusted accordingly thus requiring some iteration in the computation of an allowable temperature rise.

FIGURE 3.3

TYPICAL HORIZONTAL STABILIZER SECTION
ELEMENT NUMBERS FOR SAMPLE PROBLEM

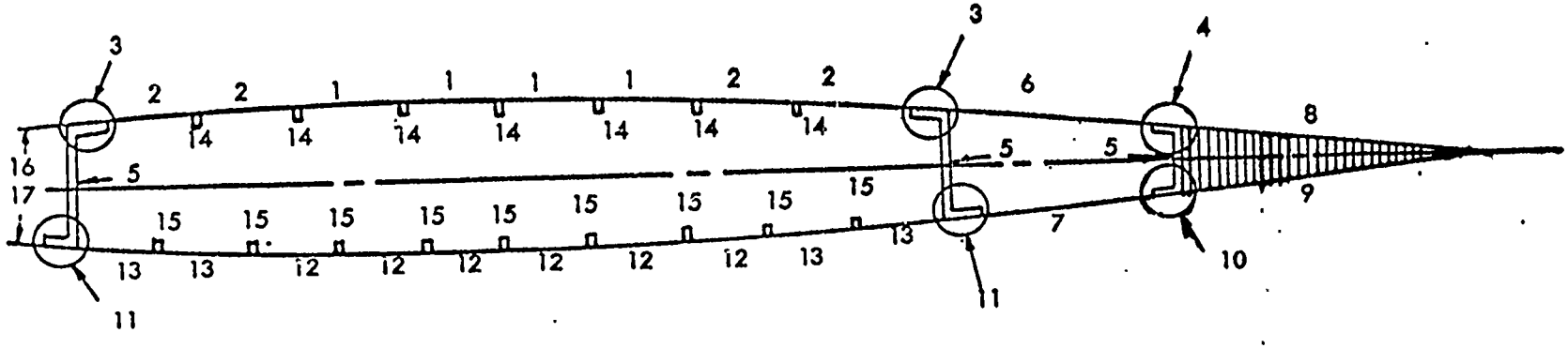

M = 171,720 IN. LB
α = 13 x 10^{-6} IN./IN

TABLE 3.1

1	2	3	4	5	6	7	8	9	10	11	12	13	14	15	16	17	18	19	20
Elt	X/ℓX	ΔT Tele-Trt	Eα (X10^{-6})	Acorr 2 x 4/E		Acorr Y 5 x 6	Ycorr 6 + Y	Acorr Ycor 5 x 8^2	αEAT Ex α	5 x 10	8 x 11	M_{th} Σ▼	M_{th} -M x 8 Σ9	M_{th} 10 + ▽t +14	$I_{th\ act}$ 15 x 5/2	$I_{th\ req'd}$ 13 x 5/2	I TOTAL 16 + 17	▽ct	I_{ex} (X10^{-3})
1	1.21	31	10200000	1.23	1.76	2.17	1.71	3.61	4,030	4,970	8,500	-13,400	11,700	1,640	1,680	-13,400	-12,005		40
2	1.21	31	10200000	1.23	1.52	1.88	1.47	2.67	4,030	4,970	7,310	-11,500	10,100	- 1,30	- 1,33	-11,700	-11,700		40
3	0.840	31	10200000	0.857	1.32	1.14	1.28	1.40	4,030	3,450	4,420	-10,000	8,770	- 1,300	-1,330	-10,200	-11,500		40
4	0.146	31	10200000	0.149	0.74	0.110	0.690	0.0708	4,030	600	414	- 5,390	4,730	- 5,350	- 5,460	- 5,500	-11,000		40
5	0.382	24	10200000	0.390	0	0.000	-0.0505	0.000992	4,420	1,720	669	395	- 346	-10,000	-10,200	403	- 9,830		40
6	0.500	31	10200000	0.510	1.10	0.561	1.05	0.562	4,030	2,050	2,160	- 8,210	7,190	- 2,880	- 2,940	- 8,370	-11,300		40
7	0.420	391	90000000	0.378	-1.10	-0.416	-1.15	0.500	50,800	19,200	22,100	9,000	- 7,890	28,800	26,000	8,100	34,100	1100 psi	34
8	0.320	82	10000000	0.320	0.45	0.144	0.400	0.0511	10,700	3,410	1,360	- 3,120	2,740	-706	-706	-3,120	-3,830		40
9	0.320	413	88000000	0.282	-0.45	-0.127	-0.500	0.0705	53,700	15,100	7,570	3,910	-3,430	36,200	31,800	3,440	35,300		34
10	0.185	123	10000000	0.185	-0.72	-0.133	-0.770	0.110	16,000	2,560	2,280	6,030	-5,280	-3,400	-3,400	6,030	2,620		39
11	0.964	74	10000000	0.864	-1.26	-1.09	-1.31	1.48	9,620	8,310	10,900	10,200	-8,980	-13,500	-13,500	10,200	-3,220		40
12	1.31	197	9800000	1.28	-1.74	-2.23	-1.79	4.12	25,600	32,900	58,900	14,000	-12,300	- 768	- 753	13,700	13,000	13300	39
13	0.960	204	9800000	0.941	-1.50	-1.41	-1.55	2.26	26,500	25,000	38,700	12,100	-10,600	1,790	1,750	11,900	13,600	13500	38
14	1.11	31	10200000	1.13	1.42	1.60	-1.37	2.12	4,030	4,550	6,230	-10,700	9,390	- 687	- 701	-10,900	-11600		40
15	1.16	149	9900000	1.15	-1.42	-1.63	-1.47	2.49	19,400	22,300	32,700	11,500	-10,100	-4,810	-4,770	11,400	6,620		39
16	0.283	31	10200000	0.289	0.90	0.260	0.850	0.209	4,030	1,170	990	-6,640	5,820	-4,250	-4,340	-6,780	-11,100		40
17	0.283	258	9600000	0.272	-0.90	-0.245	0.950	0.246	33,500	9,130	8,680	7,430	-6,520	12,900	12,400	7,140	19,500		
				11.5		.579		22.0		162,000	-151,000								
			Y = -	.579 / 11.5	= - .0505				▽T = -	162,000 / 11.5	- 14,100								

TABLE 3.2

1	2	3	4	5	6	7	8	9	10	11	12	13	14	15	16	17	18	19	20
ELE	AREA	$\frac{\Delta T}{\text{Tele-Tr}}$	E_0 (X10^{-6})	A_{corr} 2 x 4/E	Y	A_{corr} Y 5 x 6	Y_{corr} 6 + Y	I_{corr} Y^2_{corr} 5 x 8^2	$\frac{\beta E \Delta T}{\text{Ex } 3}$	5 x 10	8 x 11	$\frac{M_b}{\Sigma 9}$ M > 8	$\frac{M_{bi}}{\Sigma 9}$ -M' x 8	f_{th} 10 + σ_t · 14	$f_{th\ act}$ 15 x 5/2	f_{bact} 13 x 5/2	f TOTAL 16 + 17	σ_{cr}	F_{cx} X10^{-3}
1	1.2	31	10200000	1.23	1.76	2.11	1.66	3.39	4030	4970	8240	-13300	10200	1750	1790	-13600	-11800		40
2	1.21	31	10200000	1.23	1.52	1.81	1.42	2.48	4030	4970	7050	-11400	8760	272	277	-11600	-11400		40
3	0.846	31	10200000	0.857	1.33	1.10	1.23	1.29	4030	3450	4240	- 9880	7580	- 903	- 921	-10100	-11000		40
4	0.147	31	10200000	0.149	0.74	0.103	0.637	0.0603	4030	600	382	- 5130	- 3930	- 4550	- 4640	- 5230	- 9870		40
5	0.382	31	10200000	0.390	0	-0.0197	-0.103	0.00417	4470	1720	- 179	833	- 639	- 8730	- 8910	850	- 6060		40
6	0.500	31	10200000	0.510	1.10	0.536	0.997	0.507	4030	2060	2050	- 8030	6160	- 2328	- 2370	- 8190	-10600		40
7	0.420	391	9000000	0.0677	-1.10	-0.0782	-1.20	0.0984	50800	3450	- 4160	9700	- 7440	30900	4990	1570	6560	1100psi	36
8	0.320	82	10000000	0.329	0.45	0.128	0.347	0.0284	10700	3410	1180	- 2790	2140	289	289	- 2790	- 2590		40
9	0.329	413	8800000	0.229	-0.45	-0.115	-0.553	0.0702	53700	12300	- 6810	4460	- 3420	37800	27000	3190	30200		34
10	0.185	123	10000000	0.185	-0.72	-0.143	-0.823	0.125	16000	2560	- 2440	6630	- 5090	- 1610	- 1610	6630	5020		39
11	0.164	74	10000000	0.864	-1.26	-1.13	-1.36	1.61	9620	8310	-11300	11000	- 8430	-11300	-11300	11000	- 336		40
12	1.31	197	9000000	1.28	-1.74	-2.30	-1.84	4.36	25600	32900	-60400	14900	-11400	1700	1670	14600	16200	13500	39
13	0.950	204	9000000	0.936	-1.50	-1.45	-1.50	2.41	26500	24800	-39800	12900	- 9910	4100	3990	12600	16600	13500	38
14	1.11	31	10200000	1.13	1.42	1.54	1.32	1.96	4030	4550	5990	-10600	8110	- 346	- 353	-10800	-11200		40
15	1.16	149	9000000	1.15	-1.42	-1.69	-1.52	2.67	19400	22300	-33900	12300	- 9420	- 2560	- 2530	12200	9620		39
16	0.283	31	10200000	0.289	0.90	0.246	0.797	0.183	4030	1170	928	- 6420	4920	- 3560	- 3630	- 6550	-10200		40
17	0.283	258	9600000	0.0754	-0.90	-0.0717	-1.00	0.0759	33500	2530	- 2540	8080	- 6200	14800	3940	2150	6070		38
				10.9		.577		213		136000	-132000								
				$\bar{Y} = -\frac{.577}{10.9}$		= -.0529			$\bar{Y} = -\frac{136000}{10.9}$		= -125								

TABLE 3.3

1	2	3	4	5	6	7	8	9	10	11	12	13	14	15	16	17	18	19	20
		ΔI							ΣAI			f_b	f_{b_1}	f_{b_1}	$f_{b_1 act}$	$f_{b act}$	TOTAL	σ_{cr}	F_{cy}
		Tab. - Eq' (X10-6)		$\Delta\sigma_{cr}$		$\Delta\sigma_{cr} Y$		$\sigma_{cr} Y$				M x 8	-Mt x 8	$10^{-6}\sigma_t$	15 x 5/2	13 x 6/2	16 + 17		(X10-3)
						5 x 6		+ Y	$\Delta\sigma_{cr} Y_{cor}$	5 x 10	8 x 11	$\Sigma 9$	$\Sigma 9$	+ 14					
									5 x 8^2	Ex 3									
	1	31	10200000	1.23	1.76	2.04	1.62	3.22	4030	4970	8040	-13500	975	1750	1750	-13700	-12000		40
	2	31	10200000	1.23	1.52	1.75	1.38	2.34	4030	4970	6840	-11500	8310	276	276	-11700	-11400		40
	3-2	31	10200000	0.857	1.33	1.05	1.19	1.20	4030	3450	4090	- 9890	7160	- 877	- 895	-10100	-11000		40
4	0.145	31	10200000	0.149	0.74	0.0948	0.595	0.0528	4030	600	357	- 4970	3600	- 4440	- 4530	- 5070	- 9600		40
	0.3-2	3a	10200000	0.390	0	-0.0403	-0.345	0.00914	4420	1720	- 249	1210	- 873	- 8520	- 8690	1430	- 7460		40
	0.490	31	10200000	0.510	1.10	0.505	0.955	0.466	4030	2040	1960	- 7970	5770	- 2200	- 2310	- 8130	-10400	1100psi	40
7	0.422	321	2000000	0.0278	-1.10	-0.0335	-1.24	0.0431	50800	1410	- 1760	10400	- 7510	31350	2020	688	2760	1100psi	34
8	0.310	42	10200000	0.320	0.45	0.111	0.305	0.0299	10700	3410	1040	- 2550	1840	439	439	- 2550	- 2110		40
	0.350	413	8800000	0.237	-0.45	-0.131	-0.595	0.0938	53700	12700	- 7570	4960	- 3590	38000	28200	3630	31900		34
	0.1-3	123	10000000	0.185	-0.72	-0.152	-0.865	0.138	16000	2260	- 2560	7210	- 5220	- 1300	- 1300	2210	5920		39
	0.1-4	74	10000000	0.864	-1.26	-1.18	-1.40	1.70	9620	8310	-11700	11700	- 8480	-10900	-10900	11700	791		40
		132	2800000	1.17	-1.74	-2.15	-1.88	4.16	25600	30000	-56500	15700	-11400	2170	1940	14100	16000	13500	39
3	0.240	231	9800000	0.844	-1.50	-1.35	-1.64	2.28	26500	22400	-36800	13700	- 9920	4120	3980	12100	16000	13500	38
14	1.11	31	10200000	1.13	1.42	1.49	1.28	1.84	4030	4550	5800	-10600	7700	- 334	- 340	-10900	-11200		40
	1.16	142	9800000	1.15	-1.42	-1.75	-1.56	2.81	19400	22300	-34800	13 00	- 5450	- 2140	- 2120	12900	10800		39
16	0.263	31	10200000	0.259	0.90	0.230	0.755	0.165	4030	1170	680	- 6300	4560	- 3470	- 3540	- 6430	- 9970		40
17	0.283	258	9600000	0.0374	-0.90	-0.0375	-1.04	0.0408	33500	1250	- 1310	8710	- 6310	15200	2000	1150	3150	1500	38
				10.6		.437		20.6		128000 -	124000								

$\bar{Y} = \frac{.437}{10.6} = .0411$

$\sigma_I = \frac{128000}{10.6} = 12,100$

TABLE 2.4

1	2	3	4	5	6	7	8	9	10	11	12	13	14	15	16	17	18	19	20
		ΔT										f_b	f_{b_1}	f_{b_2}	$f_{b_{act}}$	$f_{b_{act}}$	f TOTAL	σ_{cr}	F_{cy}
		$T_{elo}-T_{rt}$	$(\kappa,10^{-6})$	2 x 4/E		5 x 6	6 + Y	Acorr Ycorr 5×8^2	$\alpha E \Delta T$ Ex 3	5 x 10	8 x 11	M x 8 Σ^9	-Mt x 8 Σ^9	$\frac{10}{I}\alpha_t$ + 14	15 x 5/2	13 x 5/2	16 + 17		
1	21	31	10200000	1.23	1.76	1.99	1.58	3.10	4030	4970	7880	-13600	9440	1710	1740	-13900	-12100		40
2	12	31	10200000	1.23	1.52	1.70	1.34	2.23	4030	4970	6692	-11500	8010	276	281	-11800	-11500		40
3	0.845	31	10200000	0.857	1.33	1.02	1.15	1.14	4030	3450	3990	- 9910	6880	- 856	- 873	-10100	-11000		40
4	0.145	21	10200000	0.149	0.74	0.0887	0.565	0.0475	4030	600	339	- 4840	3360	- 4370	- 4460	- 4940	- 9400		40
5	0.01	31	10200000	0.3 9	0	-0.0563	-0.175	0.0129	4420	1720	- 302	1500	- 1040	- 8180	- 8560	1530	- 7020		40
6	0.545	31	10200000	0.510	1.10	0.437	0.925	0.436	4030	2260	1900	- 7930	5510	- 2310	- 2270	- 8090	-10400		40
7	0.020	381	9500000	0.0176	-1.10	-0.0219	-1.28	0.0266	50800	893	1110	10900	- 7600	31500	1320	458	1770	100psi	34
8	0.09	62	10000000	0.320	0.45	0.0978	0.275	0.0241	10700	3410	937	- 2360	1640	532	532	- 2360	- 1820		70
9	0.220	4.3	8800000	0.232	-0.45	-0.138	-0.625	0.0908	53700	12300	- 7820	5370	- 3720	38200	27700	2390	31600		34
10	0.145	23	9000000	0.185	-0.72	-0.169	-0.895	0.148	16000	2960	- 2650	7680	- 5330	- 1110	- 1110	7680	6570		35
11	0.864	74	10200000	0.864	-1.26	-1.21	-1.44	1.78	9620	8310	-11900	12300	- 8550	-10700	-10700	12300	1620		40
12	1.08	197	9500000	1.08	-1.74	-2.03	-1.92	3.85	25600	27600	-52800	16400	-11400	2440	2000	13500	15500	13500	39
13	0.850	204	9800000	0.774	-1.50	-1.27	-1.68	2.17	26500	20500	-34400	14400	- 9980	4780	3850	11600	15500	13500	38
14	1.11	31	10200000	1.13	1.42	1.44	1.24	1.75	4030	4530	5650	-10700	7410	- 320	- 326	-10900	-11200		40
15	1.16	149	9800000	1.15	-1.42	-1.80	-1.60	2.93	19400	22300	-35500	13700	- 9500	- 1900	- 1880	13500	11700		39
16	0.262	31	10200000	0.289	0.80	0.218	0.725	0.152	4030	1170	844	- 3220	4320	- 3420	- 3490	- 6340	- 9830		40
17	0.263	258	9600000	0.0258	-0.90	-0.0270	-1.08	0.0298	33500	856	- 931	9230	- 6410	15400	1400	840	2240	1500	38
				10.4		.322		20.0		123000	-119000								
				$\bar{Y} = \frac{.322}{10.4} = .0309$					$\bar{T} = \frac{12300}{10.4} = 1180$										

TABLE 3.5

1	2	3	4	5	6	7	8	9	10	11	12	13	14	15	16	17	18	19	20
						Acorr Y	Ycorr												
						5 x 6	6 + Y	AcorrYcorr											
								5 x 8²	Ex 3			Σ9	Σ9						
	1.21	31		1.23	1.76	-1.96	1.56	3.01	4030	4970	7770	-13700	9220	1690	1720	-14000	-12200		40
	1.21	31		1.23	1.52	1.66	1.32	2.16	4030	4970	6580	-11600	7810	270	276	-11800	-11500		40
	0.740	31		0.857	1.33	0.989	1.13	1.10	4030	3450	3910	- 9920	6680	- 852	- 869	-10100	-11000		40
	0.140	31		0.149	0.74	0.0841	0.542	0.0438	4030	600	325	- 4750	3200	- 4340	- 4420	- 4850	- 9270		40
	0.140	34		0.260	0	-0.0683	-0.198	0.0153	4420	1220	- 341	1730	- 1170	- 8320	- 8480	1770	- 6710		40
	0.120	31		0.510	1.10	0.422	0.902	0.415	4030	2060	1850	- 7910	5330	- 2210	- 2250	- 8060	-10300		40
	0.420	391		0.0138	-1.10	-0.0176	-1.30	0.0233	50800	703	- 913	11400	- 7660	31600	1040	325	1420	1100 psi	34
	0.320	87		0.320	0.45	0.0879	0.252	0.0203	10700	3410	860	- 2210	1490	582	582	- 2210	- 1630		40
	0.320	413		0.231	-0.45	-0.145	-0.648	0.0971	53700	12400	- 8040	5680	- 3830	38300	27700	4100	31800		34
	0.320	413		0.231	-0.45	-0.145	-0.648	0.0971	53700	12400	- 8040	5680	- 3830	38300	27700	4100	31800		39
	0.185	123		0.185	-0.72	-0.166	-0.918	0.156	16000	2960	- 2720	8040	- 5420	- 997	- 997	8040	7050		40
	0.[illegible]	74		0.864	-1.26	-1.24	-1.46	1.84	9620	8310	-12100	12800	- 8610	-10600	-10600	12800	2220		39
	1.21	197		1.00	-1.74	-1.92	-1.94	3.77	25600	25700	-49800	17000	-11400	2600	1990	13000	15000	13500	38
	0.910	274		0.724	-1.50	-1.21	-1.70	2.09	26500	19200	-32600	14900	-10000	4930	3720	11200	14900	13500	38
	1.11	31		1.13	1.42	1.40	1.22	1.68	4030	4550	5560	-10700	7220	- 320	- 327	-10900	-11300		40
	1.14	149		1.15	-1.42	-1.83	-1.62	3.01	19100	22300	-36000	14200	- 9550	- 1750	- 1730	14000	12300		39
	0.233	31		0.289	0.90	0.210	0.702	0.143	4030	1170	818	- 6150	4150	- 3390	- 3460	- 6280	- 9230		40
	0.283	258		0.0211	-0.90	-0.0227	-1.10	0.0255	33500	709	- 778	9620	- 6480	15500	1150	717	1870	1500	38
				10.3		.233		196		119000 -	116000								

$\bar{Y} = -\frac{.233}{10.3} = -.0226$ $\quad \alpha_T = -\frac{119000 - 116000}{10.3}$

4.0 GENERAL HONEYCOMB PANEL BUCKLING

The general buckling equation was derived in Reference 6. The equation was derived to handle sandwich panels with faces of unequal thickness and dissimilar materials. This equation then fits the general production honeycomb panel exposed to thermal radiation exactly. The production honeycomb panel, with faces of unequal thickness because of external damage requirements, have been difficult to handle. The addition of a temperature gradient and change of material properties especially in the hot facing has complicated the problem to a point where testing of panels was the only solution. While now, through the use of the generalized panel buckling equation, the differences of facing thickness and material properties can be accounted for theoretically. With this capability, aircraft thermal limits can be derived directly through the use of a theoretical analysis. The use of the general buckling equation also provides the capability of designing honeycomb structures to withstand the anticipated thermal loading.

The testing of the honeycomb panels and configurations are described in appendix A. The panels were tested to provide correlation data for the general honeycomb buckling equation proposed for use in this study. The data compiled in appendix A showed very good repeatability and consistency from one test to the other. In a comparison of the test data with computed allowables, agreement was wide spread. Portions of this spread can be explained in several ways. The allowable equation shows a high sensitivity of the allowable load to the hot face temperature. A study of the equation sensitivity to temperature shows that this sensitivity increases with temperature. See Fig. (4.1). Reading and measurement errors for the thermocouple installation used on these tests was estimated at ± 25 °F and -5°F. A second source of error in the computed allowable results from the fact that a temperature gradient exists across the panel to an extent of 5% lower temperature rise at the edge as compared to that at the center of the panel. This results in a lower average temperature than that measured.

An evaluation of panel construction tolerances was also made to establish induced computed allowable errors. This study revealed that an increase of the core depth of $\pm$ 5% had a direct effect on the allowable by $\pm$ 5%. A $\pm$ 5% tolerance on the thickness of the hot face produced a $\pm$ 4% change in the panel allowable load. A thickness change in the cold facing produced negectable allowable load change.

The test data and computed allowable data is compiled in table (4.1) and plotted in fig. (4.2). The computed allowables were computed using equation (2.1.62) which was also used in the "Allowable Stress Program" as subroutine HKN. Although the comparison of the computed data and test data shows a wide range of scatter, the inaccuracies of the test and the sensitivity of the equation must be considered in the evaluation of the equation. Since the equation shows good results compared to test data at room temperature, and again crosses the 0% error line in the area of 600°F., it is the opinion of the writer that the equation is satisfactory for predicting thermal limits in honeycomb structures.

NORTH AMERICAN AVIATION, INC.
COLUMBUS DIVISION
COLUMBUS 16, OHIO

FIGURE 4.1

LOAD CHANGE VERSUS TEMPERATURE CHANGE

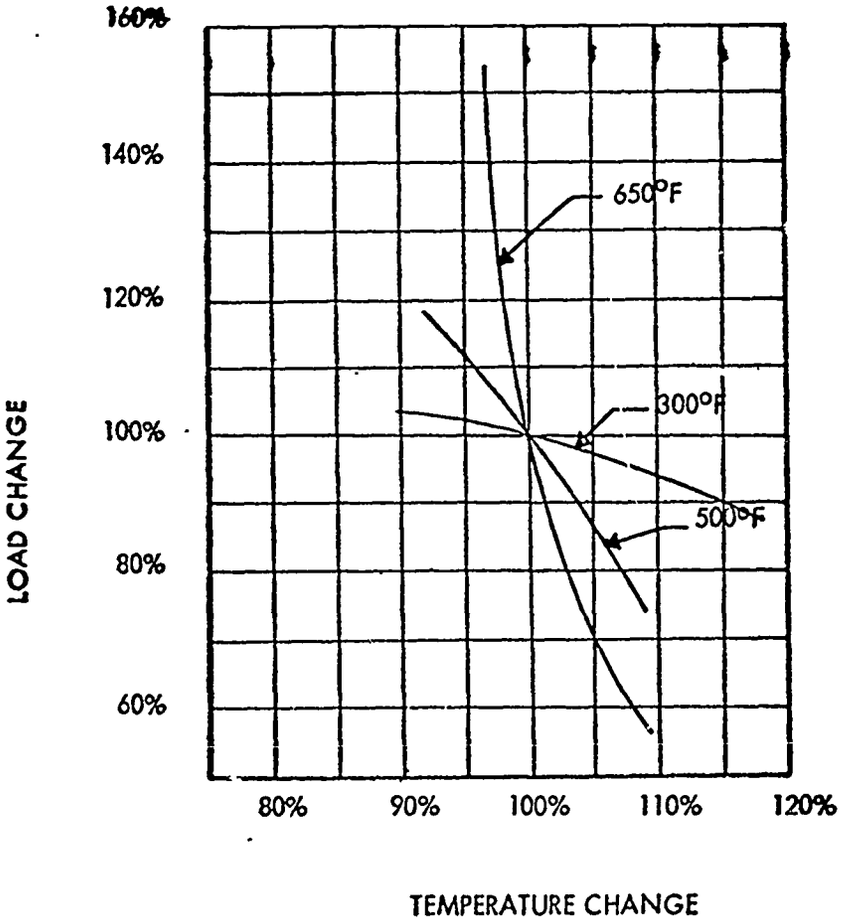

NORTH AMERICAN AVIATION, INC
COLUMBUS DIVISION
COLUMBUS 16, OHIO

FIGURE 4.2

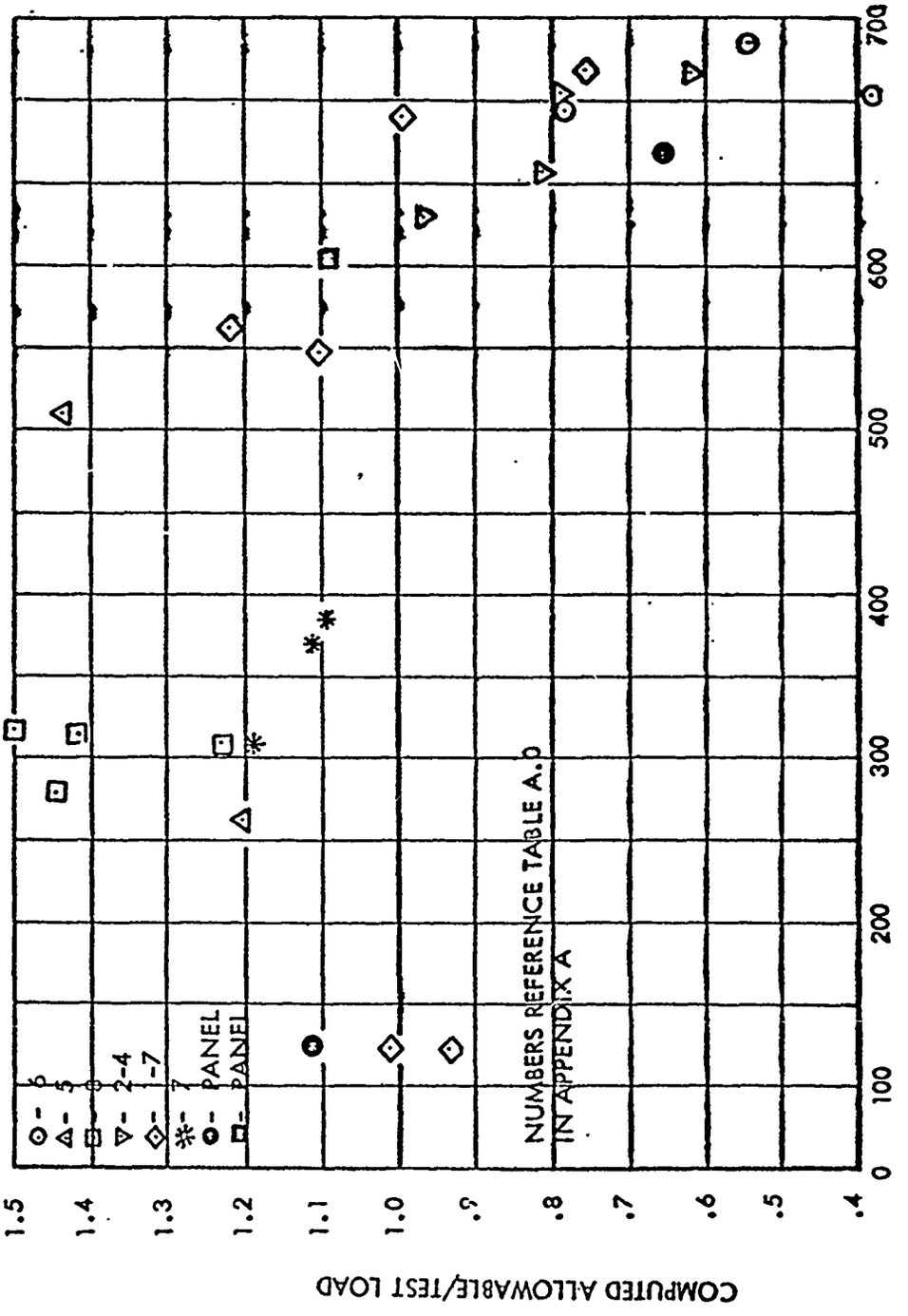

HONEYCOMB PANEL GENERALIZED BUCKLING TEST DATA

TABLE 4.1

Config.	Spec. No.	Hot Face Temp.	Cold Face Temp.	Test Failure Load	Computed Failure Load
5	1	NO RESULTS			
6	2	649	336	2040	1610
6	3	687	363	2140	1170
6	4	675	325	2700	
6	5	657	290	3510	1260
7	6	260	88	11700	14080
7	7	336	110	11900	13090
7	8	322	112	11650	13080
5	9	218	85	6750	8190
5	10	461	181	4100	5900
8	11	260	94	8100	10100
8	12	231	85	7100	10330
8	13	268	92	6650	10010
4	14	610	331	3050	2480
4	15	584	302	3350	3260
4	16	640	336	3000	
2	17	670	388	2650	1640
2	18	653	372	2700	2140
3	19	670	428	3350	2560
3	20	644	394	2900	2920
3	21	501	260	4980	5540
1	22	514	255	4500	5550
2	23				
2	24	527	333	3400	7190
8	25	268	110	7150	10290
8	26	331	136	7250	8490
1	27	R.T.	R.T.	9380	8800
1	28	R.T.	R.T.	8620	8800
2	29				
2	30	408	177	2110	4835

5.0 THERMAL STRESS SUBSTANTIATION TEST

A test program was conducted in the Structures Laboratory, Columbus Division of North American Aviation, Inc. in support of a Generalized Thermal Stress analysis for existing aircraft structure incorporating honeycomb sections as proposed in Phase I of Reference (8).

The test program consisted of two parts. The first part, as outlined in Appendix A, provides test data for correlation of a general buckling equation for honeycomb panels subjected to thermal blast. The second part, which is presented in Appendix B, was conducted to substantiate methods for predicting the stress distribution in a typical composite structure subjected to load-temperature environment.

The test methods and instrumentation used in both parts of this test were designed to provide the most accurate test results possible based on experience gained during previous thermal tests and research. The most valuable experience, especially in test instrumentation, was obtained during the thermal tests conducted for the FJ-4B "Hardtack Project" of Reference (9). Problems were encountered during the "Hardtack Project" in devising an adequate strain gage and thermocouple system. A strain gage installation, which consisted of nichrome gages and ceramic cement for readings to 600°F., proved to be inadequate. The ceramic cement acted as an insulator on the heated surface which produced local stress concentrations due to thermal gradients. Investigations were conducted on several strain gage systems and a compromise of temperature reducing the maximum to 400°F. was found to be necessary in order to use a phenolic cement with the nichrome gage. This system provided acceptable results and was adopted for future elevated temperature tests. Another problem was encountered in obtaining a positive thermocouple installation on aluminum surfaces. The previous practice involved welding the chromel alumel wire to the aluminum surface (generally non weldable 7075 material). Excessive labor time required to replace the thermocouples necessitated the investigation of other methods for installation. A successful method which was adopted consisted of drilling a small hole in the surface, installing the thermocouple wire, and peening it in place. The 400°F. strain gage and the peened thermocouple systems were used in the test in this chapter.

The recording and temperature controlling devices used during this are considered to be some of the best thermal testing equipment available at this time. The Sanborn Recorder, which was used during the honeycomb panel test, is a direct writing instrument which can record a number of variables simultaneously. The final record is permanent and in true rectangular coordinates. The Gilmore Data Logger, used in recording load, temperature, deflection, and strain on the composite structure, is capable of printing out 100 channels of test data in a total elapsed time of 20 seconds. The Research Inc., Ignitron Unit used in controlling temperatures on both tests, is a high quality temperature controller which electronically senses and controls error in specimen temperature.

The following test instrumentation and procedures are recommended for combined load and thermal testing. In preparing the specimen for test, install Tatnall Strain Gages (C12-142 for aluminum) with GA-50 phenolic cement for an adequate strain measuring system up to 400°F. After installation per manufacturers recommended procedures, the gages are to be cured for two hours at 350°F. and one-half hour at 450°F. for the best results. At the present time, strain gages designed for temperatures higher than 400°F. have produced unreliable results. The temperature on the test specimen can be measured or controlled by chromel alumel thermocouples. It is recommended that these thermocouples be installed at the strain gages for strain-temperature correlation and at locations on the specimen where a certain temperature or heat rate is desired. The thermocouples, which establish a certain temperature or heat rate, are used in conjunction with a temperature controller unit such as the aforementioned Research Inc. Ignitron to automatically regulate power input to the heating elements. All thermocouples are to be installed on aluminum by drilling holes for the wires and peening them fast at the surface. After instrumenting the test specimen, the strain gages were coated with a black MIL-L-19537 acrylic lacquer to prevent gage shorts and the entire heated area is sprayed with an aqua-dag suspension for heat absorbsion and stray potential shielding. The quartz lamp radiant heating units such as the standard ALT8-612 unit are used in most cases to provide a heating system; however, for unique specimen configurations or in restricted areas, tubular (Cal-Rod) heaters may be used.

6.0 DISCUSSION OF OPTIMUM DESIGN PROCEDURES

The preceding sections of this report have dealt with the analysis of aircraft structures subjected to temperature gradients. In the past it has been the practice to design an aircraft for normal flight conditions and then analyze the aircraft to establish the limit temperature conditions it would withstand. This method is completely unsatisfactory in many cases, specifically for the case of determining the vulnerability of a weapon system structure. The required performance of the weapon system can only be designed into the structure, not analyzed into it.

The work presented in this section is a first attempt to establish an optimum design procedure for aircraft structures with a temperature gradient. The results of this study have been gratifying in that a relatively simple procedure has been developed. This section presents design procedures for two different types of construction techniques. The first presented, in Section 6.1, is for a honeycomb panel with fixed load and fixed strain conditions. These panel optimization methods can be used for designing the isolated honeycomb panels for a given load or the non-structural honeycomb panel with a given strain induced by the primary structure. The more detailed requirements for these design methods will be presented in Section 6.1.

The two honeycomb panel methods just outlined are also used as a part of a honeycomb box beam design procedure. The design of a box beam to resist thermal gradients can be approached through two structural concepts. The first is to use conventional construction and design for the induced stresses which may require extra material and therefore extra weight. The second method is to reduce the thermal stresses as much as possible with corrugated spar webs. The second method should be lighter in weight than the conventional construction but the induced thermal deflections are larger than those in the conventional structure. In each of these cases the box beam section is optimized for given applied primary and secondary moments with some limit heat input. The secondary moment is the critical moment in the reverse direction from the primary moment. The honeycomb box beam optimization procedure computes the minimum weight, producible configurations for the upper and lower skin panels as well as the spar spacing.

A second box beam optimization method was developed to determine the minimum weight configuration for skin stringer type construction. This method includes the two types of spar construction as mentioned in the discussion of the honeycomb box beam method. The skin stringer box beam design uses two spars and integrally machined skin stringers. The skin thickness and stringer spacing for the upper and lower skins are the prime objectives in the optimization procedures.

The method applied in these optimization procedures have not used the allowable stress methods as originally planned. The basic idea of the allowable stress method is used however, in that the design methods are based upon the element strain rather than stress.

Historically, optimization methods were relatively simple when only a few parameters were involved. In many cases the optimum configuration could be found directly from the differentiation or minimization of a weight equation which was expressed in the terms of the allowable equations. With attempts to optimize more complex structural arrangements the weight equation become too complex to permit direct solution. At this point the high speed computer became a tool to minimize the weight equation through calculation of several configurations and selecting the minimum configuration from a simple equation through these points. With the introduction of temperature gradients into the problem the interdependencies of the structural parameters becomes even more complex. It becomes extremely difficult to solve this problem in the terms of applied stress and allowable stresses as past optimization problems have been handled. Therefore, it became necessary to develop a new procedure or concept. It was known that by assuming the total strain of one element the strain of the other elements could be determined independent of the element areas for an axially loaded member. Thus several configurations can be determined from different assumed strains to obtain the strain at which the minimum weight configuration occurs. More details of this technique will be discussed in the following sections of this report. With the addition of bending into the problem, an expression for the bending strain must also be included in the element strains. This was accomplished by assuming a maximum bending strain on an element with a straight line distribution between elements (plane sections remain plane). This assumed bending strain is iterated until a balance with the bending moment is achieved. Again several configurations are computed and a minimum weight configuration determined using these points.

The optimum configuration thus derived may then be used as a basis of the final design development. The final design then must be checked against the design limits using the allowable stress program presented in Section 2.0 of this report. Any changes in the configuration during the final design development phase may be referenced to the non-optimum configurations generated during the optimization process. A reference to these configurations will indicate the weight penalties involved in the changes and possibly indicate the direction in which the change should be made.

6.1 HONEYCOMB COMPRESSION PANEL OPTIMIZATION

This section discusses the optimization of honeycomb panels (Fig. 6.1) as individual structural elements. Two different conditions were considered for the honeycomb panel design. A method for the optimum design of a honeycomb compression panel for a given load was first derived. A second honeycomb panel design method was derived for a given axial strain. The fixed strain procedure lends itself to the design of secondary structural elements dependent upon the deflection and strains of adjacent primary structure.

Both design methods have been derived for thermal gradients dependent upon the panel configuration. The dependency of the temperature distribution through the panel on facing thickness, core density, and core depth insures an accurate design solution, but also complicates the problem greatly. To reduce this complexity the facing temperatures have been expressed in an emperical tabular form as a function of the configuration parameters. With this approach a minimum amount of time is expended computing temperatures. However, since the final temperature is dependent on the configuration and the configuration dependent on the temperature an iterative process is required to achieve the final balanced design condition.

6.1.1 HONEYCOMB COMPRESSION PANEL OPTIMIZATION WITH FIXED LOAD

The honeycomb compression panel with a fixed load is designed to satisfy three failure modes. The three failure modes used in this derivation are general panel buckling, face wrinkling, and intercell buckling. The general buckling allowable load as used in the following derivation is a function of two unequal facing thicknesses, core depth, core density, edge fixity conditions, and panel size. This equation can be written as follows:

$$N = \frac{P_M A H^2}{\sigma^2} \tag{6.1.1}$$

$$A = \frac{\pi^2 t_{f1} t_{f2} E_1 E_2}{(1-\mu^2)(t_{f1} E_1 + t_{f2} E_2)} \tag{6.1.2}$$

$$H = \left(C + \frac{t_{f1} + t_{f2}}{2}\right) \tag{6.1.3}$$

$$P_M = \frac{K + \left(\frac{V_x}{c_4} + V_y\right) F}{1 + L + \frac{V_x V_y}{c_4} F} \tag{6.1.4}$$

$$K = c_1 + 2c_2 + c_3 \qquad F = c_1 c_3 - c_2^2 + \frac{1-\mu}{2} c_2 K$$

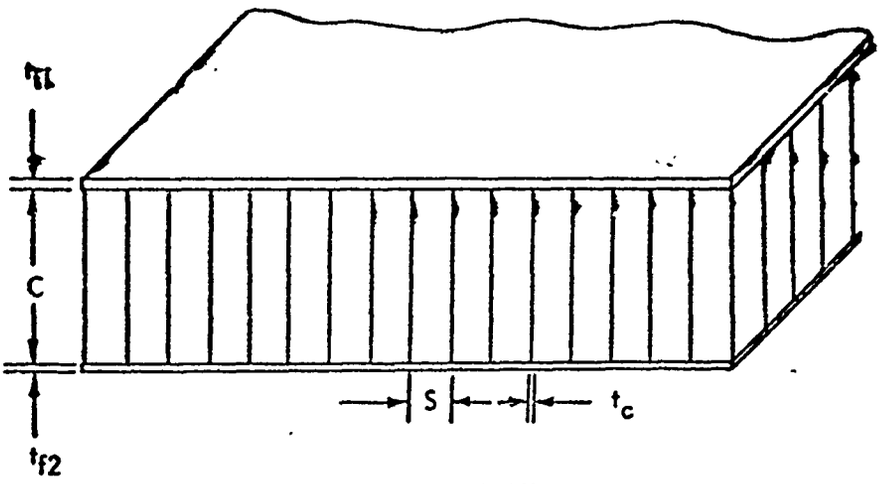

HONEYCOMB PANEL

FIGURE 6.1

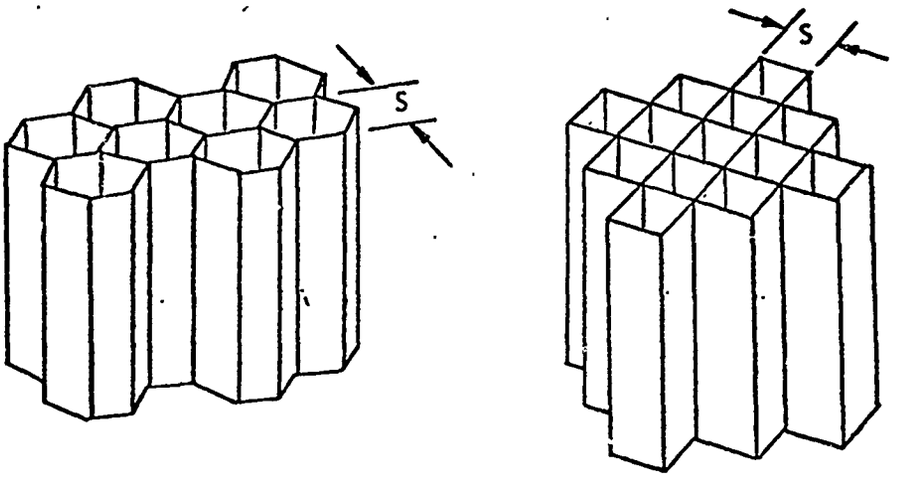

HEXCELL CORE

SQUARE CELL CORE

FIGURE 6.2

$$L = \left(c_1 + \frac{T - P}{2} c_2\right) \frac{V_x}{c_4} + \left(c_3 + \frac{T - P}{2} c_2\right) V_y$$

$$V_y = A \frac{C}{a^2 G'_{cy}} \qquad V_x = A \frac{C}{a^2 G'_{cx}}$$

$G'_{cx} = \frac{G'_{cy}}{2}$ for Hexcell Core $\qquad G'_{cx} = G'_{cy}$ for Square Cell Core (Figure 6.2)

The constants c_1, c_2, c_3, c_4 are a function of panel edge fixity, a/b ratio and number of buckling waves. The constants can be computed as follows for the four primary boundary conditions:

Simply supported panel

$$c_1 = c_4 = \frac{b^2}{n^2 a^2} \qquad c_2 = 1 \qquad c_3 = \frac{1}{c_2}$$

Loaded edge S.S., Unloaded edge clamped

$$c_1 = \frac{16}{3} \frac{b^2}{n^2 a^2} \qquad c_2 = \frac{4}{3} \qquad c_3 = \frac{n^2 a^2}{b^2} \qquad c_4 = \frac{4}{3} \frac{b^2}{n^2 a^2}$$

Loaded edge clamped, Unloaded edge S.S.

$$c_2 = 1 \qquad c_3 = \frac{n^4 + 6n^2 + 1}{n^2 + 1} \frac{a^2}{b^2}$$

$$c_1 = 3/4 \frac{b^2}{a^2} \qquad c_4 = 3 \frac{b^2}{a^2} \quad \text{for } n = 1$$

$$c_1 = c_4 \left(\frac{1}{n^2 + 1}\right) \frac{b^2}{a^2} \quad \text{for } n > 1$$

All edges clamped

$$c_1 = 4 \quad c_4 = 4 \frac{b^2}{a^2} \quad \text{for } n = 1$$

$$c_1 = 4 \quad c_4 = \left(\frac{16}{3(n^2 + 1)}\right) \frac{b^2}{a^2} \quad \text{for } n = 1$$

$$c_2 = 4/3 \qquad c_3 = \left(\frac{n^4 + 6n^2 + 1}{n^2 + 1}\right) \frac{a^2}{b^2}$$

The face wrinkling mode of failure is primarily a function of the core density and facing modulus. The allowable facing stress is expressed as follows:

$$F_{cw} = .5 \left[.066 \left(\frac{t_c}{S} \right)^2 G_c E_c (E_s + e E_T) \right]^{1/3} \qquad (6.1.5)$$

It must be noted at this point, however, that the facing moduli, E_s and E_T, are a function of F_{cw} when F_{cw} is above the proportional limit for the material. In such a case the Ramberg-Osgood stress strain relation (Section 2.0) must be used. The intercell buckling is also dependent upon the Ramberg-Osgood strain relation along with facing thickness, and cell size. The allowable intercell buckling facing stress is written as follows:

$$F_{ci} = .9 E_R \left(\frac{t_f}{S} \right)^{3/2} \qquad (6.1.6)$$

$$E_R = \frac{2 E E_T}{E + E_T} \qquad (6.1.7)$$

With the allowable Equations (6.1.1), (6.1.5) and (6.1.6) the design of a honeycomb compression panel can be accomplished. The requirements of the design for this derivation has included a temperature gradient as well as the axial compression load. The applied stress under these conditions can be expressed for the critical compression as follows:

$$F_c \text{ applied} = \alpha E \Delta T - \frac{1}{A} \sum \alpha E \Delta T \Delta A + \frac{N}{\Sigma \Delta A} \qquad (6.1.8)$$

Because of the two facings being at different temperatures and thus having different material properties and stress level, an effective area of each element must be used. The applied stress Equation (6.1.8) is made up of the full fixity stress $\alpha E \Delta T$, the axial relief stress $1/A \sum \alpha E \Delta T \Delta A$, and the applied load stress $N/\Sigma \Delta A$. No bending relief stress is used in this analysis since it is assumed that the panels are restrained in bending by adjacent structure. The above Equation (6.1.8) can now be rewritten as follows:

$$F_c \text{ applied} = \alpha_1 E_{s1} (T_1 - T_R) - \left[\frac{\alpha_1 E_{s1} (T_1 - T_R) t_{f1} + \alpha_2 E_{s2} (T_2 - T_R) t_{f2}}{t_{f1} + \frac{E_{s2}}{E_{s1}} t_{f2}} \right] + \frac{N}{t_{f1} + \frac{E_{s2}}{E_{s1}} t_{f2}} \qquad (6.1.9)$$

For the design of the minimum weight panel the allowable face wrinkling and general panel buckling stresses will be equal to the applied load stress. Therefore a relation for core density (t_c/s) can be derived by combining Equations (6.1.5) and (6.1.9) as follows:

$$.5 \left[.066 \left(\frac{t_c}{S}\right)^2 G_c E_c (E_{s1} + 3 E_T\right]^{1/3} = \alpha_1 E_{s1} (T_1 - T_R) \left(1 - \frac{t_{f1}}{t_{fT} + \frac{E_{s2}}{E_{s1}} t_{f2}}\right) + \frac{1}{t_{f1} + \frac{E_{s2}}{E_{s1}} t_{f2}} \left[N - \alpha_2 E_{s2} (T_2 - T_R) t_{f2}\right] \quad (6.1.10)$$

$$\frac{t_c}{S} = \left[\frac{\alpha_1 E_{s1} (T_1 - T_R) \left(1 - \frac{t_{f1}}{t_{f1} + \frac{E_{s2}}{E_{s1}} t_{f2}}\right)}{.5 \left[.066 G_c E_c (E_{s1} + 3 E_{T1})\right]^{1/3}} + \frac{\frac{1}{t_{f1} + \frac{E_{s2}}{E_{s1}} t_{f2}} \left[N - \alpha_2 E_{s2} (T_2 - T_R) t_{f2}\right]}{.5 \left[.066 G_c E_c (E_{s1} + 3 E_{T1})\right]^{1/3}}\right]^{3/2} \quad (6.1.11)$$

Another parameter which must be determined is the core depth (C). An expression for (C) may be derived directly from the general buckling Equation (6.1.1) as follows:

$$N = \frac{P_M A H^2}{a^2}$$

Let

$$X = \frac{t_{f1} + t_{f2}}{2} \qquad Y = \frac{t_{f1}\, t_{f2}\, E_{t1}\, E_{t2}}{t_{f1}\, E_{t1} + t_{f2}\, E_{t2}}$$

Substituting Equations (6.1.2), (6.1.3) and (6.1.4), N becomes:

$$N = \left(\frac{K + \left(\frac{V_x}{c_4} + V_y \right) F}{1 + L + \frac{V_x V_y}{c_4} F} \right) K_1 Y (C + X)^2 \qquad (6.1.12)$$

$$v_x = \frac{K_1 Y C}{C'_{cx}} \qquad V_y = \frac{K_1 Y C}{G'_{cy}}$$

$G'_{cx} = G'_{cy}$ for square cell

$G'_{cx} = G'_{cy}/2$ for Hexcell (Figure 6.2)

$$N = \frac{K K_1 (C + X)^2 Y + \left(\frac{K_1 Y C}{c_4 G'_{cx}} + \frac{K_1 Y C}{G'_{cy}} \right) F K_1 Y (C + X)^2}{1 + L + \frac{K_1^2 Y^2 C^2}{c_4 G'_{cx} G'_{cy}} F} \qquad (6.1.13)$$

$$N = \frac{K_1 K (C + X)^2 + C (C + X)^2 \left(\frac{K_1^2}{G'_{cx} c_4} + \frac{K_1^2}{G'_{cy}} \right)}{\frac{1}{Y} + \frac{L}{Y} + \frac{K_1^2 C^2}{c_4 G'_{cx} G'_{cy}} FY} \qquad (6.1.14)$$

$$\frac{N}{Y} + \frac{NL}{Y} + C^2 \left(\frac{N K_1^2 FY}{G'_{cx} G'_{cy} c_4} \right) = C^2 K_1 K + 2 C X K_1 K + X^2 K_1 K$$

$$+ (C^3 + 2C^2 X + C X^2) \left[\frac{K_1^2}{G'_{cx} c_4} + \frac{K_1^2}{G'_{cy}} \right] FY \qquad (6.1.15)$$

$$\frac{N}{Y} + \left(c_1 + \frac{1-\mu}{2} c_2\right) \frac{K_1 CN}{c_4 G'_{cx}} + \left(c_3 + \frac{1-\mu}{2} c_2\right) \frac{K_1 CN}{G'_{cy}}$$

$$+ C^2 \left(\frac{NK_1^2 FY}{G'_{cx} G'_{cy} c_4}\right) = C^3 \left[\frac{K_1^2}{G'_{cx} c_4} + \frac{K_1^2}{G'_{cy}}\right] FY$$

$$+ C^2 \left[K_1 K + 2X FY \left(\frac{K_1^2}{G'_{cx} c_4} + \frac{K_1^2}{G'_{cy}}\right)\right]$$

$$+ C \left[2 X K_1 K + X^2 FY \left(\frac{K_1^2}{G'_{cx} c_4} + \frac{K_1^2}{G'_{cy}}\right)\right] + X^2 K_1 K \qquad (6.1.16$$

$$C^3 \left[FY \left(\frac{K_1^2}{G'_{cx} c_4} + \frac{K_1^2}{G'_{cy}}\right)\right]$$

$$+ C^2 \left[K_1 K + 2X FY \left(\frac{K_1^2}{G'_{cx} c_4} + \frac{K_1^2}{G'_{cy}}\right) - \frac{NK_1^2 FY}{G'_{cx} G'_{cy} c_4}\right]$$

$$+ C \left[2X K_1 K + X^2 FY \left(\frac{K_1^2}{G'_{cx} c_4} + \frac{K_1^2}{G'_{cy}}\right)\right.$$

$$\left. - K_1 N \left(\frac{\left(c_1 + \frac{1-\mu}{2} c_2\right)}{c_4 G'_{cx}} + \frac{\left(c_3 + \frac{1-\mu}{2} c_2\right)}{G'_{cy}}\right)\right]$$

$$+ X^2 K_1 K - \frac{N}{Y} = 0 \qquad (6.1.17)$$

No further reduction of Equation (6.1.17) was attempted since the solution of the cubic will be performed on a digital computer.

All the Equations (6.1.11), (6.1.6) (6.1.17) for the design of a honeycomb panel in compression have now been presented. From these equations it is evident that the design procedure for a given panel with a thermal input is very complex if attacked directly. The complexity is primarily established by the inter-dependency of the temperature distribution with the panel configurations and the inelastic stress-strain relation inherent in an efficient design. While designing a honeycomb panel to perform a certain job it will be found that there are an infinite number of panel configurations which will perform this job with a zero margin. The structural efficiencies for these infinite number of configurations vary, however, over a very wide range. The configuration desired is the one which attains the best efficiency (or minimum weight).

The following design procedure has been derived to compute this minimum weight (optimum) configuration under the conditions previously stipulated. The basic approach to this problem has been changed from one of stress as used in the past to one of strain. By assuming the total strain on one facing of the panel the strain can be computed for the other facing. The strain on the second facing is expressed as follows:

$$\delta_2 = \delta_1 - \alpha (T_1 - T_2)$$

This equation is valid since it has been assumed that no bending occurs in the panel. The bending restraint is assumed to be provided by adjacent structure.

At this point an arbitrary facing thickness t_{f1} is also assumed. With this assumed value of t_{f1} an initial estimate of the facing temperature is computed. This initial estimate is made with a very simple equation:

$$T_1 = \frac{K_t}{t_{f1}} + T_2 \quad , \quad T_2 = \text{Boundary Layer Temperature} \qquad (6.1.18)$$

Knowing δ_1 and δ_2 and the temperature of the facings, the facing stress (F) can be computed using the Ramberg-Osgood equation. The solution of the Ramberg-Osgood equation is an iterative process of trial and error. The equation to be solved is as follows:

$$\delta = \frac{F}{E}\left[1 + 3/7\left(\frac{F}{Fy}\right)^{n-1}\right] \qquad (6.1.19)$$

The yield stress (F_y) is obtained from material properties at temperature.

Knowing the t_{f1} and the facing stresses F_{c1} and F_{c2} the second facing thickness can be computed as a function of the applied load (N). The expression for t_{f2} can be written as follows:

$$t_{f2} = \frac{N - t_{f1}F_{c1}}{F_{c2}} \qquad (6.1.20)$$

Having obtained t_{f2} (Equation 6.1.20) two other parameters remain to be determined to complete the panel configuration. These parameters tc/s, and C, can be determined from Equations (6.1.11) and (6.1.17), respectively. With the final determination of panel configuration for the given load, temperature, t_{f1}, and δ_1 a new estimate of the temperature distribution can be made. This new estimate can be made with much greater accuracy because a panel configuration has been determined. The method of determining this temperature distribution is taken from Reference 10. The curves used for aluminum honeycomb are presented in Figures 6.3 and 6.4.

The process of estimating the temperature and recomputing the panel configuration, as described, must be repeated until temperature convergence is achieved. At this time the temperature distribution and the panel configuration have become compatible. The area or relative weight of this configuration can be determined as follows:

$$A = t_{f1} + t_{f2} + K\frac{t_c}{s}C \qquad (6.1.21)$$

where

K = 2 for square cell, 3 for Hexcell

With a compatible panel configuration determined for the assumed strain δ_1 and facing thickness t_{f1} another strain δ_1 will be assumed. A compatible panel configuration is then determined for this assumed strain also. This process is repeated for a third time so that there are three different configurations for the given load and temperature condition and assumed facing thickness t_{f1}. At this time the strain at which the minimum weight configuration occurs can be determined. The process of determining this minimum is one of fitting an equation (described in Section 6.4) for area as a function of δ_1 through the three computed points and differentiating the equation and setting it equal to zero. The δ_1 which satisfies the $dA/d\delta_1 = 0$ equation is the strain at which the minimum weight (or area) configuration occurs. Using this δ_1 the optimum configuration for the assumed t_{f1} can be computed by the preceding method.

At this point in the analysis the assumed t_{f1} is changed and the complete procedure of computing three panel configurations for three different δ_1's is repeated. Again following the third δ_1 computation the optimum configuration is determined for the second assumed t_{f1}. This process is repeated for a third t_{f1} to establish three optimum δ_1 configurations as a function of t_{f1} (Figure 6.5)

NORTH AMERICAN AVIATION, INC.
COLUMBUS DIVISION
COLUMBUS 16, OHIO

FIGURE 6.3
CORRELATION OF HONEYCOMB THERMAL RESPONSE

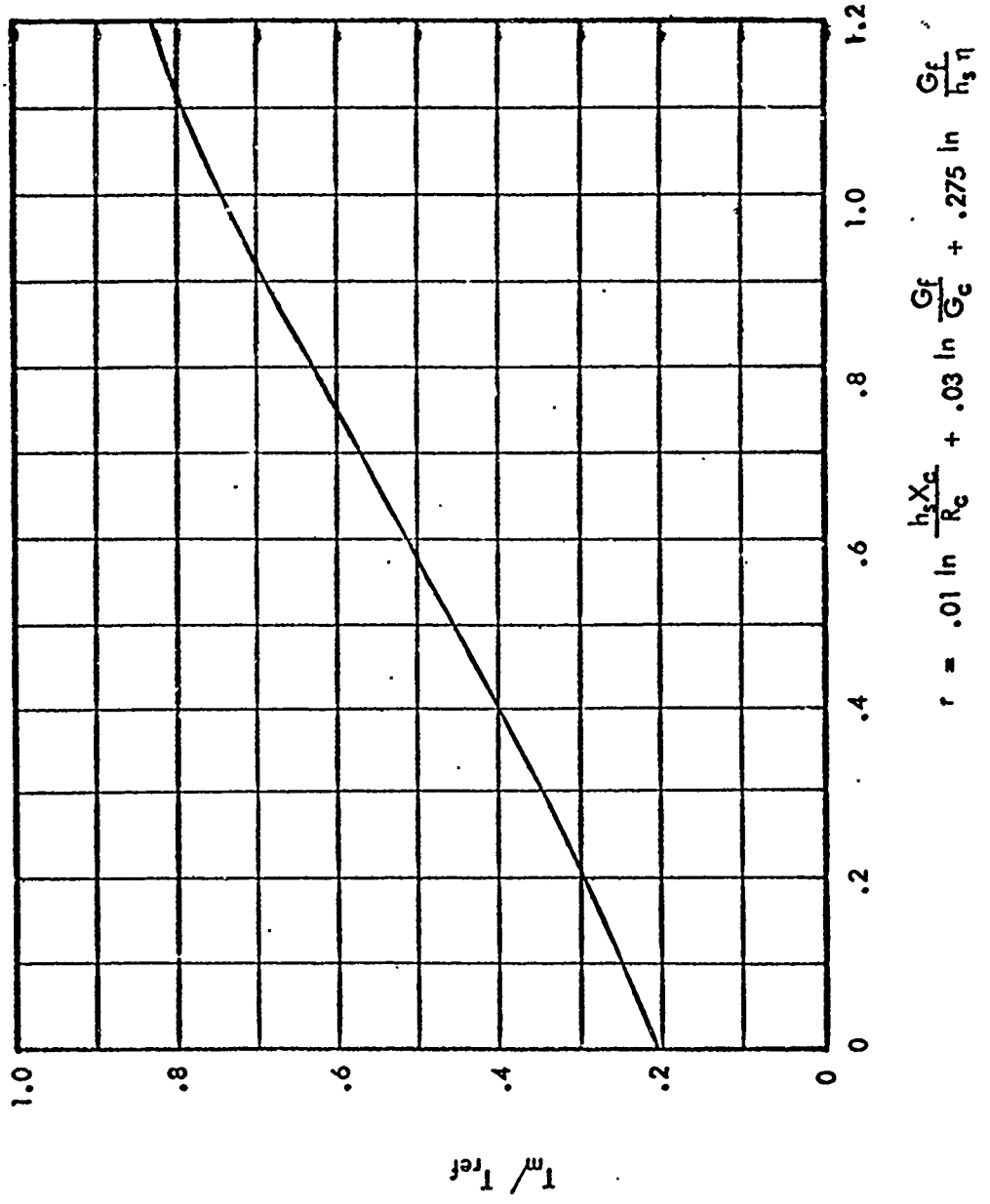

NORTH AMERICAN AVIATION, INC.
COLUMBUS DIVISION
COLUMBUS 16, OHIO

FIGURE 6.4
CORRELATION OF HONEYCOMB THERMAL GRADIENT

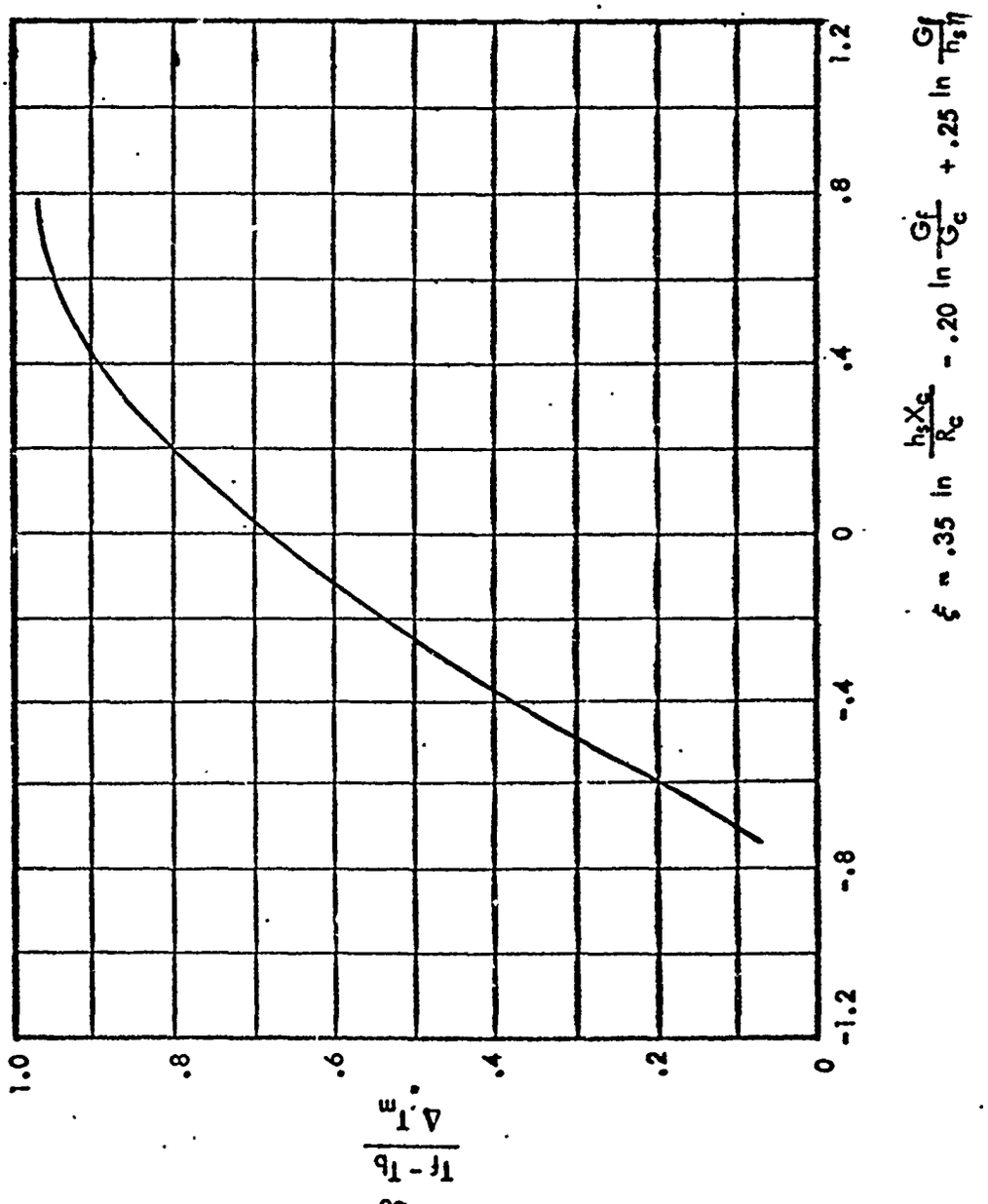

NORTH AMERICAN AVIATION , INC.
COLUMBUS DIVISION
COLUMBUS 16, OHIO

FIGURE 6.5
OPTIMIZATION CURVE

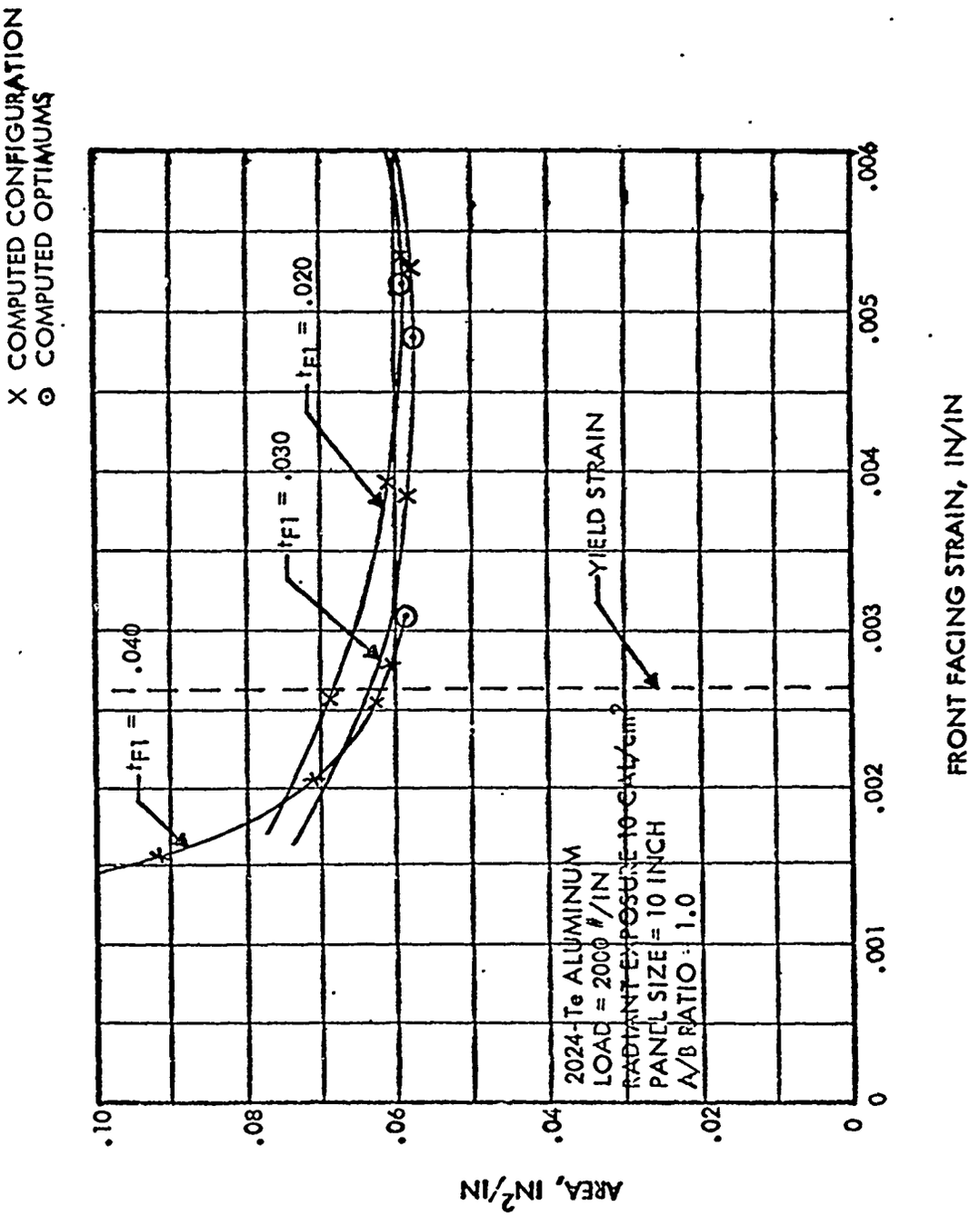

With these three points the absolute optimum can be determined. The determination of the absolute optimum point can be accomplished again by fitting an equation for the area (described in Section 6.4) through the three computed points as a function of t_{f1} and setting the derivative (dA/dt_{f1}) equal to zero. After solving this equation for the optimum t_{f1} the process must be repeated to determine the configuration compatible with the optimum t_{f1}. This final configuration will satisfy the loading and thermal conditions applied with the minimum weight configuration within the tolerances of engineering accuracy.

The preceding method was programmed as described on the IBM 709 Digital Computer as Program E2001. Details of this program such as the FORTRAN listing, block diagram, symbol listing, and input data are presented in Appendix D.

Results from this program are plotted in Figure 6.6. Each configuration computed in the described procedure is plotted to present a better picture the process to find the optimum configuration that satisfies the given loading and heating condition. This plot is also a valuable tool in selecting non-optimum configurations in a case where the optimum configuration cannot be used.

6.1.2 HONEYCOMB PANEL OPTIMIZATION WITH FIXED STRAIN

The fixed strain design procedure has been derived to satisfy the requirements of secondary structural elements. These secondary structural elements in general are not highly stressed load carrying elements but elements which are required to carry only the strain induced in them by the primary structure and thermal loadings. However, these secondary structural elements must still be capable of withstanding the induced stresses of strain. The failure modes which establish the design criteria are general panel buckling, face wrinkling, and intercell buckling. The Equations written for these failure modes in Section 6.1.1 remain basically the same, (6.1.1) (6.1.5), (6.1.6). The approach to the derivation of this method remains one of strain analysis. If δ_N is considered as the $\pm$ extensional strain induced by the primary structure the total strain for each of the two facings can be written as follows:

$$\delta_1 = \alpha_1 (T_1 - T_B) + \delta_N \qquad (6.1.22)$$

$$\delta_2 = \delta_1 - (\alpha_1 T_1 - \alpha_2 T_2) \qquad (6.1.23)$$

The initial temperature estimate is made by the following equation

$$T_1 = T_2 + \frac{KT}{t_{f1}} \qquad T_2 = T_B \qquad (6.1.24)$$

NORTH AMERICAN AVIATION , INC.
COLUMBUS DIVISION
COLUMBUS 16, OHIO

FIGURE 6.6
OPTIMIZATION CURVE

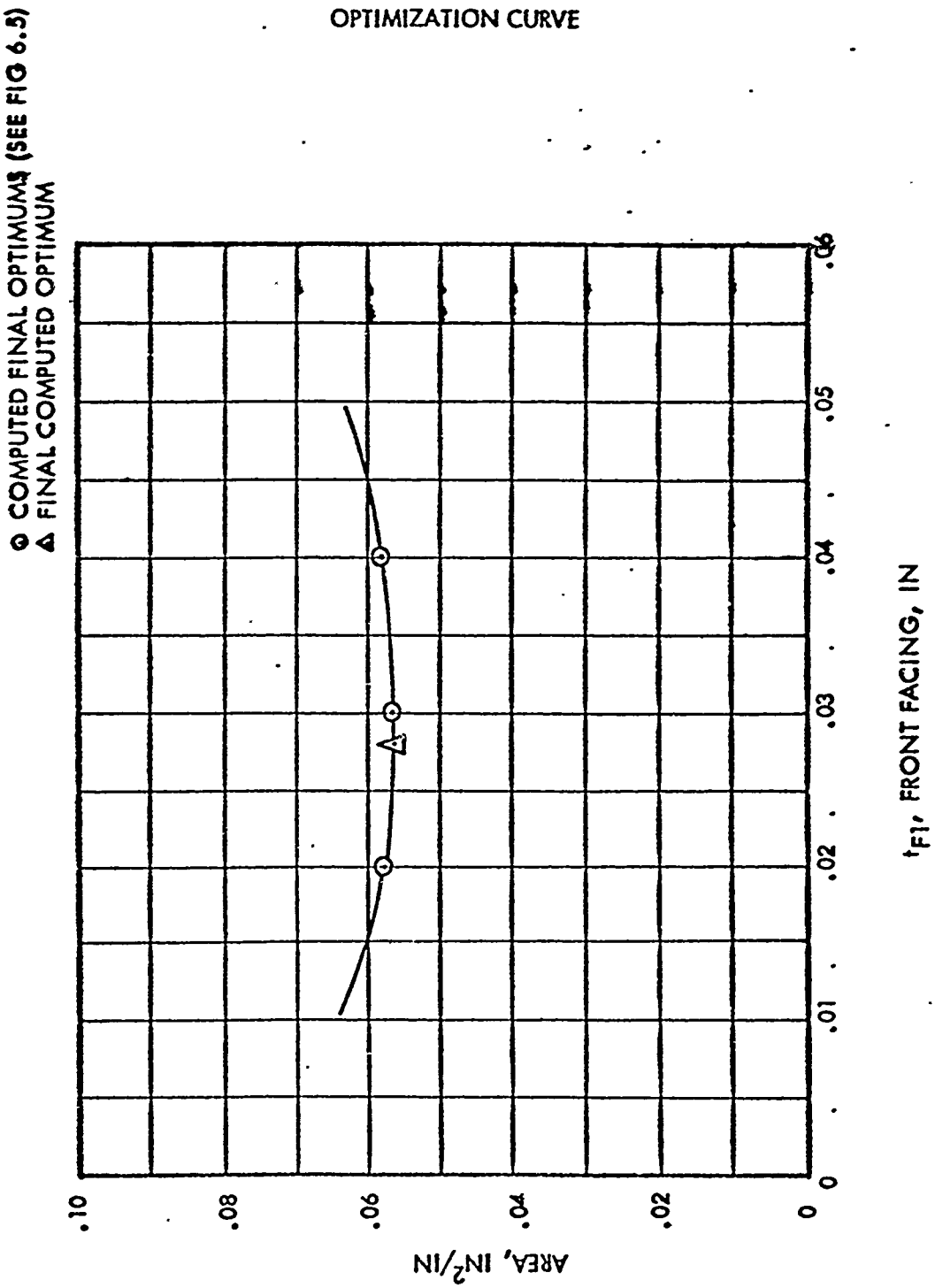

Knowing δ_1 and δ_2 the second modulus and element stress for each facing can be found from the material stress strain curve (Reference Section 2.0). At this point the core configuration can be computed having assumed a facing thickness t_{f1} with the following equation:

$$\frac{t_c}{S} = \left[\frac{\delta'_1 E_{s1}}{.5\left[.066\, G_c E_c (E_{s1} + 3E_{f1})\right]}\right]^{1/3}{}^{3/2} \qquad (6.1.25)$$

$$S = \left(\frac{.9\, E_{R1}}{F_{c1}}\right)^{2/3} t_{f1} \qquad (6.1.26)$$

The second facing thickness t_{f2} can be computed from the equation for cell size (S) as follows:

$$t_{f2} = S\left(\frac{F_{c2}}{.9\, E_{R2}}\right)^{2/3} \qquad (6.1.27)$$

The remaining panel parameter to be computed is core depth which can be derived from the general buckling equation:

$$N = \frac{K_1 (C + X^2)\left[K + \left(\frac{K_1 C}{G'_{cx} c_4} + \frac{K_1 C}{G'_{cy}}\right)\right] FY}{\frac{1}{Y} + L + \frac{K_1{}^2 C^2}{G'_{cx} G'_{cy} c_4}} \qquad (6.1.28)$$

The load N to be sustained by the panel can be expressed as follows:

$$N_A = E_{s1}\, \delta_1\, t_{f1} + E_{s2}\, \delta_2\, t_{f2} \qquad (6.1.29)$$

Setting the allowable load (Equation 6.1.28) equal to the applied load (Equation 6.1.29) the following cubic equation for the core depth C is obtained:

$$\frac{C^3\left(\frac{K_1^2}{G'_{cx}c_4}+\frac{K_1^2}{G'_{cy}}\right)}{N_A}$$

$$+C^2\left[\frac{K_1K}{N_A}+\frac{2XFY\left(\frac{K_1^2}{G'_{cx}c_4}+\frac{K_1^2}{G'_{cy}}\right)}{N_A}-\frac{K_1^2FY}{G'_{cx}G'_{cy}c_4}\right]$$

$$+C\left[\frac{FYX^2\left(\frac{K_1^2}{G'_{cx}c_4}+\frac{K_1^2}{G'_{cy}}\right)}{N_A}+\frac{2XK_1K}{N_A}-\frac{L}{C}\right]$$

$$=\frac{1}{Y}\qquad\frac{X^2K_1K}{N_A} \tag{6.1.30}$$

$$\frac{L}{C}=\left(C_1+\frac{1-\mu'}{2}C_2\right)\frac{K_1}{G'_{cx}x_4}+\left(C_3+\frac{1-\mu}{2}C_2\right)\frac{K_1}{G'_{cy}} \tag{6.1.31}$$

This cubic equation for C is solved by a trial and error iteration method on the computer. At this point in the computation the temperature distribution in the panel must be computed and compared for convergence with the last computed value. The temperature information is taken from the curves in Figures 6.3 and 6.4. If the temperature has not converged the panel configuration must be recomputed as described. Following convergence of the temperature, the area, or relative weight, of the panel can be computed from the following equation:

$$A=t_{f1}+t_{f2}+K\frac{t_cC}{S} \tag{6.1.32}$$

where K = 2 for square cell, 3 for Hexcell (See Figure 6.2)

The process described is repeated for several values of t_{f1} for the given applied load strain δ_n. This procedure produces a series of points relating the panel area (or weight) as a function of t_{f1}. It was found that this procedure did not produce a minimum, but went to zero Area for $t_{f1}=0$. At this point in the study minimum values for the facing thicknesses t_{f1} and t_{f2} were used along with core density and cell size limits. With these limits imposed a minimum practical configuration is reached.

The method discussed was programmed on the IBM 709 Digital Computer as Program E2004. Details of this program such as the FORTRAN listing, block diagram, symbol listing and input data are presented in Appendix D.

Sample results from this program are plotted in Figure 6.7. Each configuration computed in the described procedure is plotted to present a better picture of described process. Each configuration derived will satisfy the induced strain and temperature requirements of the design condition.

FIGURE 6.7
OPTIMIZATION CURVE

6.2 HONEYCOMB BOX BEAM OPTIMIZATION

To this point the optimization of honeycomb structural elements have been discussed. In general these elements appear in a primary load carrying structure which can be classified as a box beam. The honeycomb elements discussed to this point are used in this box beam as the skins or facings of the box. The spar webs and spar spacing must be designed to satisfy the design condition as well as the facings. While the honeycomb panel optimization design condition allowed for only axial loading, the box beam must be designed for bending and shear loads. The bending load can still be assumed to induce axial loads in both the upper and lower honeycomb facing panels. Besides the applied bending moment there is now a thermally induced bending moment to be accounted for. This thermal moment is dependent upon the upper panel configuration, which determines the primary temperature, and the remaining portion of the box beam.

The optimum design process developed during this study uses both the fixed load and fixed strain honeycomb panel procedures to derive the optimum box beam configuration. The details of application will be discussed later in this section.

In the design of a box beam two types of spar web construction must be considered when the thermal stress problem is present. These two web configurations are designated as straight web, Figure 6.8 and corrugated web, Figure 6.9. The two types of construction differ drastically in the presence of thermal stresses. In the case of the straight web box beam, thermal expansions of the upper facing induce loads in the spar web and lower facing as extensional forces and induced bending. In the case of the corrugated spar web the upper facing panel(including the spar attachment channels) is free to expand without inducing loads into the rest of the structure. Thus the thermal effects are retained entirely within the hot facing panel. There are certain advantages to this type of structural arrangement but the major disadvantage is the large deflection induced. If this increased deflection and warping under thermal loads can be tolerated a light weight structure is most likely possible.

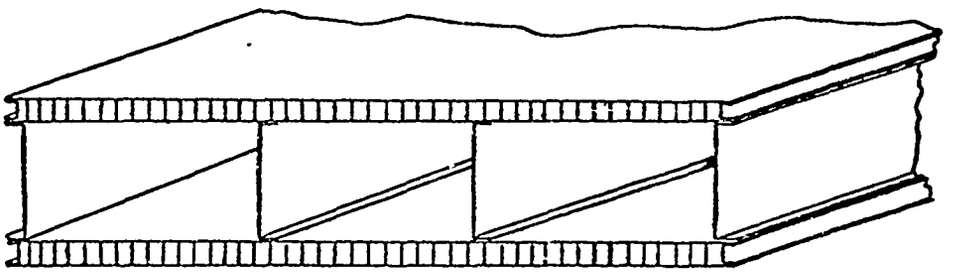

STRAIGHT WEB BOX BEAM

Figure 6.8

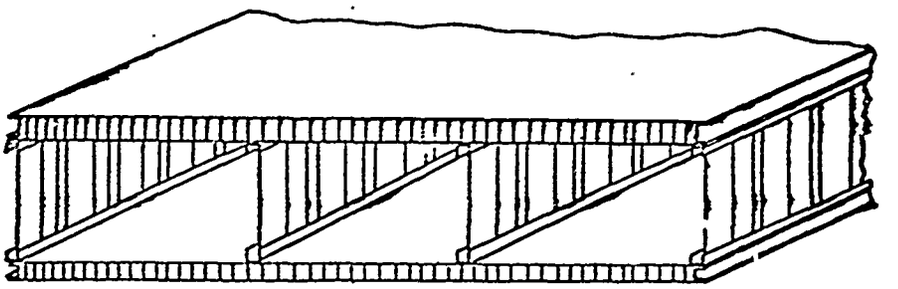

CORRUGATED WEB BOX BEAM
FIGURE 6.9

6.2.1 SPAR WEB DESIGN

In the present study two types of spar webs are used for the box beam design. The first type to be discussed is the straight spar web design to carry the average axial strain and shear strains without buckling. The allowable shear stress can be expressed as follows:

$$F_{scr} = K_{ws} \left(\frac{t_w}{b_w}\right)^2 E_{T_w} \qquad (6.2.1)$$

The allowable axial stress is expressed as:

$$F_{cr} = K_w \left(\frac{t_w}{b_w}\right)^2 E_{T_w} \qquad (6.2.2)$$

The applied shear stress and axial stresses are:

$$f_s = \frac{Q}{\left(\frac{CL}{W} + 1\right) t_w b_w} \qquad f_w = e_w E_{sw} \qquad (6.2.3)$$

$$\left(\frac{CL}{W} + 1\right) = \text{No. of Spar webs}$$

These values are combined in the shear and axial load combined stress equations to derive an expression for t_w as follows:

$$\left(\frac{f_w}{F_{cr}}\right)^2 + \left(\frac{f_s}{F_{scr}}\right)^2 = 1 \qquad (6.2.4)$$

$$\left(\frac{e_w E_{sw}}{K_w \left(\frac{t_w}{b_w}\right)^2 E_{sw}}\right)^2 + \left[\frac{\left(\frac{Q}{t_w b_w}\left(\frac{CL}{w} + 1\right)\right)}{K_{ws}\left(\frac{t_w}{b_w}\right)^2 E_{T_w}}\right] = 1 \qquad (6.2.5)$$

$$E_{T_w} = \frac{E_{sw}}{\frac{E_{sw}}{E_w}(1 - m) + m} \qquad m = \text{Ramberg-Osgood Coeff.}$$

Solving for t_w :

$$t_w^6 - t_w^2 \frac{e_w^2 b_w^4}{K_w^2} - \frac{Q^2 b_w^2}{E_{T_w}^2 K_{ws}^2 \left(\frac{CL}{w} + 1\right)^2} = 0 \qquad (6.2.6)$$

This equation (6.2.6) can now be put in the form of a simple cubic if t_w^2 is set equal to X_{tw}, which can be solved directly for X_{tw} or t_w^2.

The second type of spar web design is the corrugated web. The type of corrugation selected for this study is shown in Figure 6.10.

CORRUGATED SPAR WEB

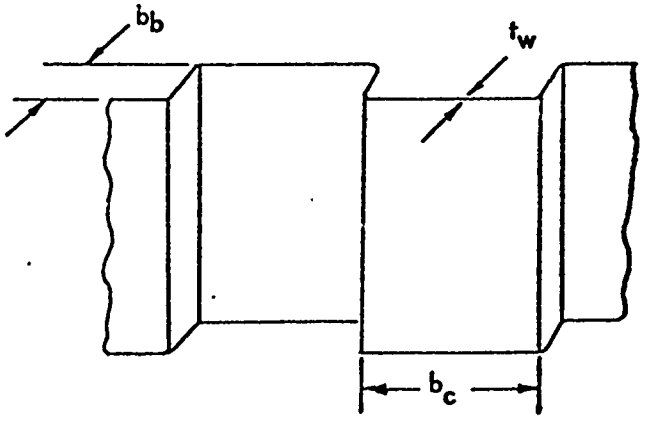

FIGURE 6.10

Since this spar web is incapable of carrying any part of the bending moment on the box beam, only the shear load must be considered in its design. This type of shear web can be designed to an ultimate shear value (F_{su}) selected by the designer. The corrugation length (b_c) can then be determined to prevent buckling of the web. The web design parameters can be computed as follows:

$$t_w = \frac{Q}{\left(\frac{CL}{W} + 1\right) b_w F_{su}} \qquad b_c = t_w \left(\frac{K_{ws} E_w}{F_{su}}\right)^{1/2} \qquad (6.2.7)$$

If $b_c < b_{c\,min}$ set $b_c = b_{c\,min}$

$b_{c\,min}$ = minimum rivet spacing

$$t_w = b_{c\,min} \left(\frac{F_{su}}{K_{ws} E_w}\right)^{1/2} \qquad (6.2.8)$$

$$\frac{\text{Bearing Load}}{\text{in.}} = t_w BR_s \qquad (6.2.9)$$

$$\text{Rivet load} = \frac{b_c Q}{b_w} \qquad (6.2.10)$$

$$\text{Rivet Dia. Req.} = \frac{b_c Q}{b_w t_w BR_s} \qquad (6.2.11)$$

If Rivet Dia. > Max. Allow Rivet Dia.

Set RD = MRD $\qquad b_c = \frac{RD\, b_w t_w BR_s}{Q} \qquad (6.2.12)$

If $b_c < b_{c\,min}$ $\qquad t_w = t_w \frac{b_{c\,min}}{b_c} \qquad (6.2.13)$

set $b_c = b_{c\,min}$

$$b_b = 2 \times BR \times t_w \qquad (6.2.14)$$

The relative area of the web can then be computed as:

$$A_w = \left[\frac{t_w b_c (b_w + 1.5) + b_b t_w (b_w + 1.5)}{b_c}\right] \frac{\left(\frac{CL}{W} + 1\right)}{CL} \qquad (6.2.15)$$

6.2.2 STRAIGHT SPAR WEB BEAM DESIGN

The method selected for the design of the upper and lower cap panels is dependent upon the type of spar web construction. The primary difference in the two spar web types considered in this study is the bending effectiveness of the spar webs. The straight web is considered to carry a share of the bending moment while the corrugated web carries no bending.

With the spar web carrying part of the bending moment the portion of the load carried by the caps is not directly obtainable. Since the configuration of the box beam is the object of the design problem no moment of inertia or size parameters are available to estimate the stress distribution. This is specifically true in the case of inelastic stress where the distribution is non-linear. Therefore strain analysis, which is more independent of the configuration, must be used. In the case of the honeycomb panels a strain on one face could be assumed and the strain on the other face computed as a function of the temperature distribution. This is no longer true since there is bending present. However, if the assumed upper panel strain is a total strain including even the bending, a bending strain distribution for the remaining elements can be assumed. This assumed bending strain will take the form of a straight line distribution of zero on the upper cap and a tension strain e_{lb} on the lower cap. At this time the total strain on each element can be computed as follows:

Average spar web strain

$$e_w = e_{u1} - (\alpha_u T_{u1} - \alpha_w T_w) + 1/2\, e_{lb} \qquad (6.2.16)$$

Lower cap strain

$$e_L = e_{u1} - (\alpha_u T_{u1} - \alpha_L T_L) + e_{lb} \qquad (6.2.17)$$

Parameters which must be given for the solution of this problem are as follows:

CL	Chord length
h or bw	Beam depth to center of faces
M_U	Primary bending moment
M_R	Secondary reverse bending moment
Q	Primary shear load
L	Rib spacing

The initially assumed parameters are as follows:

e_{uT}	Total strain on t_{f1} of upper cap
e_{Lb}	Bending strain on lower cap
t_{f1}	Upper facing thickness for upper panel
W	Spar spacing

The temperature of the upper panel face (T_{u1}) used in the element strain equations just described was taken from the fixed strain honeycomb panel optimization procedure described in Section 6.1.2. The area of the lower facing is estimated by the following equation:

$$t_{F4} + t_{F5} = \frac{M_u}{CL\ h\ F_{tu}} \qquad (6.2.18)$$

To complete the initial sizing of the configuration a spar web thickness (t_w) must be obtained. The sixth root polynomial derived in Section 6.2.1 (Equation 6.2.6) can now be solved as a function of e_w.

$$t_w^6 - t_w^2 \frac{e_w^2 b_w^4}{K_w^2} - \left(\frac{Q\ b_w}{\left(\frac{CL}{W} + 1\right) E_{T_w} K_{w_s}} \right)^2 = 0 \qquad (6.2.19)$$

Equation (6.2.19) designs the straight spar web to remain unbuckled under the shear and bending and axial stresses induced by the thermal and primary static loadings. Now that a configuration has been derived the equilibrium of the section must be checked. The first requirement for this equilibrium check is to determine the location of the neutral axis, since the moment must be computed about the neutral axis of the beam cross-section. The location of the neutral axis below the center line of the upper panel is computed from the following equation:

$$\bar{y} = \frac{\Sigma A_n y_n E_n}{\Sigma A_n E_n} \qquad (6.2.20)$$

$$\bar{y} = \frac{\frac{b_w^2}{2} t_w E_{sw} \left(\frac{1}{W} + \frac{1}{CL}\right) + b_w E_{sL} (t_{F4} + t_{F5})}{\left(\frac{1}{W} + \frac{1}{CL}\right) E_{sw} b_w t_w + E_{sL} (t_{F4} + t_{F5}) + E_{sF1} t_{F1} + E_{sF2} t_{F2}} \qquad (6.2.21)$$

Using a moment balance equation about the neutral axis, an actual e_{Lb} can be computed.

$$e_{Lb} = \Bigg[-M_u + e_{u1}E_{s1}t_{F1}CL\bar{y} + e_{u2}E_{s2}t_{F2}\,CL\,\bar{y} + (e_{u1} - \;\;F\;\; + \;\;_wT_w)\left[E_{sw}\,t_w\,b_w\left(\frac{CL}{w}+1\right)\left(\bar{y} - \frac{\;\;}{2}\right)\right] + (e_{u1} - \;\;_1T_1 + \;\;_2T_2)\left[E_{sL}T_{F3}\,CL(\bar{y} - b_w)\right] \Bigg] \times \Bigg[-.5\left[E_{sw}t_wb_w\left(\frac{CL}{w}+1\right)\left(\bar{y} - \frac{b_w}{2}\right)\right] - \left[E_{sL}\,t_{F3}\,CL\,(\bar{y} - b_w)\right] \Bigg]^{-1} \qquad (6.2.22)$$

With this computed e_{Lb} the upper panel load required for axial balance can be computed as follows:

$$P_{u1} = t_{F2}\,e_{ue}\,E_{s2}\,CL + e_{1s1}\,E_{s1}\,t_{F1}\,CL = -\left(\frac{CL}{w}+1\right)\,T_w\,b_w\,e_w\,E_{sw} - e_L\,E_{sL}\,t_{Fs}\,CL \qquad (6.2.23)$$

The load P_{u1} is then used in the fixed load honeycomb panel method to determine the optimum upper panel for the given load and optimum strain level e_{u1} for that load.

Since the P_{u1} and e_{u1} have been computed from the equilibrium equations and are compatible with e_{Lb}, convergence of e_{Lb} is all that is necessary. Therefore, by comparing the present value of e_{Lb} with the last value convergence can be determined when they become equal within a preset limit.

The only portion of the total configuration which remains undetermined at this point is the core configuration for the lower box cap. The area of the lower panel facings has previously been determined from requirements imposed by the primary bending putting the lower cap in tension. The core configuration will be determined from the compression loading imposed by the secondary bending moment and thermal input on the lower side. The compression load (P_{R2}) imposed on the lower face is estimated as follows:

$$P_{u1} = \frac{M_u}{b_w} \qquad XP_{u1} = (t_{F1} F_{c1} + t_{F2} F_{c2})\ CL \qquad (6.2.24)(6.2.25)$$

$$XP_{R2} = \frac{M_R}{b_w} \frac{XP_{u1}}{P_{u1}} \qquad (6.2.26)$$

To determine the final lower configuration three thickness ratios of t_{f5}/t_{f4} are used knowing the value of $t_{f5} + t_{f4}$ (Equation 6.2.18). By assuming an initial core density and depth, the temperatures T_4 and T_5 can be computed from the curves of Reference (10). Assuming a strain e_5, e_4 can be computed as:

$$e_4 = e_5 - (\alpha_5 T_5 - \alpha_4 T_4) \qquad (6.2.27)$$

A check of the equilibrium equation must be performed:

$$P_N = e_4 E_{s4} t_{F4} + e_5 E_{s5} t_{F5} \qquad (6.2.28)$$

the computed P_N must be equal to the XP_{R2} applied to the panel. If this is not satisfied e_5 is changed until the condition is met. When the condition is met the core density can be computed as:

$$\frac{t_c}{S} = \left[\frac{F_{c5}}{.5 \left[.066\, G_{c5} E_{c5} (E_{s5} + 3 E_{T5}) \right]^{1/3}} \right]^{3/2} \qquad (6.2.29)$$

The core depth (C) can also be computed from Equation (6.1.17) of Section 6.1.1. With the computed configuration just established a new temperature distribution in the panel must be computed and checked for convergence against the last temperature values used. If convergence has not been obtained the configuration must be recomputed as described. When convergence is obtained, the area of the lower panel is computed as:

$$A_5 = t_{F4} + t_{F5} + K \frac{t_c}{S} C \qquad (6.2.30)$$

The procedure must then be repeated for another ratio of t_{f5}/t_{f4} until three configurations have been obtained. At this time a minimum weight configuration can be estimated with the curve matching process (Section 6.4) from the values A_5 as a function of t_{f5}.

When the lower panel configuration has been determined as discussed above, the relative area of the total box beam can be computed by combining Equations (6.1.21) (6.2.30) and the spar web area

$$A_T = t_{F1} + t_{F2} + t_{F4} + t_{F5} + K \frac{t_{ci}}{S_1} C_1 + K \frac{t_{c5}}{S_5} C_5 +$$

$$(b_w + 1.5)\frac{\frac{CL}{W} + ?}{CL} t_w \qquad (6.2.31)$$

Following the computation of the total area A_T a new box beam configuration must be computed for another value of t_{f1} until three configurations are obtained. These three configurations are then used to determine the value of t_{f1} which will produce the minimum weight configuration for the given spar spacing (W).

Following the determination of the minimum configuration for the one spar spacing (W) the process is repeated for two more values of W to achieve a minimum weight configuration with respect to spar spacing (W). This total process then provides the designer with the minimum weight box beam structure to withstand all the induced thermal conditions and loads for the many parameters involved.

The details of the programmed procedure are presented in Appendix D in the form of block diagrams, FORTRAN listings, and sample data sheets. A sample plot of data for a typical design problem is presented in Figure 6.11. This plot presents each point computed in the optimization process described and presents a better picture of the procedures discussed. The plot also shows the weight savings which can be achieved by such an optimization process.

6.2.3 CORRUGATED SPAR WEB BEAM DESIGN

The corrugated spar web beam design must be considered when thermal gradients are present in the structural design requirements. Since the corrugated spar web will not restrain the hot facing panel from expanding the thermal stresses induced in the structure are much lower. These lower stresses will permit a lighter weight design when considering a strength design. However, the corrugated spar will allow greater deflections for the same relative weight, and would be considerably heavier than the straight web construction in the case of a stiffness design.

The load carried by the upper and lower caps can be determined directly for the corrugated spar case. These loads are computed as follows:

$$P_{u1} = P_{u2} = \frac{M_u}{b_w} \qquad (6.2.32)$$

This load P_{u1} can then be used directly in the fixed load honeycomb panel optimization procedure described in Section 6.1.1. Following the determination of the upper cap panel configuration the area of the lower cap can be determined. The lower cap area is assumed to be critical in tension for the primary bending moment M_u.

FIGURE 6.11
OPTIMIZATION CURVE

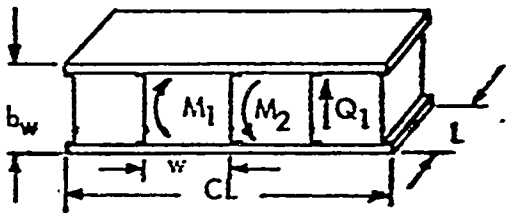

RIB SPACING-L = 10 IN
BOX DEPTH - b_w = 5 IN
BOX CHORD - CL = 40 IN
PRIMARY BENDING - $M_1 = 1 \times 10^6$ IN-LB
SECONDARY BENDING-$M_2 = 6 \times 10^5$ IN-LB
MAX SHEAR LOAD-Q_1 = 1000 LB
RADIANT EXPOSURE-Q_t = 10 CAL/cm^2
TIME TO PEAK, - η = 1.014 SEC

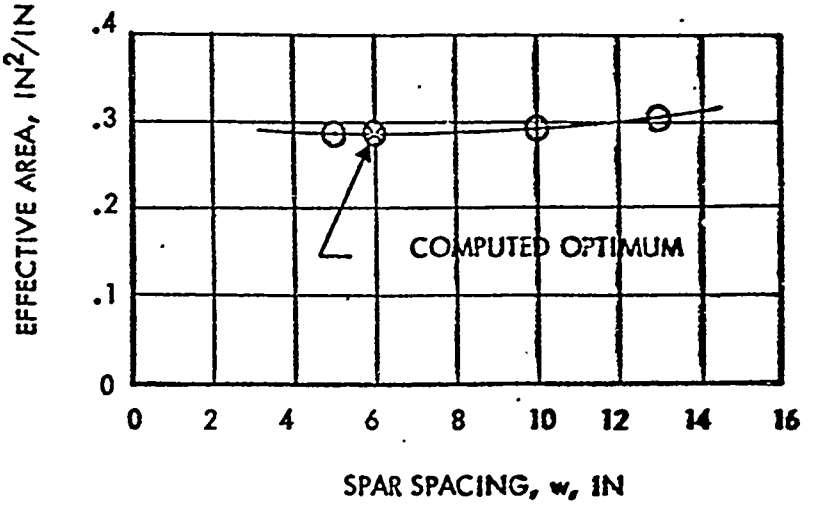

OPTIMUM CONFIGURATION

UPPER PANEL

t_{F1} = .0436 TEMP 1 = 241°F
t_{F2} = .0801 TEMP 2 = 158°F
C_1 = .33
$\frac{t_c}{S}$ = .00583 S_1 = .5676

LOWER PANEL

t_{F5} = .0499 TEMP 5 = 226°F
t_{F4} = .0334 TEMP 4 = 203°F
C_2 = .18
$\frac{t_c}{S}$ = .00326 S_2 = .7633

SPAR WEB t_w = .0530

$$t_{F4} + t_{F5} = \frac{P_{u2}}{F_{tu} CL} \qquad (6.2.33)$$

The lower panel must also withstand the compression load induced by the reverse moment M_R.

The P_{R2} can then be used in the lower panel design procedure described in Section 6.2.2. This design method ensures sufficient area in the lower panel to carry the tension loads induced by M_u and panel stability to carry the compression loads induced by M_R.

The design of the corrugated web is the only problem remaining in the box beam design. The design procedure for the corrugated web is described in Section 6.2.1.

The design procedure to this point has been for a given t_{f1} and W. As in the straight web box beam, two more values of t_{f1} are used for the fixed W. The area of each configuration is computed as:

$$A_T = t_{F1} + t_{F2} + t_{F4} + t_{F5} + K \frac{t_{c1}}{S_1} C_1 + K \frac{t_{c5}}{S_5} C_5$$

$$+ \left(\frac{t_w b_c (b_w + 1.5) + b_b t_w (b_w + 1.5)}{b_c} \right) \left(\frac{\frac{CL}{W} + 1}{CL} \right) \qquad (6.2.34)$$

The parabola method of Section 6.4 is again used to estimate the minimum area configuration as a function of t_{f1}. This process is repeated for two more values of W to provide data to estimate the minimum configuration with respect to t_{f1} and W.

The IBM program for the corrugated spar web box beam design is included in the same program with the straight web box beam presented in Appendix D . Using the same computer program, the option of straight web or corrugated web or both box beam designs is up to the engineer. Data from the corrugated box beam program is presented in Figure 6.12, for comparison with an equivalent straight web box beam.

NORTH AMERICAN AVIATION , INC.
COLUMBUS DIVISION
COLUMBUS 16, OHIO

FIGURE 6.12
OPTIMIZATION CURVE

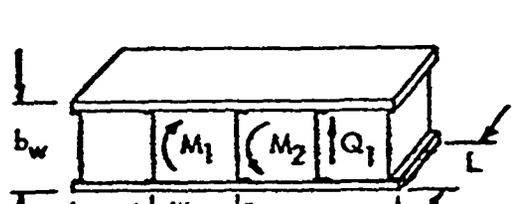

RIB SPACING - L = 10 IN
BOX DEPTH - b_w = 5 IN
BOX CHORD LENGTH-CL = 40 IN
PRIMARY BENDING-M_1=1x10^6 IN-LB
SECONDARY BENDING-M_2=3x10^{5}IN-LB
MAX SHEAR LOAD-Q_1 = 2000 LB
RADIANT EXPOSURE-Q_t = 10 CAL/cm^2
TIME TO PEAK, - η = 1.014 SEC

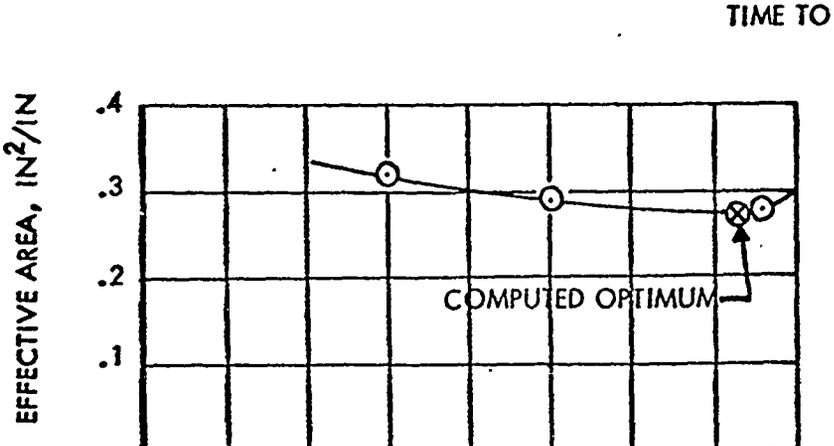

OPTIMUM CONFIGURATION

UPPER PANEL

t_{F1} = .0411	TEMP 1 = 256°F
t_{F2} = .0867	TEMP 2 = 119°F
C_1 = .90	
t_c/S = .00548	S_1 = .4925

LOWER PANEL

t_{F5} = .0445	TEMP 5 = 239°F
t_{F4} = .0389	TEMP 4 = 215°F
C_2 = .21	
t_c/S = .002	S_2 = 2.5

SPAR WEB t_w = .08

6.3 BOX BEAM WITH SKIN AND STRINGERS

The purpose of this section is to determine an optimum box beam structure under a non-uniform temperature distribution and given overall dimensions and for a given applied bending moment, shear load, and reverse applied bending moment.

Initially, for a better understanding of the problem, an I-Beam was investigated to obtain some preliminary optimization equations. It was found that the best approach was through the use of strain equations. To start with, an upper cap thickness was assumed along with an applied strain and appropriate strain and moment equilibrium equations written. The strain was then varied until the equilibrium equations were satisfied. The only restrictions placed on the cross-section were that the upper cap and web be at their critical buckling strains. The lower cap area was determined by assuming it is critical in tension and calculating the area from the applied moment. Another thickness was assumed and the applied strain varied until the equilibrium equations were satisfied. After several values of the upper cap thickness were assumed, a plot was made of total area versus upper cap thickness. The upper cap thickness at the minimum area was then taken as the optimum thickness.

It is this same general approach of using strain equations along with appropriate equilibrium equations that is used in determining an optimum box beam with skin and stringers. Two types of box beams are considered here, one with straight webs and one with corrugated webs. The box beam with straight webs will be considered first.

6.3.1 BOX BEAM WITH STRAIGHT WEBS

It is assumed that the optimum structure will be similar to the one shown below in Figure 6.13.

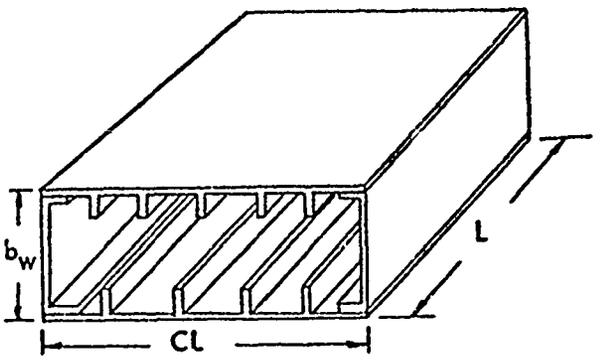

BOX BEAM WITH STRAIGHT WEBS

FIGURE 6.13

The structure is analyzed in three parts; determination of lower cap area and skin-stringer configuration (Section 6.3.1.1), determination of upper cap area and skin-stringer configuration (Section 6.3.1.2), and analysis of the box beam (Section 6.3.1.3).

6.3.1.1 DETERMINATION OF LOWER CAP AREA AND SKIN-STRINGER CONFIGURATION

The lower cap is acted on by an applied moment, M_U, and a reverse moment, M_R. The cap has a total width CL. It is assumed that the lower cap is at a uniform temperature and colder than the upper cap.

As a first approximation it is assumed that the lower cap is critical in tension. The area, A_L, of the lower cap is then calculated by:

$$A_L = \frac{M_U}{b_w F_{tuL}} \qquad (6.3.1)$$

where F_{tuL} is the ultimate tension stress at room temperature and b_w is the arm through which A_L acts (in this case the depth of the box beam).

A minimum skin thickness of .020 inch is assumed as a practical limit. Therefore, A_L must be $\geq .020$ CL. If A_L, calculated by Equation (6.3.1) is less than this value, A_L is taken as:

$$A_L = .020 \text{ CL} \qquad (6.3.2)$$

Since there is a reverse applied moment, M_R, present that will induce compression into the lower cap, the lower cap must be checked to see if it is critical in compression and add the necessary stringers for the given area, A_L, to sustain the compression load. An effective area, A_{eff}, (that part of the lower cap area that remains stable under a compression load) is determined by:

$$A_{eff} = \frac{M_R}{b_w F_{allow}} \qquad (6.3.3)$$

where F_{allow} is some allowable compression stress ($F_{allow} = F_{cy}$ is suggested.

The value of A_{eff} is then checked against A_L calculated by Equations (6.3.1) or (6.3.2). If $A_L < A_{eff}$, A_L is taken as

$$A_L = A_{eff} \qquad (6.3.4)$$

Considering the lower cap as a sheet with no stringers, the effective area may also be defined, by the method outlined in Section 2.1.6, as

$$A_{eff} = A_L \left(\frac{F_{cr}}{f_c}\right)^{1/2} \tag{6.3.5}$$

where F_{cr} is the allowable plate buckling stress given by

$$F_{cr} = K_c E_L \left(\frac{t_{max}}{CL}\right)^2$$

where t_{max} is the maximum skin thickness given by

$$t_{max} = \frac{A_L}{CL}$$

and K_c is the plate buckling coefficient ($K_c = 3.62$ for simple supported edges) or,

$$F_{cr} = K_c E_L \left(\frac{A_L}{CL^2}\right)^2 \tag{6.3.6}$$

f_c is the compression stress on the lower cap and is calculated by

$$f_c = \frac{M_R}{b_w A_L} \tag{6.3.7}$$

Now substituting Equations (6.3.6) and (6.3.7) into Equation (6.3.5),

$$A_{eff} = \left(\frac{A_L}{CL}\right)^2 \left(\frac{K_c E_L b_w A_L}{M_R}\right)^{1/2} \tag{6.3.8}$$

The maximum stress, $f_{c_{max}}$ on the lower cap is then calculated by

$$f_{c_{max}} = \frac{M_R}{b_w A_{eff}} \tag{6.3.9}$$

where A_{eff} is calculated by Equation (6.3.8), or

$$f_{c_{max}} = \left(\frac{CL}{A_L}\right)^2 \left(\frac{M_R^3}{K_c E_L b_w^3 A_L}\right)^{1/2} \tag{6.3.10}$$

The value of $f_{c_{max}}$ is then compared with F_{allow}. If $f_{c_{max}} \leq F_{allow}$ the lower cap configuration is determined as a sheet of thickness $t_L = A_L/CL$ and no stringers. On the other hand, if $f_{c_{max}} > F_{allow}$ it is necessary to add stringers to carry the compression load produced by the reverse applied moment, M_R. As an initial approximation the number of stringers, n, is assumed to be 2. The skin width, b_L, (distance between stringers) is given by

$$b_L = \frac{CL}{n+1} \tag{6.3.11}$$

The allowable buckling stress, F_{cr}, is given by

$$F_{cr} = K_{L_s} E_L \left(\frac{t_L}{b_L}\right)^2$$

where K_{L_s} is the buckling coefficient for the skin ($K_{L_s} = 3.62$ for simple supported edges). Solving for the skin thickness, t_L,

$$t_L = b_L \left(\frac{F_{cr}}{K_{L_s} E_L}\right)^{1/2} \tag{6.3.12}$$

Also,

$$F_{cr} = \left(\frac{A_{eff}}{A_L}\right)^2 \frac{M_R}{b_w A_L} \tag{6.3.13}$$

But, by Equation (6.3.3),

$$A_{eff} = \frac{M_R}{b_w F_{allow}}$$

Substituting this value of A_{eff} into Equation (6.3.13),

$$F_{cr} = \left(\frac{M_R}{b_w F_{allow}}\right)^2 \frac{M_R}{b_w A_L^3} \tag{6.3.14}$$

Substituting this value of F_{cr} into Equation (6.3.12),

$$t_L = \left(\frac{M_R^3 \; b_L^2}{b_w^3 A_L F_{allow} K_{L_s} E_L}\right)^{1/2} \tag{6.3.15}$$

This valueof t_L is then compared with the maximum possible skin thickness, t_{max} given by

$$t_{max} = \frac{A_L}{CL} \tag{6.3.16}$$

If $t_L \geq t_{max}$, then n must be changed by

$$n_i = n_{i-1} + 2 \tag{6.3.17}$$

and the above procedure repeated starting with Equation (6.3.11) until $t_L < t_{max}$. This procedure, in effect, adds stringers until the cross-section is able to sustain the compression load.

If $t_L < t_{max}$, t_L must be compared with a minimum skin thickness (.020 inch). If $t_L < .020$ t_L is set = .020 and A_L recalculated along with t_{max} in Equation (6.3.16).

The allowable compression stress, F_{allow} may be defined by

$$F_{allow} = K_{cstr}\ E_L \left(\frac{t_{str}}{b_{str}}\right)^2 \tag{6.3.18}$$

where t_{str} is the stringer thickness, b_{str} is the stringer height, and K_{cstr} is the buckling coefficient ($K_{c_{str}}$ = .385 for one edge free).

In terms of the stringer area, A_{str}, Equation (6.3.18) may be solved for t_{str} by

$$t_{str} = \left(\frac{F_{allow}\ A_{str}^2}{K_{c_{str}}\ E_L}\right)^{1/4} \tag{6.3.19}$$

The stringer area, A_{str}, may be defined by

$$A_{str} = \frac{(t_{max} - t_L)\ CL}{n} = b_{str}\ t_{str} \tag{6.3.20}$$

where $t_{max} = A_L/CL$ and n is the number of stringers. Substituting this value of A_{str} into Equation (6.3.19),

$$t_{str} = \left(\frac{F_{allow}\ (t_{max}-t_L)^2\ CL^2}{n^2\ K_{c_{str}}\ E_L}\right)^{1/4} \tag{6.3.21}$$

Equation (6.3.20) may be solved for b_{str} by

$$b_{str} = \frac{(t_{max} - t_L)\ CL}{n\ t_{str}} \qquad (6.3.22)$$

The effective skin width, b_{eff}, (width of skin that remains stable under the compression load) may be calculated by

$$\frac{b_{eff}}{b_L} = \frac{A_{eff}}{A_L} = \left(\frac{M_R}{b_w F_{allow}}\right)\left(\frac{1}{A_L}\right)$$

or

$$b_{eff} = \frac{b_L\ M_R}{b_w\ A_L\ F_{allow}} \qquad (6.3.23)$$

The cross-section must now be checked to determine if it is critical as a column. The column allowable, F_c, is calculated by

$$F_c = \frac{\pi^2 E_L}{(L/\rho)^2} = \frac{\pi^2 E_L \times I \times 1.5}{(t_{str}\ b_{str} + t_L\ b_{eff})\ L^2} \qquad (6.3.24)$$

where L is the length of the column and the moment of inertia, I, is calculated by

$$I = t_L\ b_{eff}\ \bar{y}^2 + b_{str}\ t_{str}\left(\frac{t_L}{2} + \frac{b_{str}}{2} - \bar{y}\right) + \frac{t_{str}\ b_{str}^3}{12} \qquad (6.3.25)$$

where $\bar{y}$ is the distance from the upper skin to the neutral axis and is given by

$$\bar{y} = \frac{\Sigma A_n Y_n}{\Sigma A_n} = \frac{t_L^2\ b_{eff} + (b_{str} + 2t_L)^2\ t_{str}}{2\ (t_L\ b_{eff} + b_{str}\ t_{str})} \qquad (6.3.26)$$

This value of the column allowable, F_c, calculated by Equation (6.3.24) must then be compared with F_{allow}. If $F_c < F_{allow}$, the number of stringers, n, must be increased as in Equation(6.3.17) and the above procedure repeated, starting with Equation (6.3.11) until $F_c \geq F_{allow}$.

If $F_c \geq F_{allow}$ the configuration is determined and the last values of A_L, t_L, t_{str}, b_{str}, and n are taken as the optimum values.

A diagram of a typical configuration is shown in Figure 6.14 below

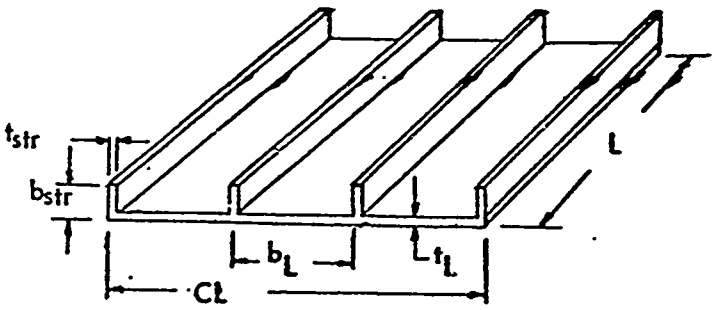

LOWER CAP

FIGURE 6.14

6.3.1.2 DETERMINATION OF UPPER CAP AREA AND SKIN-STRINGER CONFIGURATION

The upper cap will consist of skin and stringers similar to that shown in Figure 6.15 below.

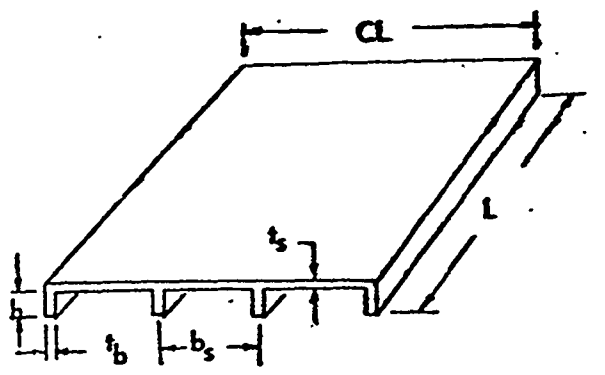

UPPER CAP

FIGURE 6.15

For the purpose of analysis only one T-section will be considered. The temperature of the upper skin and stringers are a function of the skin thickness, t_s, and stringer depth, h, respectively as outlined in Reference 4. A typical temperature-thickness curve is shown in Figure 6.16.

It is assumed that for optimum design, the section will be critical as a column, the stringer will be stable, and the skin will be subject to local buckling. The loading on the upper cap is assumed to be an applied strain, e_u, (produced by the applied moment M_u).

For a given skin thickness, t_s, and stringer spacing, b_s, a ratio, R, of stringer area to skin area ($R = t_b h / t_s b_s$) is assumed along with the temperature of the stringer, T_b. At failure the stringer is at yield strain, e_{yb}. In order to determine the stringer geometry, the stringer strain, e_b, is assumed to be at the critical plate buckling strain, e_{cr_b}, or:

FIGURE 5.16
SKIN TEMPERATURE VERSUS SKIN THICKNESS

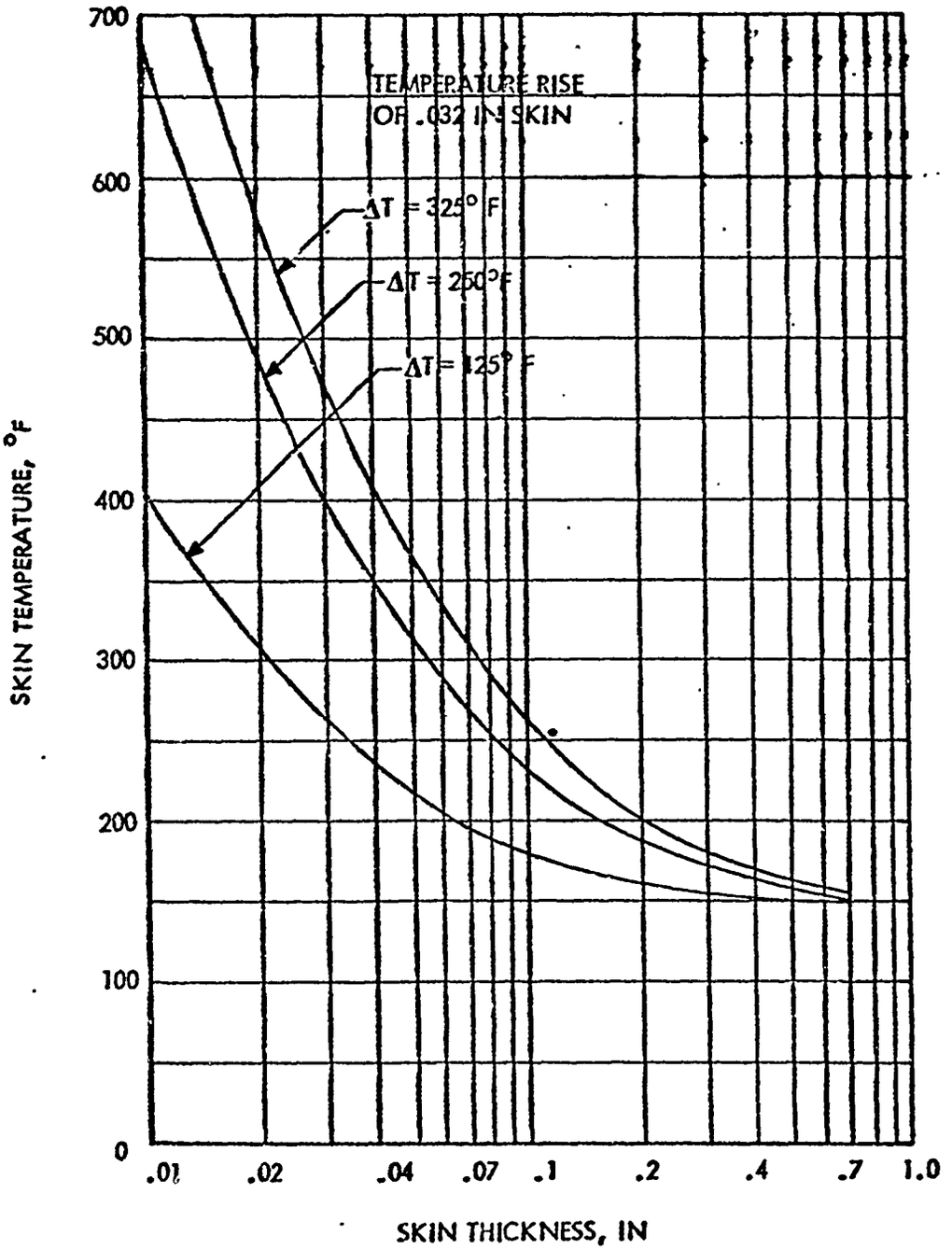

$$e_b = e_{y_b} = e_{cr_b} = K_{c_b}\left(\frac{t_b}{h}\right)^2 \qquad (6.3.27)$$

where K_{c_b} is the buckling coefficient (K_{c_b} = .385 for one edge free). e_{y_b} may be found from the Ramberg-Osgood relationship described in Section 2.0 as

$$e_{y_b} = \frac{F_{y_b}}{.7E_b} \qquad (6.3.28)$$

Solving Equation (6.3.27) in terms of e_{y_b} and R_b

$$h = \left(\frac{.7\,E_b\,K_{c_b}}{F_{y_b}}\right)^{1/4} (t_s\,b_s\,R)^{1/2} \qquad (6.3.29)$$

The temperature of the stringer, T_b, may now be found from Figure 6.16 and compared with the value of T_b assumed; a new value of T_b assumed and the above procedure repeated until the value of T_b obtained from Figure 6.16 agrees with the value assumed. At this point the stringer depth, h, is defined for the assumed value of R.

The strain on the upper skin, e_s, is defined by

$$e_s = \alpha T_s + (e_{ap} + e_p + e_T) = e_u \qquad (6.3.30)$$

where e_u is some known strain.

The strain on the stringer, e_b, is calculated by

$$e_b = \alpha T_b + (e_{ap} + e_p + e_T) \qquad (6.3.31)$$

Solving Equation (6.3.30) for $(e_{ap} + e_p + e_T)$ and substituting in Equation (6.3.31),

$$e_b = e_u + \alpha(T_s - T_b) \qquad (6.3.32)$$

and

$$e_s = e_u \qquad (6.3.33)$$

The allowable crippling stress, F_{cc}, as defined in Section 2.1.6 is found by

$$F_{cc} = \frac{\Sigma F_n E_n A_n C_n}{\Sigma E_n A_n} = \frac{F_s E_s t_s b_s C_s + F_b E_b t_b\, h\, C_b}{E_s t_s b_s + E_b t_b\, h} \qquad (6.3.34)$$

where F_n is the stress associated with the strain found by the Ramberg-Osgood relationship explained in Section 2.0 and C_n is the effective area coefficient outlined in Section 2.1.6.

Since the stringer is a stable element $C_b = 1$. On the other hand, the skin element is subject to local instabilities and therefore from Section 2.1.6,

$$C_s = \left(\frac{e_{cr_s}}{e_s}\right)^{1/2} = \frac{t_s}{b_s}\left(\frac{K_{c_s}}{e_s}\right)^{1/2}$$

$$= \frac{t_s}{b_s}\left[\frac{K_{c_s}}{\frac{F_s}{E_s}\left[1+\frac{3}{7}\left(\frac{F_s}{F_{y_s}}\right)^{m-1}\right]}\right]^{1/2} \quad \text{if } e_s > e_{cr_s}$$

or (6.3.35)

$$C_s = 1 \quad \text{if } e_s \leq e_{cr_s}$$

The stringer stress, F_b, is assumed to reach a cutoff stress where $F_b = F_{yb}$ for the optimum design.

Substituting thes values of C_s and F_b into Equation (6.3.34)

$$F_{cc} = \frac{t_s^2\sqrt{K_{c_s}E_s^3}\,(F_s)^{1/2}\left[1+\frac{3}{7}\left(\frac{F_s}{F_{y_s}}\right)^{m-1}\right]^{-1/2} + F_{yb}t_b\,h\,E_b}{E_s t_s b_s + E_b t_b h} \qquad (6.3.36)$$

The maximum crippling stress $(F_{cc})_{max}$ is found by differentiating Equation (6.3.36) and equating the derivative to zero.

$$\frac{dF_{cc}}{dF_s} = \frac{t_s^2\sqrt{K_{c_s}E_s^3}\,(F_s)^{-1/2}\left[1+\frac{3}{7}\left(\frac{F_s}{F_{y_s}}\right)^{m-1}\right]^{-1/2}}{2\,(E_s t_s b_s + E_b t_b h)}$$

$$- \frac{t_s^2\sqrt{K_{c_s}E_s^3}\,(F_s)^{1/2}\left[1+\frac{3}{7}\left(\frac{F_s}{F_{y_s}}\right)^{m-1}\right]^{-3/2}\left[\frac{3(m-1)F_s^{m-2}}{7F_{y_s}^{m-1}}\right]}{2\,(E_s t_s b_s + E_b t_b h)}$$

$$= 0 \qquad (6.3.37)$$

Solving Equation (6.3.37) for F_s,

$$F_s = F_{y_s}\left[\frac{7}{3(m-2)}\right]^{\frac{1}{m-1}} \qquad (6.3.38)$$

Substituting this value of F_s into Equation (6.3.36) and putting $t_b h$ in terms of R,

$$(F_{cc})_{max} = \frac{\frac{t_s}{b_s}\sqrt{K_{c_s} E_s^3}\left[F_{ys}\left(\frac{m-2}{m-1}\right)\left(\frac{2.333}{m-2}\right)^{\frac{1}{m-1}}\right]^{1/2} + F_{yb} E_b R}{E_s + E_b R} \quad (6.3.39)$$

The neutral axis is located by

$$y = \frac{\Sigma E_n A_n y_{n_r}}{\Sigma E_n A_n} = \frac{E_s\left(\frac{t_s}{2}\right) C_s + E_b R\left(\frac{h}{2} + t_s\right)}{E_s + E_b R} \quad (6.3.40)$$

The allowable column stress, F_c, is calculated by Johnson's Parabola.

$$F_c = (F_{cc})_{max}\left[1 + \frac{(F_{cc})_{max}\Sigma A_n C_n}{4\pi^2 (f/L)^2 \Sigma E_n A_n}\right] \quad (6.3.41)$$

$$= (F_{cc})_{max}\left[1 + \frac{(F_{cc})_{max} L^2 (C_s + C_b R)^2}{6\pi^2 R (E_s + E_b R)\left(\frac{y^2 C_s}{R} + \left[\frac{t_s + h}{2} - y\right]^2 C_b + \frac{h^2}{12}\right)}\right]$$

The elastic applied strain, e_{ap}, on the cross-section may then be calculated by:

$$(e_{ap})_{calc} = \frac{F_c \Sigma A_n C_n}{\Sigma E_n A_n} = \frac{F_c (C_s + C_b R)}{E_s + E_b R} \quad (6.3.42)$$

Also e_{ap} may be calculated from the equilibrium equation by

$$e_{ap} = \frac{\Sigma F_n A_n C_n}{\Sigma E_n A_n} = \frac{F_s C_s + F_b C_b R}{E_s + E_b R} \quad (6.3.43)$$

where F_s and F_b are the stresses associated with the strains e_s and e_b respectively, calculated in Equations (6.3.32) and (6.3.33).

This value of e_{ap} calculated in Equation (6.3.43) is then compared with $(e_{ap})_{calc}$ found by Equation (6.3.42).

$$\Delta e_{ap} = e_{ap} - (e_{ap})_{calc} \quad (6.3.44)$$

The value of R (ratio of stringer area to skin area) is then changed and the above procedure is repeated starting with Equation (6.3.29) until $e_{ap} = (e_{ap})_{calc}$ or $\Delta e_{ap} = 0$. This then satisfies the conditions of equilibrium and the cross-section is at the critical column stress and the optimum cross-section has been achieved for a given stringer spacing. b_s, skin thickness, t_s, and

applied strain, e_u.

The total area of the upper cap is then calculated by:

$$A_u = \frac{CL}{b_s}(t_s b_s + t_b h) = CL\, t_s (1 + R) \qquad (6.3.45)$$

6.3.1.3 BOX BEAM

The box beam, consisting of two spar webs, and upper and lower caps, is similar to that shown in Figure 6.17 below.

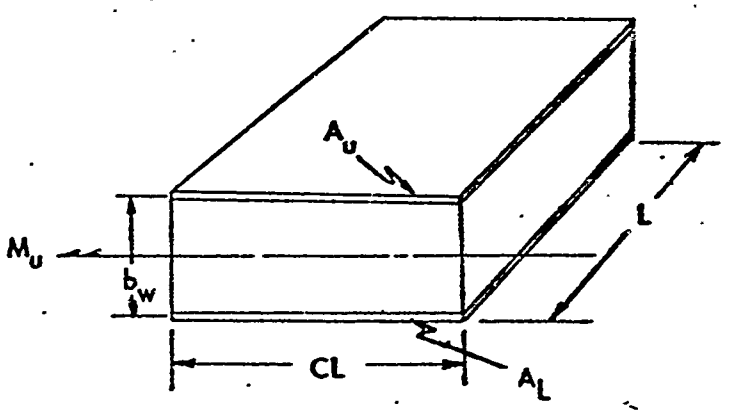

BOX BEAM

FIGURE 6.17

The box beam is assumed to be loaded by an applied moment, M_u, producing compression in the upper cap, or a reverse moment, M_R, producing tension in the upper cap, and a shear load, Q, on the webs. It is assumed that the temperature of the webs and lower cap are known, and the temperature of the upper cap is a function of the upper cap thickness.

First, the lower cap area, A_L, and skin-stringer configuration are determined by the method presented in Section 6.3.1.1.

To start, a value of the upper cap stringer spacing, b_s, is assumed along with values of the upper cap skin thickness, t_s, and the upper cap applied strain e_u.

The web strain, e_w, is calculated by

$$e_w = \alpha_u (T_u - T_B) - \alpha_w (T_w - T_B) + e_u + e_{bw} \qquad (6.3.46)$$

where e_{bw} is an assumed bending strain consisting of both thermal and applied bending strains. T_w and T_u are the temperatures of the web and upper cap skin (discussed in Section 6.3.1.2) respectively; T_B is some reference temperature (room temperature); α_u and α_w are the coefficients of thermal expansion of the web and upper cap.

The lower cap strain, e_L, is calculated by

$$e_L = \alpha_u (T_u - T_B) - \alpha_L (T_L - T_B) + e_u + e_{b_L} \qquad (6.3.47)$$

where e_{b_L} is a bending strain consisting of both applied and thermal strains and T_L is the temperature of the lower cap.

The spar web strain, e_w, is assumed to be the strain at the centroid of the web; therefore,

$$e_{b_w} = \frac{e_{b_L}}{2} \qquad (6.3.48)$$

Substituting this value of e_{b_w} into Equation (6.3.46),

$$e_w = \alpha_u (T_u - T_B) - \alpha_w (T_w - T_B) + e_u + e_{b_L/2} \qquad (6.3.49)$$

and

$$e_L = \alpha_u (T_u - T_B) - \alpha_L (T_L - T_B) + e_u + e_{b_L} \qquad (6.3.50)$$

A value of e_u is assumed (compression) and to start, let $e_{b_L} = 0$.

From the strains, e_u, e_w, and e_L, the stresses associated with these strains may be calculated by the Ramberg-Osgood relationship described in Section 2.0. With these stresses, f_u, f_w, and f_L, the corresponding Secant Moduli, E_{s_u}, E_{s_w}, and E_{s_L}, may be found by:

$$E_s = \frac{f}{e} \qquad (6.3.51)$$

The optimum structure is one in which the spar webs are at both the critical compression buckling stress and the critical shear buckling stress. From this assumption it is possible to calculate the spar web thickness, t_w, by the method described in Section 6.2.1.

At this point the upper cap area, A_u, and the skin-stringer configuration are determined by the method outlined in Section 6.3.1.2 for a given skin thickness, t_s, stringer spacing, b_s, and strain, e_u. However, if the value of h (stringer height) exceeds some maximum value (such as $b_w/2$) a new value of e_u must be chosen and the entire procedure started over again.

The neutral axis is located by

$$\bar{y} = \frac{\Sigma E_{sn} A_n Y_{nr}}{\Sigma E_{sn} A_n} \qquad (6.3.52)$$

where Y_{nr} is the distance from some reference axis to the centroid of element n. In this case the reference axis is taken to be an axis passing through the centroid of the upper skin. Therefore,

$$\bar{y} = \frac{E_{s_w} t_w b_w^2 + E_{s_L} A_L b_w}{2 E_{s_w} t_w b_w + E_{s_L} A_L + E_{s_u} A_u} \qquad (6.3.53)$$

At this point the moment equilibrium may be written as:

$$M_u = \sum e_n E_n A_n y_n \qquad (6.3.54)$$

or

$$M_u = -\left(e_u E_{s_u} CL\, t_s C_s + F_b \frac{CL}{b_s} t_b h\right) \bar{y} - e_w E_{sw} 2 b_w t_w \left(\bar{y} - \frac{b_w}{2}\right) + e_L E_{s_L} A_L (b_w - \bar{y}) \qquad (6.3.55)$$

The strains e_w and e_L may be written in terms of e_u from Equations (6.3.49) and (6.3.50). Equation (6.3.55) then becomes

$$M_u = -\left(e_u E_{s_u} CL\, t_s C_s + F_b \frac{CL}{b_s} t_b h\right) \bar{y}$$

$$- \left[e_u + \alpha_u (T_u - T_B) - \alpha_w (T_w - T_B)\right] E_{s_w} 2b_w t_w \left(\bar{y} - \frac{b_w}{2}\right)$$

$$+ \left[e_u + \alpha_u (T_u - T_B) - \alpha_L (T_L - T_B)\right] E_{s_L} A_L (b_w - \bar{y}$$

$$+ e_{b_L} \left[E_{s_L} A_L (b_w - \bar{y}) - E_{s_w} b_w t_w \left(\bar{y} - \frac{b_w}{2}\right)\right] \qquad (6.3.56)$$

Solving Equation (6.3.56) for e_{b_L},

$$e_{b_L} = \Bigg\{ M_u + (e_u E_{s_u} CL\, t_s C_s + F_b \frac{CL}{b_s} t_b h)\, \bar{y}$$

$$- \left[e_u + \alpha_u (T_u - T_B) - \alpha_w (T_w - T_B)\right] E_{s_w} 2b_w t_w \left(\bar{y} - \frac{b_w}{2}\right)$$

$$- \left[e_u + \alpha_u (T_u - T_B) - \alpha_L (T_L - T_B)\right] E_{s_L} A_L (b_w - \bar{y}) \Bigg\} \Big/ \left[E_{s_L} A_L (b_w - \bar{y})\right.$$

$$\left. + E_{s_w} t_w b_w \left(\bar{y} - \frac{b_w}{2}\right)\right] \qquad (6.3.57)$$

The value of e_{b_L} calculated by Equation (6.3.57) is then compared with the value of e_{b_L} assumed in Equations (6.3.49) and (6.3.50). A new value of e_{b_L} is assumed and the steps outlined in Equations (6.3.49) through (6.3.57) are repeated until the value of e_{b_L} calculated by Equation (6.3.57) is compatible with the value of e_{b_L} assumed.

Next, the axial strain equilibrium equation may be written.

$$\Sigma e_n E_n A_n = 0 \qquad (6.3.58)$$

or

$$e_u E_{s_u} C_s CL\, t_s + F_b \frac{CL}{b_s} t_b h + 2 e_w E_{s_w} t_w b_w + e_L E_{s_L} A_L = 0$$

where F_b is the stress associated with the strain on the stringer calculated in the upper cap in Section 6.3.1.2. Solving Equation (6.3.58) for e_u,

$$e_u = \frac{- F_b \frac{CL}{b_s} t_b h - 2 e_w E_{s_w} t_w b_w - e_L E_{s_L} A_L}{E_{s_u} C_s CL\, t_s} \qquad (6.3.59)$$

The value of e_u calculated by equation (6.3.59) is then compared with the value of e_u assumed in Equation (6.3.49). A new value of e_u is assumed and the above procedure, starting with Equation (6.3.49), is repeated until the value of e_u calculated by Equation (6.3.59) is compatible with the assumed value of e_u.

The structure is now in complete equilibrium since the conditions imposed by Equations (6.3.57) and (6.3.59) have been satisfied.

Next, a new value of upper skin thickness, t_s, is assumed and the entire procedure outlined above is repeated until the necessary equilibrium conditions are satisfied. After several values of the upper skin thickness have been assumed, a plot may be made of the total area, A_T ($A_T = A_u + 2b_w t_w + A_L$), versus t_s for a given stringer spacing, b_s, as shown in Figure 6.18 (a). This curve exhibits a minimum value of A_T at some value of t_s. This point is the optimum design for a given stringer spacing b_s. The minimum point may be calculated by determining three points and assuming a parabola through them as discussed in Section 6.4.

A new value of the stringer spacing, b_s, is assumed and the above procedure repeated for several values of t_s to determine another curve of A_T versus t_s. A typical graph of A_T versus t_s for several different values of b_s is shown in Figure 6.18 (b). A plot is then made of $(A_T)_{min}$ versus b_s as shown in Figure 6.18 (c).

The stringer spacing, b_s, at the minimum of the curve shown in Figure 6.18 (c) is the optimum stringer spacing and the optimum structure has been defined. However, it is possible that the upper cap may fail in tension when the reverse moment, M_R, is applied. Thus the upper cap area must be tested to see if it is capable of sustaining such a tension load and, if necessary, adjust the upper cap area and skin stringer configuration to sustain the tension load produced by M_R. The minimum upper cap area, A_{min}, required to sustain a tension load produced by the reverse moment, M_R, is calculated by

$$A_{min} = \frac{M_R \Sigma E_n A_n}{b_w \Sigma F t_{u_n} E_n A_n}$$

$$= \frac{M_R (E_s t_s b_s + E_b t_b h)}{b_w (F t_{u_s} E_s t_s b_s + F t_{u_b} E_b t_b h} \qquad (6.3.60)$$

where Ft_{u_s} and Ft_{u_b} are the ultimate tension stresses of the upper skin and stringers respectively. If the minimum area shown in Figure 6.18(d) is less than A_{min} calculated by Equation (6.3.60) a new b_s must be chosen such that

FIGURE 6.18
OPTIMIZATION CURVES

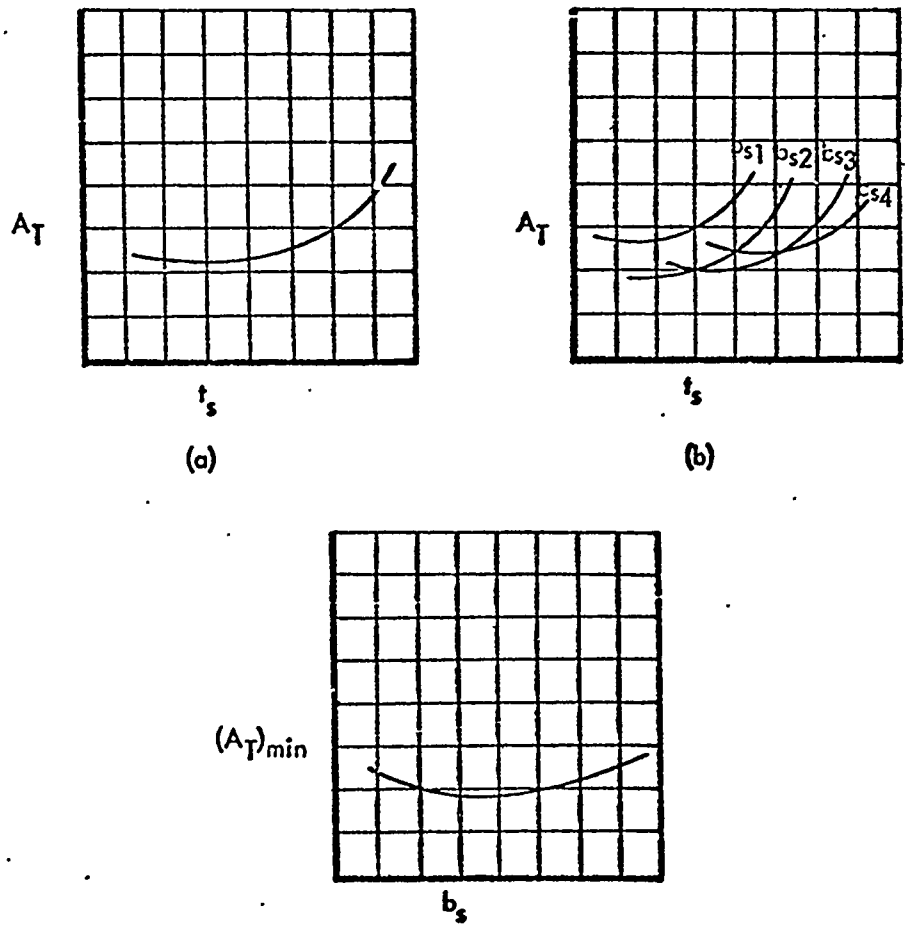

$\left[(A_T)_{min} \right]_{min} \geq A_{min}$ and the entire procedure is repeated one more time for this new value of b_s. This, then is this final optimum design of the box beam. It should be noted, however, that this is an optimum design for a given rib spacing, L, chord length, CL, box depth, b_w, applied primary moment, M_U, reverse moment, M_R, shear load, Q, and temperature distribution through the spar webs and lower cap.

The IBM program to perform this optimization is presented in Appendix D.

6.3.2 BOX BEAM WITH CORRUGATED WEBS

It was pointed out in Section 6.2.3 that the corrugated spar web design should be considered when thermal stresses are present since the corrugated spar web will not restrain the hot upper cap from expanding and the thermal stresses induced in the structure are much lower, thus permitting a lighter weight design. However, the corrugated spar webs will allow greater deflections and a considerable weight penalty must be paid in the case of a stiffness design.

The load, P, carried by the upper and lower caps can be determined directly for the corrugated spar web case. P may be calculated by:

$$P = \frac{M_U}{b_w} \qquad (6.3.61)$$

The upper cap area, A_U, and skin-stringer configuration is determined by the method described in Section 6.3.1.2 after a value is assumed for the upper cap applied strain e_U. P may then be calculated by:

$$P = f_s t_s CL + f_b \frac{CL}{w_s} t_b h \qquad (6.3.62)$$

where f_s and f_b are the stresses associated with the strains on the upper skin and stringers respectively. The load calculated by Equation (6.3.62) is then compared with the actual load calculated in Equation (6.3.61) and a new value of e_U is chosen and the procedure repeated until the calculated load is compatible with the actual load.

The lower cap area, A_L, and skin-stringer configuration is determined by the method outlined in Section 6.3.1.1.

The design of the corrugated web is then determined by the procedure described in Section 6.2.1.

The design procedure to this point has been for a given upper skin thickness, t_s, and stringer spacing, b_s. As in the straight web case, two more values of t_s are chosen for a given b_s. The area of each configuration is computed by:

$$A_T = A_U + 2\,A_W + A_L \qquad (6.3.63)$$

The parabola method of Section 6.4 is again used to determine the minimum area configuration as a function of the skin thickness, t_s. This procedure is repeated for two more values of b_s to determine the minimum area configuration with respect to t_s and b_s.

The IBM program for both the straight and corrugated spar webs is presented in Appendix D.

6.4 PARABOLA CURVE FITTING METHOD

The parabola curve fitting method is used in this study for the primary purpose of describing the optimization curves generated by the high speed computer data. The general form of the equation used in this method is:

$$y = Ax^2 + Bx + C \tag{6.4.1}$$

To compute the exact equation for the optimization curves, a minimum of three points are required. These three points can be described as x_1y_1, x_2y_2, and x_3y_3. Using these points in the general equation, the following three equations can be written:

$$\begin{aligned} y_1 &= Ax_1^2 + Bx_1 + C \\ y_2 &= Ax_2^2 + Bx_2 + C \\ y_3 &= Ax_3^2 + Bx_3 + C \end{aligned} \tag{6.4.2}$$

Solving these three equations simultaneously the following values for the constants A, B, and C are obtained:

$$A = \frac{\frac{(y_2 - y_3)}{(x_2 - x_3)} - \frac{(y_1 - y_2)}{(x_1 - x_2)}}{(x_2 + x_3) - (x_1 + x_2)} \tag{6.4.3}$$

$$B = \frac{y_1 - y_2}{x_1 - x_2} - \frac{A}{x_1 + x_2} \tag{6.4.4}$$

$$C = y_3 - Ax_3^2 + x_3 \frac{(y_1 - y_2)}{(x_1 - x_2)} - \frac{Ax_3}{x_1 - x_2} \tag{6.4.5}$$

Substituting these constants into the general equation, an equation through the three chosen points is obtained. In this study the primary objective is to estimate the minimum value of the parameter y with respect to x. The point on the curve at which this minimum occurs has a slope equal to zero. From calculus it is known that the first derivative of an equation gives the slope at any point on the curve. The derivative of the general equation is:

$$\frac{dy}{dx} = 2Ax + B \tag{6.4.6}$$

If the slope dy/dx is set equal to zero the equation can be solved for the parameter x.

$$\frac{dy}{dx} = 2Ax + B \qquad (6.4.7)$$

$$x = -\frac{B}{2A}$$

This value of x is then the point at which the minimum or maximum value of y occurs. Certain controls have been placed in the computer program to insure that it is a minimum which is computed and that the value is a relatively accurate value.

6.5 CONCLUSIONS

In summary, optimization methods have been developed for four types of box beams; honeycomb box beam with straight or corrugated webs and integral sking-stringer box beam with straight or corrugated webs. One of the principle features of these optimization methods is their ability to handle variable temperature gradients. However, as with all programs, certain restrictions and limitations must be imposed. The following paragraphs describe some of these restrictions and limitations along with some suggested applications of the programs.

It must be pointed out the optimization program presented in Section 6 is for a variable mold line since the box beam depth, b_w, is taken as the distance between the centroids of the upper and lower caps. Thus the mold line will vary, depending on the skin thickness and stringer depth. However, this variation in mold line will be small and a good approximation may be made of the optimum design.

The optimization methods presented here are for a fixed rib spacing, L. However, the designer may easily optimize for the rib spacing by calculating the optimum design for several different rib spacings and including an additional term to account for the weight of the rib as a function of the rib spacing.

The optimum design at elevated temperatures may not be optimum at room temperature and may, in fact, not be able to sustain the applied load at room temperature. Therefore, the programs presented here must be run for room temperature to see if the box beam is indeed critical at room temperature. A plot may be made of the room temperature optimum curve as shown in Figure 6.19. The intersection of these two curves is then the optimum design point when both room temperature and elevated temperature are considered, except when the minimum of one of the curves lies inside the envelope described by the two curves.

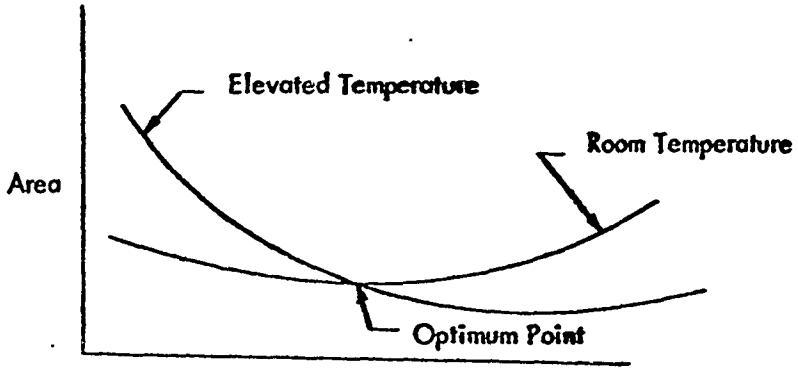

SUPERPOSITION OF ROOM AND ELEVATED TEMPERATURE OPTIMIZATION CURVES

Figure 6.19

This principle of superposition of optimum curves may be extended to other parameters produced by different flight conditions and a design envelope established to determine an optimum structure that will satisfy all of the conditions imposed upon it. A typical example is shown in Figure 6.20 below.

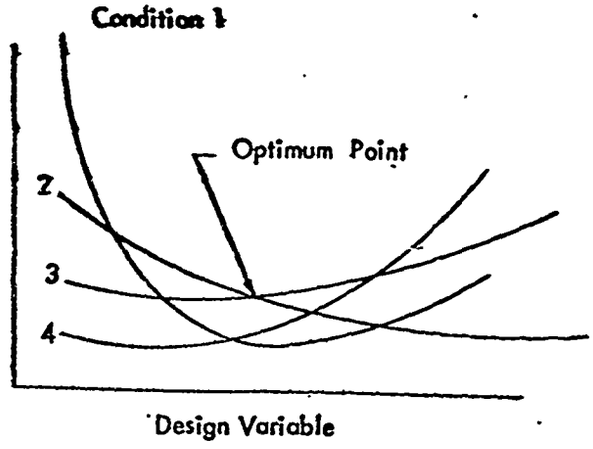

SUPERPOSITION OF MULTI-CONDITION OPTIMIZATION CURVES

FIGURE 6.20